



 **Universität Trier**

NUMERICAL MODELLING OF THE FLIGHT BEHAVIOUR OF  
BATS TO ESTIMATE THE COLLISION RISK WITH WIND  
TURBINES

**Dissertation**

zur Erlangung des akademischen Grades  
einer Doktorin der Naturwissenschaften (Dr. rer. nat.)

im Fachbereich IV der Universität Trier  
vorgelegt von

**Christina Müller**

November 2017

SUPERVISORS:  
Prof. Dr. Ekkehard W. Sachs  
Prof. Dr. Michael Veith  
Prof. Dr. Volker Schulz

## ACKNOWLEDGEMENTS

---

First of all, I would like to express my special gratitude to my advisors Prof. Dr. Ekkehard W. Sachs and Prof. Dr. Michael Veith for giving me the opportunity of writing this thesis and for their support during the last years. I am very thankful for the interdisciplinary topic of this thesis. I also want to thank Prof. Dr. Volker Schulz not only for supervising this thesis but also for the opportunity of being an associate member of the Research Training Group on *Algorithmic Optimization*.

Further I want to thank my colleagues of the Department of Mathematics at Trier University for the fruitful discussions and the moral support especially during the past weeks. My special thanks goes to Laura Somorowsky, Christina Schenk, Bernd Perscheid and Gennaji Heidel for proofreading this thesis and to Ulf Friedrich for the practical advise in so many situations.

I also have to thank my colleagues of the Department of Biogeography at Trier University for not only accepting me in your Department but also for sharing their expertise concerning bats and especially the many enjoyable lunch breaks.

My special thanks goes to Johannes, who always encouraged me in writing this thesis and believing in me all the time.

Finally I want to thank the research initiative *Trier Center for Sustainable Systems* of Trier University funded by the federal state Rhineland-Palatinate, the Research Training Group on *Algorithmic Optimization* funded by the German Research Foundation and Bianca Schröder for their financial support. Additionally, I want to thank the *Statistical and Applied Mathematical Science Institute* for giving me the opportunity of two research stays and for the financial support.

Christina Müller  
Trier, November 2017



## DEUTSCHE ZUSAMMENFASSUNG

---

Das Ziel dieser Arbeit ist es, die Effekte von Windenergieanlagen auf lokale Fledermauspopulationen zu modellieren und Aussagen über deren Gefahr für den Erhalt der betrachteten Population zu treffen. Dabei simulieren wir die Nachtaktivität der Fledermauspopulation und nehmen dabei Rücksicht auf die speziellen Verhaltensweisen und Eigenschaften dieser Säugetiere. Wir modellieren außerdem unterschiedliche Landschaftstypen und das jeweilig zugehörige Verhalten der Tiere. Hierbei betrachten wir zwei unterschiedliche Ansätze, ein individuenbasiertes Modell und einen dichteabhängigen Ansatz. Ersteres erstellen wir mit Hilfe von verschiedenen stochastischen Prozessen, zweiteres mit partiellen Differentialgleichungen. Schließlich stellen wir die Vor- und Nachteile und die jeweiligen Ergebnisse beider Ansätze gegenüber.

Beim ersten Modell handelt es sich um ein sogenanntes Individuenbasiertes Modell (IBM). Bei diesem wird jedes Einzelindividuum separat modelliert. Anschließend wird mit Hilfe einer Monte-Carlo Simulation ein durchschnittliches Verhalten für jedes Tier ermittelt und somit auch die durchschnittliche Gefahr, dass es in die Nähe einer Windenergieanlage fliegt, quantifiziert. In Summe erhalten wir somit das Verhalten der Gesamtpopulation und so auch das Gesamtrisiko. Der große Vorteil dieses Ansatzes ist, dass es hier möglich ist Einzelpräferenzen darzustellen und das Verhalten jedes Einzelindividuums anhand der produzierten Flugwege nachzuvollziehen.

Wir wenden dieses Modell auf ein reales Habitat an. Dabei wählen wir den Bereich um den Ort Lettweiler in Rheinland-Pfalz. Dieser Ort ist in besonderem Maße für ein erstes Anwendungsbeispiel geeignet, weil dort einerseits Sommerquartiere von Zwergfledermäusen zu finden sind und andererseits eine Kollegin dort, im Rahmen ihrer Forschungsarbeit, empirische Daten zu dieser Population erhebt.

Im zweiten Ansatz betrachten wir ein äquivalentes partielles Differentialgleichungsmodell. Dieser Ansatz modelliert einheitliche Präferenzen der Gesamtpopulation und benötigt wesentlich weniger Berechnungsaufwand als das IBM. Allerdings gehen bei diesem Ansatz einige Informationen verloren. So ist es nur möglich die Gesamtpräferenzen darzustellen und nicht etwa, wie im ersten Modell, Rivalitätsverhalten zwischen den Einzelindividuen zu berücksichtigen. Des Weiteren erhalten wir bei diesem Modell nur eine Dichteverteilung der Gesamtpopulation, keine Einzelflugwege der Tiere.

Um unser Modell verifizieren zu können stellen wir ein Kalibrierungsproblem auf und erläutern die Übertragung auf unsere spezifischen Modelleigenschaften. Insbesondere gehen wir dabei auf die Adjungiertengleichung ein, die uns die Möglichkeit gibt den Rechenaufwand der Kalibrierung zu reduzieren.

Anschließend an die beiden Ansätze stellen wir eine Formel auf, die uns die geschätzte Anzahl an getöteten Tieren in Abhängigkeit von Rotorradius, -höhe und Windgeschwindigkeit liefert. Somit erlaubt dieses Modell den durch Windenergieanlagen hervorgerufenen Einfluss auf die Mortalität zu schätzen.

Im nächsten Teil dieser Arbeit führen wir in die Theorie von Populationsmodellen ein. Dabei stellen wir sowohl altersunabhängige als auch altersabhängige Modellansätze vor und betrachten dabei jeweils einen diskreten und einen stetigen Ansatz. Danach passen wir diese Modelle an die speziellen Eigenschaften von Fledermäusen an und setzen die erhöhte Sterberate in das Modell ein. Dadurch erhalten wir die gewünschte Aussage über das Fortbestehen der betrachteten Population.

Als Erweiterung des Modells betrachten wir zuletzt ein partielles Integro-Differentialgleichungsmodell zur Modellierung von Schwärmen. Dabei gehen wir insbesondere auf Existenz- und Eindeutigkeitsaussagen ein.

# CONTENTS

---

1	MOTIVATION	1
1.1	Introduction . . . . .	1
1.2	Outline . . . . .	3
2	LITERATURE REVIEW	9
2.1	Random walk theory . . . . .	9
2.2	Movement from A to B . . . . .	11
2.3	Movement modelling based on Partial Differential Equations . . . . .	13
2.4	Partial integro-differential equations . . . . .	14
3	MODEL ASSUMPTIONS	19
3.1	Biologically induced assumptions . . . . .	19
3.2	Practically induced assumptions . . . . .	21
4	FIRST APPROACH: INDIVIDUAL BASED MODEL	23
4.1	Sample path . . . . .	23
4.2	Attraction zones . . . . .	24
4.2.1	One-dimensional attraction zone . . . . .	25
4.2.2	Two-dimensional attraction zone . . . . .	26
4.3	Voronoi diagram . . . . .	33
4.4	Algorithm . . . . .	36
4.5	Monte-Carlo Simulation . . . . .	38
4.6	Numerical results . . . . .	39
5	APPLICATION	45
6	SECOND APPROACH: PARTIAL DIFFERENTIAL EQUATION MODEL	53
6.1	Transfer to our model . . . . .	53
6.1.1	Sample path and one-dimensional attraction zone . . . . .	54
6.1.2	Two-dimensional attraction zone . . . . .	55
6.2	Numerical results of the PDE model . . . . .	57
6.3	Comparison of the two approaches . . . . .	59
7	MODEL CALIBRATION USING THE ADJOINT EQUATION	65
7.1	General calibration model . . . . .	65
7.2	Gauß-Newton method . . . . .	66
7.3	Adjoint equation . . . . .	67
7.3.1	Model characteristics of the IBM . . . . .	67
7.3.2	Transitions between different parts . . . . .	70
7.3.3	Calibration model for bats flight behaviour . . . . .	70
7.3.4	Lagrange function and necessary first order conditions . . . . .	71
8	RISK OF WIND TURBINES	79
8.1	Model structure . . . . .	79
8.2	Probability density functions . . . . .	80

8.3	Killing rate . . . . .	80
8.4	Numerical implementation . . . . .	82
9	POPULATION GROWTH MODELS . . . . .	85
9.1	Introduction . . . . .	85
9.2	Time-dependent population models . . . . .	87
9.2.1	Discrete model . . . . .	87
9.2.2	ODE model . . . . .	89
9.2.3	Age-independent models for a local bat population . . . . .	91
9.3	Age-dependent population models . . . . .	94
9.3.1	Discrete age-dependent model: the Leslie matrix . . . . .	94
9.3.2	Continuous age-dependent models . . . . .	103
9.3.3	Age-dependent models for a local bat population . . . . .	105
10	SWARM BEHAVIOUR . . . . .	111
10.1	Simulating animal swarms . . . . .	112
10.2	Weak formulation . . . . .	113
10.3	Linear Case I . . . . .	114
10.4	Linear Case II . . . . .	117
10.5	Non-linear case . . . . .	118
11	CONCLUSION AND OUTLOOK . . . . .	121
11.1	Conclusion . . . . .	121
11.2	Outlook and possible applications . . . . .	124
11.2.1	Numerical calibration . . . . .	124
11.2.2	Planning tool . . . . .	125
11.2.3	Comparison to existing models . . . . .	126
	BIBLIOGRAPHY . . . . .	129



## MOTIVATION

---

### 1.1 INTRODUCTION

Since the nuclear phase-out, Germany has to find other options for satisfying its huge power demand and guaranteeing a stable power supply. One possibility for alternative power production are fossil fuel power plants like gas- or coal-fired power plants. Unfortunately, these power plants produce very high emissions such that new options are necessary in order to fulfil international climate targets. Therefore, renewable energy plants are in the focus of politics, economists, ecologists and environmental activists. They produce clean energy with low or no emissions and without reducing the amount of non-renewable resources. However, there are also some problems caused by renewable energy production, like the dependence on specific weather conditions or the enormous need of expansion of the power grid systems because of the decentralized production places.

One type of renewable energy production is wind energy. In 2016 27,797 onshore and 947 offshore wind power plants have been operating in Germany and they produced 49,975 MW which represents 12.4% of the power production in Germany (Durstewitz et al., 2017). Usually offshore wind plants are much more efficient than onshore plants because of the more hours of full load but they only produce energy in the north of Germany whereas the main demand of power is located in the south of Germany. That means the power has to be transported a very long way from north to south but the power grid is unable to cope with this high amount of power. For limiting the need for a huge expansion of the power grid, Germany needs to spread the energy production more over the country. One way to do so is building onshore wind turbines. However, the effects of these wind turbines on the surrounding wildlife are still not predictable at the moment. Some of these effects are positive (e.g. new edge habitats because of the aisles in forests) but most of them are negative for the surrounding environment (e.g. loss of habitat, collision risk of birds, noise disturbance, forest clearance).

The wildlife is faced by a huge interference caused by the wind energy production. Especially birds and bats are threatened by death caused by collisions with the rotor blades of wind turbines (Rydell et al., 2012; Voigt et al., 2015). The development of mitigation strategies

of bat fatalities at wind turbines is therefore a focal issue in conservation biology (Peste et al., 2015). One common way of reducing the number of bat fatalities is to shut down the wind turbines during times of high bat activity. However, it is not known how many bats are killed by wind turbines and how many bats are saved by the shutting down algorithms. Apart from counts of bats killed by wind turbines there is almost no information about the impact of such extra mortality on the viability of local bat populations. Discussing and setting maximum thresholds for the number of killed bats per wind turbine and year may therefore be important for conservation purposes and political reasons (Arnett, Barclay, and Hein, 2013). Additionally the cumulative risk of several wind turbines of a whole wind park has to be considered and the recommended thresholds have to be adapted to this cumulative risk.

Recent attempts to model the impact of wind turbine induced mortality on bat populations primarily tried to identify landscape characteristics that influence the probability of bats being killed using species distribution models (Santos et al., 2015) and similar correlative approaches (Amorim, Rebelo, and Rodrigues, 2012). The few attempts of predicting population trends following wind turbine induced bat mortality relied on deterministic growth models and lead to a decrease in population size inevitably (Rydell et al., 2012).

In this thesis we present a new approach for estimating the effects of wind turbines for a local bat population. We build an individual based model (IBM) which simulates the movement behaviour of every single bat of the population with its own preferences, foraging behaviour and other species characteristics. This behaviour is normalized by a Monte-Carlo simulation which gives us the average behaviour of the population. The result is an occurrence map of the considered habitat which tells us how often the bat and therefore the considered bat population frequent every region of this habitat. Hence, it is possible to estimate the crossing rate of the position of an existing or potential wind turbine.

We compare this individual based approach with a partial differential equation based method. This second approach produces a lower computational effort but, unfortunately, we lose information about the movement trajectories at the same time. In a next step we predict the average number of fatalities for each wind turbine in the habitat, depending on the type of the wind turbine and the behaviour of the considered bat species. This gives us the extra mortality caused by the wind turbines for the local population. This value is used for a population model and finally we can calculate whether the population still grows or if there already is a decline in population size

which leads to the extinction of the population.

Using the combination of all these models, we are able to evaluate the conflict of wind turbines and bats and to predict the result of this conflict. Furthermore, it is possible to find better positions for wind turbines such that the local bat population has a better chance to survive.

## 1.2 OUTLINE

Here we want to give a short overview over the structure and the content of this thesis. Therefore, we shortly describe the content of each chapter and point out the major parts of this thesis.

### CHAPTER 2: LITERATURE REVIEW

We start this thesis with a literature review. In Chapter 2 we summarize the recent results concerning simulating types of animal movement behaviour with different mathematical techniques. Animal behaviour is a well studied topic in literature and of special interest for lots of biological phenomenon. In many cases it is easy to track individuals with radio transmitters, but especially for small individuals, like e.g. bats, this is not always possible or it is too expensive and needs a lot of man power. Therefore, many authors have built several models to simulate individual movement behaviour without the high effort of collecting empirical data.

We start with simple random walk models, then we look at more specific models which treat specific types of animal movement, like searching or foraging behaviour. After that we introduce partial differential equations which are used for simulating the occurrence density profiles of whole populations. Then we present the extension to swarm models, which simulate the behaviour inside animal swarms with partial integro-differential equations. Swarming is a very significant and often observed movement type, where the animals not only orientate on the surrounding landscape but in fact on their surrounding conspecifics. We give an overview of the latest techniques and findings for all this models and we finish the chapter by pointing out the difficulties when it comes to bats and the reason to build a special model for them.

### CHAPTER 3: MODEL ASSUMPTIONS

For building our own model we have to make many assumptions concerning the foraging behaviour of bats. In Chapter 3 we present the general assumptions for our model. Most of them are biologically

motivated and are well documented in recent literature and studies on the movement behaviour of bats. Additionally we rely on the work of Cosima Lindeman, who does a movement behaviour study on the common pipistrelle (*Pipistrellus pipistrellus*) near the village Lettweiler (Germany). Here we use information on this habitat for validating our model and for giving a first idea on how the model can be used for biologically induced questions.

Unfortunately, we also have to make assumptions for simplification purposes to make it possible to implement the model. All these practical induced assumptions are made to reduce the computational effort but we try to guarantee that the effect on the model result is deniable, so we still can accept these restrictions. These assumptions are very important for building our bats' movement model and make it realisable in a acceptable amount of time.

#### CHAPTER 4: INDIVIDUAL BASED MODEL

To fully understand the wind-turbine-induced increase of individual mortalities and their consequences for the viability of an entire bat population we simulate the behaviour of every individual of a considered model population in an individual based model (IBM) in Chapter 4. We estimate the probability of a moving bat to come close enough to a wind turbine in the corresponding landscape. In principle, our approach is based on several stochastic processes. However, we adapt the mathematical model to three different scenarios which are determined by the different flight behaviour types of bats. This includes a flight along a path or a one-dimensional attraction zone, e.g. an alley or a forest edge, which bats usually use for orientating inside their habitat or for hunting along, respectively. Both behaviours are simulated by a two dimensional stochastic process along the predefined path or hunting zone, whereby the bat flies only once along a path but several times along a hunting zone. The third habitat structure is a model for a foraging behaviour over a two-dimensional attraction zone, such as a lake or a forest. This is simulated by a two-dimensional reflected Brownian motion (RBM) and we discretize it by a symmetric Euler-Maruyama scheme (Bossy, Gobet, and Talay, 2004) which we adapt to our special model characteristics.

In addition, the model contains a randomly chosen decision variable which models different preferences for various attraction zones. We also include several elements to be able to simulate different types of territoriality, e.g. a Voronoi separation inside the foraging zones or different attraction values for each zone and each individual.

In order to obtain an average behaviour of the local population we

include a Monte-Carlo simulation to our model. The result is an occurrence profile of the simulated habitat for one bat or the whole population, respectively. We finish the chapter by presenting the numerical results of the IBM and the Monte-Carlo simulation.

#### CHAPTER 5: APPLICATION

In Chapter 5, we present the numerical implementation of the before described IBM to a realistic model landscape. Therefore, we choose the village Lettweiler and use the data set of C. Lindemann, who does a behaviour study on the common pipistrelle (*Pipistrellus pipistrellus*) in this area. We show the model results for different parameter settings and illustrate the possibilities to apply our first approach on a realistic scenario.

#### CHAPTER 6: PARTIAL DIFFERENTIAL EQUATION MODEL

In Chapter 6 we introduce a second approach to simulate animal movement behaviour: a partial differential equation (PDE) based approach. Our first model has lots of advantages when it comes to adaptability of individual behaviour but this advantage generates one problem: a high computational effort. It is well discussed in literature that IBM approaches are often limited concerning the number of simulated individuals (Grimm et al., 2006). So, we want to simulate the behaviour of the bat population by a much faster PDE based approach. Therefore, we derive the corresponding PDE model to our IBM by using the well known theory concerning the connection between stochastic differential equations (SDE) and partial differential equations. Furthermore, we find a possibility to combine the behaviour of the bats over the foraging zones, which we describe by a reflected Brownian motion (RBM) in the IBM, with a parabolic PDE with Neumann boundary conditions (Bossy, Gobet, and Talay, 2004).

In this approach, we simulate the behaviour of a homogeneous population and we obtain a probability density function for the occurrence probabilities. Therefore, it is not possible to show different preferences inside the population or to get trajectories of single individuals. The main advantage of the PDE model is the very low computation time. But on the other side we have a loss of information and adaptability. At the end it is dependent on the application, which of the two approaches is preferable.

#### CHAPTER 7: CALIBRATION

The most important step of this work is the calibration of our model results to an empirical data set. In Chapter 7 we present several nu-

merical methods for solving general calibration problems. In particular we use the adjoint equation and fit this method to the special characteristics of our movement model. Especially the adaptation of the calibration model for the two-dimensional foraging zones and the transitions between the three different behaviour models is challenging.

#### CHAPTER 8: MODEL FOR THE DEATH RISK OF WIND TURBINES

In Chapter 8 we derive a model which predicts the rate of a bat being killed by a wind turbine. Therefore, we calculate the probability of the bat reaching the dangerous circle area that is created by the three turning blades of the wind turbine. Then we derive the rate of a bat being hit by one of these blades depending on the wind strength. Finally we obtain the death rate of the considered wind turbine for the local bat population.

We consider this death rate as an additional death risk for the local bat population which is endangered by the wind turbine. With this value and a proper population model we can estimate the changes in population viability and therefore we can make a prediction whether the considered population is endangered by extinction or whether the increased death rate caused by the wind turbines can be compensated by the intrinsic growth rate of the bat population.

#### CHAPTER 9: POPULATION MODEL

In Chapter 9 we concentrate on the theory of population modelling. Therefore, we give a short overview over the general theory of population models. Then we start by introducing a simple discrete version and derive an ordinary differential equation (ODE) model. We include a carrying capacity  $K$  to our models, fit both approaches to the specific characteristics of our simulated bat species and compare their results. At the end we include the increased death rate caused by the wind turbines and examine its effect on the population growth rate.

Bats usually have different fertility and death rates during their lifespan. Therefore, we present age-structured population models which make it possible to consider these different rates. Again we present a discrete and a continuous approach. In the discrete case we introduce the so called Leslie matrices and present some of the findings concerning the growth rate of the population.

In the continuous case, we derive a hyperbolic partial differential equation which describes the population size development depending on continuous time and age variables. The inclusion of a carrying

capacity  $K$  into this age-dependent models is much more challenging than in the age-independent cases. Therefore, we have a closer look at the possibilities to include such a carrying capacity into the model formulations in order to obtain a realistic result. At the end we fit again both models to the bats' characteristics and include the increased death rate.

#### CHAPTER 10: MODELLING SWARM BEHAVIOUR WITH PARTIAL INTEGRO-DIFFERENTIAL EQUATIONS (PIDE)

Finally we want to present a possible extension of the partial differential equation model to a partial integro-differential model in Chapter 10. We point out the effects of the integral term describing the non-local effects in a animal swarm, e.g. a fish school or a bird swarm. The choice of the kernel function inside the integral term is responsible for the existence of the swarm and determines how long the swarm will sustain. To point out these effects and further assumptions we have a closer look at the approach Mogilner and Edelstein-Keshet, 1999. In further steps we analyse some existence and uniqueness results of this approach.

#### CHAPTER 11: CONCLUSION AND OUTLOOK

At the end of this thesis we present a conclusion and an outlook. We present again the main contents of this work and summarize our findings and results. After that we point out the main issues and give some ideas for extensions and for future research topics in the field of behaviour simulation of bats and the conflict with the increasing number of onshore wind turbines.





## LITERATURE REVIEW

Understanding the movement of animals has been a focal issue in animal behavioural ecology over the past two decades, especially with respect to the increasing number of human-wildlife conflicts. The technological progress in tracking devices produced a large number of empirical studies with increasing levels of data accuracy concerning the spatio-temporal animal behaviour. Simultaneously, various approaches to simulate animal movement have been developed. In this chapter we want to review the most important publications and the therein described techniques for simulating different animal movement behaviour types.

## 2.1 RANDOM WALK THEORY

A very common and plausible way to simulate movement behaviour of animals is the random walk. In 1827 the botanist Robert Brown noticed a random movement of particles inside a fluid and called it a Brownian motion (Brown, 1828). For a definition of a Brownian motion see Chapter 4.

After him, lots of mathematicians and physicians used and carried on on this topic (Einstein, 1905; Langevin, 1908; Smoluchowski, 1906, e.g.). In mathematics a Brownian motion is usually simulated by a special stochastic process. Therefore, we introduce the general definition of a stochastic process:

**Definition 1.** *Stochastic process (Øksendal, 2003)*

*A stochastic process is a parametrized collection of random variables*

$$\{X_t\}_{t \in T}$$

*defined on a probability space  $(\Omega, \mathcal{F}, P)$  and  $\{X_t\}_{t \in T}$  assuming values in  $\mathbb{R}^n$ . Hereby  $T$  is an index set,  $\Omega$  is a non-empty set,  $\mathcal{F}$  is a  $\sigma$ -algebra and  $P$  is a probability measure on  $\mathcal{F}$ .*

The stochastic process which is used to simulate a Brownian motion is called Wiener process, named after the mathematician Norbert Wiener. This process has special properties which are summarized in the following definition:

**Definition 2.** *Wiener process (Karatzas and Shreve, 1991)*

*Be  $(\Omega, \mathcal{F}, P)$  a probability space. Then a Wiener process is a continuous, adapted process  $W = \{W_t, \mathcal{F}_t, 0 \leq t < \infty\}$  on this probability space with the following properties:*

- $W_0 = 0$  almost surely
- the increments of  $W$  are independent and Gaussian distributed ( $W_{t+s} - W_t \sim N(0, s)$ )

The basic model for animal movement is an unbiased random walk. That means the direction of each new step is independent of all past movements. The resulting movement is therefore absolutely random because no direction is preferred (Codling, Plank, and Benhamou, 2008).

A more realistic approach uses correlated random walks (CRWs). Hereby the movement directions are correlated, which means the animal is more likely to move in the same direction as before, then into the opposite direction (see e.g. Bovet and Benhamou, 1988; Codling, Plank, and Benhamou, 2008; Patlak, 1953).

Another approach is a biased random walk (BRW). The directions of the BRW are not chosen randomly but in a way, such that the resulting process is a biased movement to a certain point or into a certain direction (see e.g. Codling, Plank, and Benhamou, 2008). The possibility of simulating animal movement to a certain destination is a very interesting research field. Another way to simulate this type of behaviour is a mean-reversion process. It is also possible to simulate movement inside a home range (Harris and Blackwell, 2013) with this process. The mathematical formulation of such behaviour can be described by a Ornstein-Uhlenbeck process (Uhlenbeck and Ornstein, 1930).

**Definition 3.** *Ornstein-Uhlenbeck process (Gardiner, 2009)*

*Let  $W_t$  be a Wiener process, then the Ornstein-Uhlenbeck process  $X_t$  satisfies the following stochastic differential equation:*

$$dX_t = \theta(\mu - X_t)dt + \sigma dW_t$$

*for constants  $\theta, \sigma, \mu > 0$ .*

Again, this process is a Wiener process but the mean of the process converges to a certain point, such that the process itself converges to a certain point. An extension of this model presents the work of Blackwell (Blackwell, 1997), who uses not only one Ornstein-Uhlenbeck process to simulate animal movement behaviour but several Ornstein-Uhlenbeck processes with different parameters to simulate different behaviour patterns. Another recent extension of this work is the incorporation of group dynamics of Langrock et al. (Langrock et al., 2014).

For a detailed overview of random walk models and their wide range of applications see Codling, Plank, and Benhamou, 2008. In their review they give a very detailed summary about different animal behaviour in different dimensions, the corresponding random walk

based models and other interesting applications of these model formulations. Additionally they also linked most of the models to corresponding partial differential equation based models.

## 2.2 MOVEMENT FROM A TO B

Empirical studies make it possible to make further assumptions concerning animal behaviour. In many cases animals move from a certain point to a certain destination point, e.g. from their home to a hunting area. Therefore, we know the beginning and ending point of the movement but not the movement trajectory itself. In general this behaviour can be described as movement from point A to point B.

One possibility of simulating such a behaviour is the Brownian bridge approach (see e.g. Bullard, 1991). A Brownian bridge is a Wiener process as well, but the variance parameter converges to zero and the mean converges to the ending point B.

**Definition 4.** *Brownian Bridge (Mansuy and Yor, 2008)*  
 Be  $W(t)$  a Wiener process, then

$$B(t) = W(t) - \frac{t}{T}W(T), \quad t \in [0, T]$$

is a Brownian Bridge.

Therefore, only the starting and the ending point are required as input data. The model gives us a random path between these two points by decreasing the variance parameter over time. It is comparable with the mean reversion process described above.

Another assumption is the ability of reaching a point in a certain amount of time. The velocity of animal movement is restricted. Therefore, only a limited radius is possible for one step. This is included in the recent developed space-time-prism approach (see e.g. Miller, 2005; Song and Miller, 2014; Technitis et al., 2015). These models generate individual trajectories between two points, which are randomly placed in space and time. The model then simulates the accessibility of any point within the envelope of all possible space-time paths between an origin and a destination. Therefore, they define an origin point  $x_i$  and a destination point  $x_j$  and an available amount of time  $t_j - t_i$ . Further let  $V_m$  be the maximum travel velocity. Then the reachable area for the animal in a fixed amount of time  $t - t_i$  is given by

$$p_j(t) = \{(x, y) | \sqrt{|x - x_j|^2 + |y - y_j|^2} \leq (t_j - t) \times V_m\}$$

and the area which the animal has to reach such that it is still possible to get to the destination point in the available amount of time  $t_j - t$  is given by

$$f_i(t) = \{(x, y) | \sqrt{|x - x_i|^2 + |y - y_i|^2} \leq (t - t_i) \times V_m\}.$$

The feasible points for this movement step are then given by the intersection of these two sets:  $Z_{ij} = f_i(t) \cap p_j(t)$ .

In combination with the random walk methods it allows the implementation of an unequal distribution of visit probabilities within a prism. This makes it possible to simulate a movement inside a habitat with areas of different attraction to a moving animal. An example of the construction of such a path is given in Figure 1.

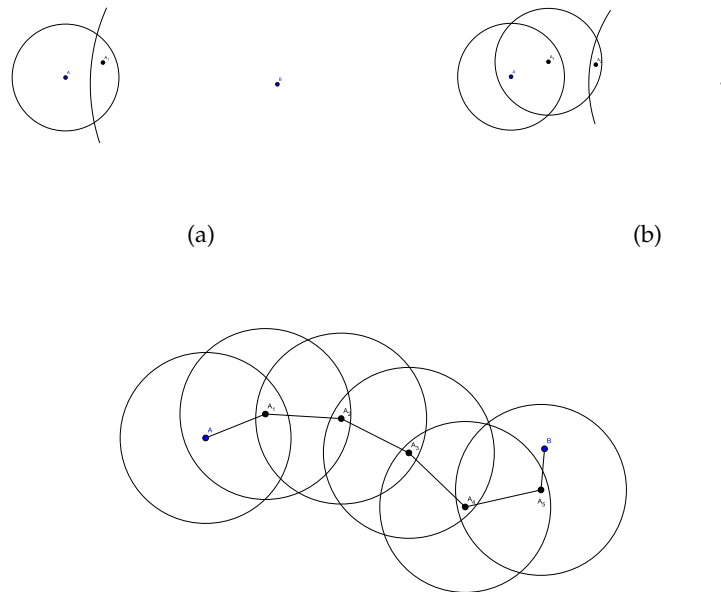


Figure 1: Example of deriving feasible steps between the starting point A and the ending point B for a space-time-prism approach.

The main differences between this approach and the simple Brownian bridges approach is the relevance of time. In this model only paths are accepted which the animal is able to move in the given time horizon. This approach is a perfect way to interpolate incomplete empirical data sets.

### 2.3 MOVEMENT MODELLING BASED ON PARTIAL DIFFERENTIAL EQUATIONS

All the models which we described above are usually implemented by an individual based model (IBM), which is really complex to implement and produces a high computational effort (Grimm et al., 2006). Another approach is more efficient to implement: the use of partial differential equations (PDE) or stochastic differential equations (SDE). This is a very wide and well studied topic in behavioural ecology (e.g. Brillinger, 2003; Brillinger et al., 2002; Codling, Plank, and Benhamou, 2008; Holmes et al., 1994; Murray, 2011; Okubo, 1980; Okubo and Levin, 2001; Preisler et al., 2001). Hereby the movement behaviour is simulated by probabilities. The result is therefore a probability density profile of the movement behaviour. It is often possible to link a random walk model to a corresponding partial differential equations model (see e.g. Codling, Plank, and Benhamou, 2008).

However, we only want to give a short overview about this topic. For a more detailed review on this research field please see Codling, Plank, and Benhamou, 2008 or Holmes et al., 1994.

The basic PDE model for describing animal movement is a diffusion model which corresponds to an unbiased random walk model (Murray, 2011; Okubo, 1980):

$$\frac{\partial p(x, y, t)}{\partial t} = D \left( \frac{\partial^2 p(x, y, t)}{\partial x^2} + \frac{\partial^2 p(x, y, t)}{\partial y^2} \right).$$

Here  $p(x, y, t)$  describes the spatial and temporal dependent density of animals,  $(x, y)$  is the spatial coordinate and  $D$  is the diffusion coefficient.

This model is especially suitable for a homogeneous environment, where the animals have no special tendency to move to certain places. For inhomogeneous landscape structures we can include a drift term in the above equation and obtain (Banks, Kareiva, and Zia, 1988; Helland, Hoff, and Anderbrant, 1984):

$$\begin{aligned} \frac{\partial p(x, y, t)}{\partial t} = & D \left( \frac{\partial^2 p(x, y, t)}{\partial x^2} + \frac{\partial^2 p(x, y, t)}{\partial y^2} \right) \\ & - u_x \frac{\partial p(x, y, t)}{\partial x} - u_y \frac{\partial p(x, y, t)}{\partial y}, \end{aligned}$$

where  $u_x$  and  $u_y$  denote the drift velocities. This model allows to include preferences of the animals towards special regions in their habitat.

The suitable PDE based model for a CRW is the so called telegraph

equation (Goldstein, 1951; Holmes, 1993; Othmer, Dunbar, and Alt, 1988):

$$\frac{\partial p(x, y, t)}{\partial t} = \frac{v^2}{2\lambda} \left( \frac{\partial^2 p(x, y, t)}{\partial x^2} + \frac{\partial^2 p(x, y, t)}{\partial y^2} \right) - \frac{1}{2\lambda} \frac{\partial^2 p(x, y, t)}{\partial t^2}.$$

Here  $1/2\lambda$  denotes the measure of correlation and  $v$  is the velocity of the individuals.

The movement directions are correlated in this approach. Therefore, it is possible to simulate a more directed movement behaviour, i.e. the animal tends to move in a similar direction as before.

In contrast to the random walk models, the PDE approach does not produce trajectories of single individuals and the fitting to very complex or detailed animal behaviour is often not possible. However, it is a good method to obtain fast results for simple or biased random walk models without implementing the behaviour of every single individual but the behaviour of a homogeneous population.

#### 2.4 MODELLING SWARM BEHAVIOUR BY USING PARTIAL INTEGRO-DIFFERENTIAL EQUATIONS

Another very interesting animal movement behaviour is swarming. The understanding of this movement type has been studied by many different researchers of many different fields (e.g. Grünbaum, 1994; Mogilner and Edelstein-Keshet, 1999; Okubo and Levin, 2001; Topaz and Bertozzi, 2004). Here single individuals do not only fit their movement behaviour to the target they want to reach. Instead they fit their movement decisions to the decisions of the animals surrounding them. This can be represented by non local terms in the mathematical problem formulation. Therefore, we also give a short overview on the most important works on this topic.

Grünbaum (Grünbaum, 1994) describes the differences between Lagrangian models, which represent individual based modelling, and Eulerian models, which use PDE formulations. The former models give a good description of the behaviour of single individuals. However, the number of simulated individuals is limited by the implementation process. With the latter ones it is possible to simulate a large number of individuals, but it is only possible to describe the population density and to predict group properties. Hence, Grünbaum builds a mixed model to describe density-dependent social animal behaviours (e.g. fish schools), in his case a PIDE model:

$$\frac{\partial p(x, t)}{\partial t} = D \frac{\partial^2 p(x, t)}{\partial x^2} - \frac{\partial}{\partial x} [p(x, t)(V + \gamma \phi(x, t))].$$

Here  $p(x, t)$  is the population density at site  $x$  at time  $t$ ,  $D$  is the diffusion coefficient,  $V$  is the environmental advection velocity,  $\gamma$  is the

characteristic aggregation velocity and  $\phi$  is the local expected value of the behavioural decision and is represented by an integral term.

Mogilner and Edelstein-Keshet modified this standard approach in (Mogilner and Edelstein-Keshet, 1999) and present their version of simulating animal aggregation:

$$\frac{\partial p(x, t)}{\partial t} = \frac{\partial}{\partial x} \left( D \frac{\partial p(x, t)}{\partial x} - V(p)p(x, t) \right).$$

Here the diffusion coefficient  $D$  is independent of the density  $p$  and they assume the population growth to be negligible. Furthermore, the velocity  $V$  is given by the convolution

$$V(p) = K * p = \int_{\mathbb{R}} K(x - x')p(x', t)dx',$$

where  $K$  is a kernel function and  $K(x - x')$  describes the strength of interaction between the individual at site  $x$  and the individual at site  $x'$ .  $R$  is the radius that allows interactions between individuals. It is a sort of sensation radius of the individual.

Topaz et al. present a first attempt to simulate swarm behaviour in more than one dimension (Topaz and Bertozzi, 2004). The authors use the standard formulation

$$\frac{\partial p(x, t)}{\partial t} + \nabla(V(x, t)p(x, t)) = 0,$$

where the coordinate  $x$  is assumed to be at least two-dimensional. That means  $V(p)$  is a velocity field and is described by the convolution

$$V(p) = \int_{\mathbb{R}^2} k(|x - y|, t)p(y, t)dy = K * p.$$

In a more recent work Topaz et al. consider a density-dependent diffusion (Topaz, Bertozzi, and Lewis, 2006). The corresponding model is therefore more complex. The model equations stays the same, but the description of the velocity is given by:

$$V(p) = V_a(p) + V_d(p),$$

where  $V_a = \frac{Vl}{\alpha} \nabla(K * p)$  describes aggregation and  $V_d = -\frac{Vr}{\alpha^2} p \nabla p$  describes dispersal. Here  $V$  is the attractive movement speed and  $l$  is the sensation radius of the individuals, i.e. inside this radius they can sense other individuals and can react to their behaviour.  $K$  is again the interaction kernel and  $r$  is the ratio from aggregative to repulsive velocity. The original model equation then can be reformulated to

$$\frac{\partial p(x, t)}{\partial t} + \nabla(Vl^{n+1}pK * \nabla p - Vr^{2n+1}p^2 \nabla p) = 0.$$

Many authors also examined the existence and uniqueness of solutions of the above equation formulations. Burger et al. (Burger, Capasso, and Morale, 2006) consider weak and entropy solutions for

$$\begin{aligned}\frac{\partial p(x, t)}{\partial t} &= -\nabla(p(x, t)\nabla(G * p(x, t))) + \Delta a(p(x, t)), \\ (x, t) &\in \mathbb{R}^d \times (0, T] \\ p(x, 0) &= p_0, \quad (x, t) \in \mathbb{R}^d \times \{0\}.\end{aligned}$$

Here  $p(x, t)$  is the population density,  $G$  is the interaction kernel and  $a(u) = \frac{1}{2}p(x, t)|p(x, t)|$ . They show that every entropy solution is also a weak solution and prove existence and uniqueness for this more general formulation.

Finally Fetecau, Huang, and Kolokolnikov, 2011 present a general study on equilibria, stability analysis, well posedness and steady states for the general formulation

$$\begin{aligned}\frac{\partial p(x, t)}{\partial t} + \nabla(pV) &= 0 \\ V(p) &= -\nabla K * p.\end{aligned}$$

Again the population density  $p(x, t)$  is considered and the velocity  $V(p)$  is described by a convolution of a kernel function  $K$  and the population density.

There are some similarities between the swarming approaches but the assumptions concerning the kernel function vary a lot and the corresponding results concerning existence and uniqueness of solutions are dependent on these assumptions. In Chapter 10 we have a more detailed look on this.

The model approaches for animal movement behaviour is as complex as the different movement types themselves. For every simulated species it is challenging to find the approach which fits best to the real movement behaviour.

The foraging behaviour of bats is very specific due to their orientation via echolocation. Bats have a special movement behaviour depending on the corresponding landscape structures. Therefore, it is not possible to simply use a common approach. Hence, we have to build a fitted model for the very complex movement behaviour of bats. Hereby we include some of the above mentioned approaches for simulating specific movement types. In our first approach we present a random walk model with different types of stochastic processes, amongst others a reflected Brownian motion inside two-dimensional



hunting areas (see Chapter 4). Additionally, we present a PDE based model for bat's movement behaviour (see Chapter 6). We compare the results of both models at the end of Chapter 6 and explain the importance of the differences between these models for our special problem formulation.

In a first step we present the relevant assumptions for our model in the next chapter. They are necessary for building a suitable model for simulating bats foraging behaviour and then we point out the relevance for a new fitted model.



## MODEL ASSUMPTIONS

---

When building a mathematical model of a real biological phenomenon it is not possible to reflect every little detail of reality. Instead it is necessary to simplify and choose the most relevant characteristics for the model. In our case it is not possible to consider every characteristic of the real behaviour of the simulated bat species or to reproduce every feature of the landscape area. Therefore, we determine the most essential properties and formulate them as model assumptions, e.g. we define different foraging zones and the position of the roost.

Most of our assumptions are biologically motivated, however, some are necessary for the practical implementation of the model. On one hand some characteristics of the bats' flight behaviour exist which are very complex to implement and require lots of computation time. On the other hand they are not extremely relevant for the resulting movement profile and only have a small effect on the outcome of our model. In such cases, it is necessary to simplify the model, to achieve a balance in between the complexity of the model and the reflection of reality.

### 3.1 BIOLOGICALLY INDUCED ASSUMPTIONS

As mentioned above most of the assumptions are biologically induced. However, we derived them from literature reviews and in cooperation with experienced researchers in this field. We start with these biologically induced assumptions:

#### 1. Female individuals

We only simulate the behaviour of roost colonies. This means we model only the behaviour of female individuals. We assume that the reproduction is never limited by a shortage of male individuals. This is a common assumption in population ecology (Caswell, 2001).

#### 2. Edge structures

We assume that the individuals orientate on landscape structures, e.g. tree lines and hedge rows (Hillen et al., 2011; Kelm et al., 2014; Verboom and Huitema, 2010). They use them to get from a particular point A to another point B in their habitat and for orientating themselves inside the model habitat. These sample paths are defined as lines along the edge structures and lead through the whole habitat. We define sample path  $i$  by

$S_i = \{\overline{S_{i_1} S_{i_2} \dots S_{i_{l_i}}}\}$  for  $i = 1, \dots, I_S$ , where  $l_i$  is the number of points  $S_{i_j}$  which are contained in path  $i$ . Every sample path starts and ends at the roost  $R$ . That means  $S_{i_1} = S_{i_{l_i}} = R$  for all  $i$ . The bat flies along these sample paths. Additionally the bats can change between two or more sample paths at certain crossing points  $S_{i_j}$  which are contained in more than one path. For example they can change between path  $S_j$  and  $S_k$  for  $j \neq k$  at crossing point  $S_{j_5}$  if  $S_{j_5} \in S_j$  and  $\in S_k$ .

### 3. Foraging zones

We assume that the population has preferred foraging zones which they use for hunting and satisfying their water demand. We define these foraging zones as lines (e.g. along forest edges or alleys) or as polygonal structured (e.g. lakes or forests). Let the one-dimensional attraction zones be given by  $P_i$ ,  $i = 1, \dots, I_{\overline{P}}$  and  $P_i$ ,  $i = I_{\overline{P}} + 1, \dots, I_P$  represent the two-dimensional attraction zones.

Furthermore, we assume attraction values  $\rho_{i,j} \in [0, 1]$ , which give us an indication how attractive zone  $i$  is for bat  $j$ .  $\rho_{i,j}$  close to one means a high attraction and  $\rho_{i,j}$  close to zero means almost no attraction. These values differ due to different landscape types (e.g. water bodies, fields, street lights) as well as inside the colony. This means that every individual has different preferences concerning different attraction zones inside the simulated habitat. With these preference values it is possible to make a first step in modelling territorial behaviour. If the preference values differ highly inside the colony they show highly different behaviour characteristics and they hardly meet each other during night. If the values are very similar, the individuals show similar behaviour, i.e. frequent similar paths and similar foraging zones. These values also make it possible to model homogeneous behaviour or very heterogeneous behaviour inside a colony.

### 4. Territorial behaviour

We assume that bats show territorial behaviour adverse other colonies as well as within their own population. This means that they in general use their own hunting areas and only in exceptional cases, they fly to areas frequented by other individuals of their own or other bat colonies. As mentioned above, this is achieved by using different attraction values  $\rho_{ij}$  in our model, such that every attraction zone has a different attraction value for every bat. For large foraging zones it is also possible to simulate a sort of division behaviour. This means that individuals separate this large zone in several smaller hunting zones. This is implemented by a Voronoi separation, which automatically splits an attraction zone in a predefined number  $N_i$  of smaller

zones. Then every smaller zone is related to one or several bats. However, this behaviour is only suitable for several specimens and for large attraction zones.

#### 5. **Maximum flight distance**

We assume a maximal flight distance per night denoted by  $D$  with  $D \geq 0$  for every individual. This should guarantee a realistic flight distance per night and individual. In the roost every bat checks whether it has already reached its flight distance. If that is the case, it stops its activity and stays in the roost for the rest of the night. If the distance is not reached yet, it starts a new flight and continues its activity period. This means that the bat covers a distance  $\bar{D} \geq D$  every night, but  $\bar{D}$  does not exceed  $D$  by far. We have to take this into account by choosing  $D$  in order to obtain a realistic flight distance  $\bar{D}$ .

#### 6. **Wind turbines**

The main purpose of our model is to estimate the danger of existing or planned wind turbines in our model area. We choose  $I_W$  points  $(w_x, w_y)_i \in \mathbb{R}^2, i = 1, \dots, I_W$  in the habitat which represent existing or planned wind turbine locations. The bats may collide with these wind turbines when they exactly fly towards them. However, we also assume that the wind turbine itself presents an attraction for the bats (tallest tree hypothesis (Cryan et al., 2014)). This means that if the bat flies in a pre-defined distance to this wind turbine it also may be attracted by it and therefore, a collision is possible. It is known that bats also tend to fly up and down along the wind turbine because of curiosity (Budenz et al., in press). This increases their risk of being killed by a wind turbine. This effect is not directly covered by our movement model but by a second model. This model describes the behaviour of bats near wind turbines. Hence, it yields an estimate for the number of fatalities caused by every wind turbine.

### 3.2 PRACTICALLY INDUCED ASSUMPTIONS

Unfortunately, we can not reproduce every characteristic of the bats' flight behaviour or every landscape structure. In order to limit the model complexity to a reasonable level we have to make some assumptions that restrict the representation of reality but whose effect on the model outcome is expected to be small, such that the result stays valuable.

#### 1. **Roost**

The first assumption we have to make is to consider just one roost. In reality the local bat population uses several roosts at

the same time and they can vary them very often during their activity period. However, these several roosts are located close to each other, such that the bats use similar landscape structures and hunting zones. This means that practically only the starting and ending point of their activity change.

## 2. **Dimension**

The next practical assumption is associated with the dimension of our model. We only model a two-dimensional behaviour, that means we do not simulate the flight height. For our main goal, calculating the effect of wind turbines, the height of the bats' flight is only of interest if the individuals reach the position of the wind turbine. Furthermore, the flight height of bats near wind turbines is not correlated with the flight height across a field or inside a forest. As each wind turbine itself poses a point of attraction for a bat, the individual would show a different flight behaviour near a wind turbine compared to near other landscape structures. Therefore, we consider the flight height in a second model, already mentioned earlier, which will estimate the number of fatalities for each wind turbine (see Chapter 8).

## 3. **Incomplete model landscape**

We are only able to reproduce an incomplete model landscape. The structures of a real landscape are way too fragmented for our simulation. We have to define a less complex model area in order to be able to deal with an acceptable computing time. Only the relevant structures are represented by the model to guarantee closeness to reality. This means that we predefine edge structures which the bats use for their orientation. We also predefine a fixed number of relevant hunting areas in the habitat and relate preference values to them, already mentioned in this chapter.

As you can see from the assumptions above, bats' movement behaviour is very dependant on the surrounding habitat type. Therefore, it is not possible to use just one model to represent their behaviour. Moreover, we have to combine several mathematical techniques and methods to achieve a realistic model for bat's foraging behaviour.

In the following chapter we will introduce our full individual based model which is constructed to fulfil all the assumptions, defined in this chapter. This model reflects the single trajectories of each individual as well as an occurrence profile of the simulated population.

## FIRST APPROACH: INDIVIDUAL BASED MODEL

---

Our first approach is an individual based model (IBM) which simulates the behaviour of every single animal. Hence, the result of the model generates trajectories which correspond to every simulated individual. That makes it possible to incorporate different preferences and behaviour types inside the colony, e.g. preferred hunting zones, a special visiting order of special places or other behaviour characteristics. The result is a very complex occurrence profile which reproduces every individual behaviour characteristic as wanted by the user. Besides this we have to guarantee a random movement of the animals such that the behaviour is not deterministic or predefined by the program. In this case, the model would be useless. So we have to include enough stochastic parameters which regulate the bats' behaviour in a random way.

A bat's action usually depends on the area it crosses. Therefore, we define three different habitat types: the sample paths, the linear attraction zones and the two-dimensional attraction zones. The one and two-dimensional attraction zones are preferred foraging areas. The linear zones are represented by simple lines, where the bats are hunting along (e.g. a clearing) and the two-dimensional zones are represented by polygons, where the bats are hunting above (e.g. a lake). While the attraction zones are used to hunt in, the sample paths are to be understood as corridors between these areas to get from one foraging zone to another or back to the roost again. These sample paths are often characterised through special landscape structures, based on which the bats orientate themselves (e.g. hedgerows or alleys).

### 4.1 SAMPLE PATH

We assume that bats do not move in a completely random way but, in general, follows certain paths. These paths often follow natural structures such as forest edges, rivers or similar landscape elements. This assumption is based on empirical studies (see e.g. Hillen et al., 2011; Kelm et al., 2014; Verboom and Huitema, 2010). We therefore define many different sample paths. In each flight simulation the bat chooses randomly one sample path. The model also allows switching between the different paths during the flight. The only fixed point which is visited in each flight is the roost  $R \in \mathbb{R}^2$ . This point is defined as the starting and ending point of each activity.

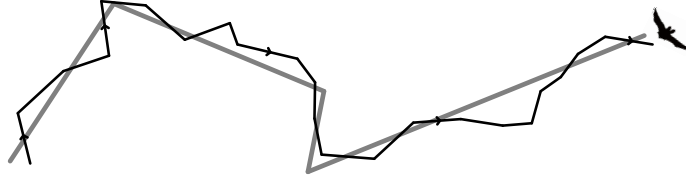


Figure 2: Example for a movement (green line) along a sample path (black line).

In order to make the model more realistic, we add a stochastic term to the sample path coordinate. Consequently, the bat does not follow the path exactly but shows some variance in its flight behaviour, which influences the probability of a bat to spontaneously leave a given sample path (see Figure 2).

We then simulate the behaviour along the sample paths with a stochastic process  $\{X_t\}$ . With Definition 1 we follow for the  $t + 1$ th step over the sample path:

**Definition 5.** *Behaviour over the sample path*

Let  $[t_0, T]$  be the time interval which the bat spends over the sample path, then the position of a bat at time  $t$  is given by

$$\begin{aligned} X_{t+1} &= X_t + h d(X_{t+1}) + \sigma B_t, \quad t = t_0, \dots, T - h, T \\ X_{t_0} &= X_0 \end{aligned}$$

where  $X_t \in \mathbb{R}^2$  is the location of the bat at time  $t$ ,  $X_{t_0}$  is the starting point (in our case the roost),  $d(X_{t+1})$  is the normalized corresponding direction of the sample path and  $h$  is the constant step size.  $B_t \in \mathbb{R}^2$  denotes a two-dimensional Brownian motion and  $\sigma = \begin{pmatrix} \sigma_1 & 0 \\ 0 & \sigma_2 \end{pmatrix}$  is the coefficient matrix which determines the amount of stochastic variation. In our model it is constant and rather small.

**Remark 1.** For  $\sigma_1$  and  $\sigma_2$  near to zero, the bat sticks close to the chosen path. The higher these parameters get, the more the bat tends to leave the sample path. Then the area the bat can visit during one night extends and consequently the danger that the bat reaches a wind turbine that is located near a path. Hence, these constants have a high effect on the occurrence profile of each bat and therefore they also effect the death probability caused by the wind turbines.

#### 4.2 ATTRACTION ZONES

In addition to the sample paths, we define attraction zones which are the preferred foraging areas of the bats. This could typically be a lake, a forest or other habitat structures where the food supply is



high. Another attraction factor is the opportunity to satisfy the water demand. Within these attraction zones the bat flies completely at random. We simulate this behaviour by reflecting the process at the boundaries at the zones. Consequently, the bat can only leave the attraction zone if it has reached the predefined duration of stay.

#### 4.2.1 One-dimensional attraction zone

We usually represent these attraction zones by polygons. In this regard, the one-dimensional attraction zone is an exception. Instead of using a polygonal structure, it is simply represented by a straight line between beginning and ending point,  $F_b = (F_b(1), F_b(2))^T$ ,  $F_e = (F_e(1), F_e(2))^T \in \mathbb{R}^2$ . Examples for this one-dimensional type of attraction zones are forest edges or clearings. We want to simulate the behaviour of the bats inside an attraction zone as a sort of searching behaviour.

For the one-dimensional attraction zone we simulate the behaviour in a similar way as for the sample paths. The only difference is, that we do not let the bat fly along the zone just once, but for several times. Hence, the bat is flying several times along the zone by changing its direction at certain changing points. By choosing these points randomly we guarantee that the bat does not change its direction always at the same point and the simulated behaviour becomes more realistic. We introduce the following definition:

**Definition 6.** *Behaviour over the one-dimensional attraction zone*

*The behaviour over the one-dimensional attraction zone is given by the following stochastic process*

$$X_{t+1} = F_b + \delta_{t+1} d_F + \sigma B_{t+1}, \quad t = t_0, \dots, T.$$

Here  $T - t_0$  represents the amount of time, which the bat spends over the zone,  $\delta_{t+1} \in [0, 1]$  is the step size of time step  $t + 1$  and  $d_F = (F_e(1) - F_b(1), F_e(2) - F_b(2)) \in \mathbb{R}^2$  the direction of the zone, e.g. the direction of the forest edge. Therefore, we do not vary the flight behaviour by a change in the direction but by the step size  $\delta_t$ .  $\sigma = \begin{pmatrix} \sigma_1 & 0 \\ 0 & \sigma_2 \end{pmatrix} \in \mathbb{R}^{2 \times 2}$  is again the coefficients matrix which determines the amount of stochastic variation and  $B_{t+1} \in \mathbb{R}^2$  is a two-dimensional Brownian motion.

**Remark 2.**

*In each time step we choose a convex combination of the beginning and ending point of the zone. That guarantees that the new point is always inside the zone and replaces a reflection rule.*

After the bat has reached the predefined step number of a specific zone, it will continue flying along the sample path which leads to the next attraction zone or back to the roost.

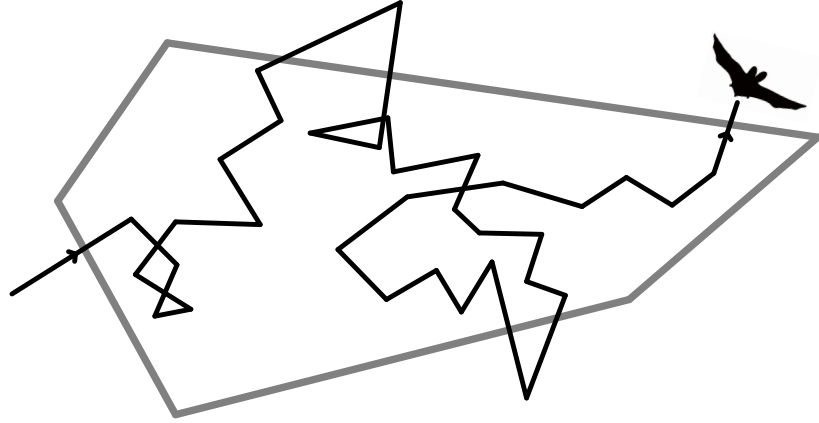


Figure 3: Example for a movement inside a two-dimensional attraction zone.

#### 4.2.2 Two-dimensional attraction zone

In the two-dimensional case, we again want the bat to fly completely random over the zone. If it reaches a boundary we do not want it to leave the zone but to change direction and continue flying over the zone until it has reached the predefined step number (see Figure 3 for an illustration). This behaviour can be described by a two-dimensional reflected Brownian motion (RBM) (see e.g. Kushner and Dupuis, 1992). We therefore introduce the definition of a Brownian motion, which is a special type of stochastic process:

**Definition 7.** *Brownian motion (Karatzas and Shreve, 1991)*

Let  $(\Omega, \mathcal{F}, \mathbb{P})$  be a probability space. Then a Brownian motion is a continuous, adapted process  $B = \{B_t, \mathcal{F}_t, 0 \leq t < \infty\}$  on  $(\Omega, \mathcal{F}, \mathbb{P})$  with the following properties:

- $B_0 = 0$
- the increment  $B_t - B_s$  is independent of  $\mathcal{F}_s$  for  $0 \leq s < t$  and is normally distributed with mean zero and variance  $t - s$ .

Now we define a RBM:

**Definition 8.** *Reflected Brownian Motion (RBM) (Bossy, Gobet, and Talay, 2004)*

A RBM is a Brownian motion inside a domain with reflecting barriers which we describe by the following stochastic process

$$X_t = X_0 + \int_0^t b(X_s) ds + \int_0^t \sigma(X_s) dW_s - \int_0^t \gamma(X_s) d\xi_s, \quad (1)$$

where  $W_s$  is a Brownian motion and  $\xi_t$  only increases for  $X_t \in \partial D$  for the domain  $D$ , such that:  $\xi_t = \int_0^t 1_{\{X_s \in \partial D\}} d\xi_s$ .

**Remark 3.**

The first three terms of Equation 1 describe a simple stochastic process with normal distributed stochastic term. The last term guarantees that the process stays in the predefined domain in the direction of the vector field  $\gamma$ , which we will define later. This can be achieved by reflecting the stochastic process back into the domain, if the process would leave the domain.

**EULER-MARUYAMA SCHEME**

In order to implement the RBM process, it is necessary to discretize Equation 1. In the literature, projected Euler schemes are often used to discretize the problem formulation above (see e.g. Costantini, Pacchiarotti, and F., 1998; Pettersson, 1995; Saisho, 1987; Słomiński, 1994). We present this common discretization scheme in this section.

Therefore, we consider the approach of Costantini et al. (Costantini, Pacchiarotti, and F., 1998) and adapt it to pure reflecting boundary problems.

Let  $D$  be a bounded convex domain in  $\mathbb{R}^2$  and of polygonal structure. Then the boundary of  $D$  is piecewise  $C^1$ . Further let  $b : [0, T] \times \bar{D} \rightarrow \mathbb{R}^2$  and  $\sigma : [0, T] \times \bar{D} \rightarrow \mathbb{R}^{2 \times 2}$  be continuous functions. Then we can define the diffusion process  $X = \{X_t\}_{t_0 \leq t \leq T}$  with coefficients  $b$  and  $\sigma$  which is reflected at the boundaries of  $\bar{D}$ . Therefore let  $n = \{n_t\}_{t_0 \leq t \leq T}$  be a unique stochastic process, such that  $n_t$  is the outward normal vector at site  $X_t \in \partial D \setminus \partial_s D$ , where  $\partial_s D$  the set of points  $x \in \partial D$  where no unique normal vector exists, namely the vertices of the polygon. Further let  $\xi = \{\xi_s\}_{t_0 \leq t \leq T}$  be a stochastic process as well. Then we consider a similar formulation as in Definition 8.

$$X_t = X_0 + \int_{t_0}^t b(s, X_s) ds + \int_{t_0}^t \sigma(s, X_s) dW_s - \int_{t_0}^t n_s d\xi_s, \quad t_0 \leq t \leq T$$

(2)

$$\xi_s = \int_{t_0}^s \mathbb{I}_{\partial D}(X_r) d\xi_r, \quad t_0 \leq t \leq T$$

where  $W$  is a standard Brownian motion.

In the next chapter, we will present a PDE approach for this movement behaviour. Therefore, we mention here the connection of the above RBM process to a Neumann boundary condition problem which Costantini, Pacchiarotti, and F., 1998 present in their paper.

**Remark 4.** *Neumann boundary condition problem*

For  $X_0 = x$ , the expected value of  $X_T$  can be represented as the solution

$u(t, x)$  of the backward partial differential equation with Neumann boundary conditions:

$$\begin{aligned} \frac{\partial u}{\partial t} &= -\frac{1}{2} \sum_{i,j=1}^d a_{ij}(t, x) \frac{\partial^2 u}{\partial x_i \partial x_j}(t, x) - \sum_{i=1}^d b_i(t, x) \frac{\partial u}{\partial x_i}(t, x), \\ t &\in [0, T], x \in D \\ u(T, x) &= f(x), \quad x \in \bar{D} \\ \frac{\partial u}{\partial n}(t, x) &= 0, \quad t \in [0, T], x \in \partial D - \partial_s D \end{aligned}$$

where  $a_{ij} = \sum_{k=1}^d \sigma_{ik}(t, x) \sigma_{jk}(t, x)$ .

We now present a projected Euler scheme to discretize Equation 2. Therefore let  $\{\Delta_{p+1}\eta\}$  be a sequence of i.i.d. random variables which are independent of  $X_0$  and let  $h$  be the chosen step size.

- Let  $t = 0$ ,  $t_p = t_0 + ph$ ,  $X_0^h = X_0$ ,  $\xi_0^h = 0$
- We set

$$\tilde{X}_{t_{p+1}}^h = X_{t_p}^h + hb(t_{p+1}, X_{t_p}^h) + \sqrt{h}\sigma(t_{p+1}, X_{t_p}^h)\Delta_{p+1}\eta.$$

- Then
  - If  $\tilde{X}_{t_{p+1}}^h \notin \bar{D}$

$$\begin{aligned} X_{t_{p+1}}^h &= \pi(\tilde{X}_{t_{p+1}}^h) \\ \xi_{t_{p+1}}^h &= \xi_{t_p}^h + P(\tilde{X}_{t_{p+1}}^h) \end{aligned}$$

Here  $\pi$  denotes the normal projection on  $\bar{D}$ . If a unit outward normal vector exists at  $\pi(w)$ ,  $P$  is given by the distance between  $w$  and its projection  $\pi(w)$ :

$$P(w) = |\pi(w) - w|.$$

- If  $\tilde{X}_{t_{p+1}}^h \in \bar{D}$

$$\begin{aligned} X_{t_{p+1}}^h &= \tilde{X}_{t_{p+1}}^h \\ \xi_{t_{p+1}}^h &= \xi_{t_p}^h \end{aligned}$$

The above scheme converges to the solution of the stochastic process and we can cite the following result:

**Theorem 1.** (Costantini, Pacchiarotti, and F., 1998)

If  $\Delta_{p+1}\eta$  is bounded and furthermore  $u_s$  is a Hölder continuous function of  $s$  of exponent  $1/2$  and  $u_{x_i, x_j}$ ,  $i, j = 1, \dots, d$ , is a Lipschitz continuous function of  $x$ , then it holds for  $h < 1$  that the Euler-Maruyama scheme

converges to the solution of the stochastic process with the convergence rate  $1/2$ :

$$\sup_{t \leq T, x \in \bar{D}} |\mathbb{E}[f(X_t^h, \xi_t^h)] - \mathbb{E}[f(X_T, \xi_T)]| \leq C(T)h^{1/2}$$

for some constant  $C(T)$ , depending only on  $T$ .

Hereby,  $f(X_t^h, \xi_t^h)$  denotes the solution of the discretization and  $f(X_T, \xi_T)$  denotes the solution of the stochastic process.

For the proof of this theorem please see Costantini, Pacchiarotti, and F., 1998.

In addition to the above discretization scheme, we want to look at the symmetrized Euler-Maruyama scheme which was firstly proposed by Bossy et al. (Bossy, Gobet, and Talay, 2004). With this scheme, it is possible to improve the convergence rate. In Figure 4 we illustrate the difference between the two schemes. In the Euler-Maruyama scheme we reflect the process simply on the boundary of the domain. In contrast, the symmetrized Euler-Maruyama scheme projects the point outside the domain not just on the boundary, but it projects the point inside the domain by using the algebraic distance  $F^\gamma$ .

**Remark 5.**  $F^\gamma$

The algebraic distance  $F^\gamma$  parallel to the vectorfield  $\gamma$  of the point outside the domain  $\tilde{x}$  to the boundary is equal to the algebraic distance of the new point  $x$  to the boundary:  $F^\gamma(\tilde{x}) = F^\gamma(x)$ .

Now, we summarize the assumptions of Bossy, Gobet, and Talay, 2004 which we need for the convergence result later:

**Assumption 1.** The boundary  $\partial D$  is bounded and of class  $C^5$ .

**Assumption 2.** The unit vector field  $\gamma$  is of class  $C^4$  and there exists a  $p_0 > 0$  such that  $\gamma(s)n(s) \geq p_0$ ,  $\forall s \in \partial D$

**Assumption 3.** The functions  $b$  and  $\sigma$  are  $C_b^4(\bar{D}, \mathbb{R}^d)$  and  $C_b^4(\bar{D}, \mathbb{R}^d \otimes \mathbb{R}^d)$  functions.

**Assumption 4.** The matrix  $\sigma\sigma^T$  is uniformly elliptic:  $\forall x \in \bar{D}$  holds  $\sigma\sigma^T(x) \geq \sigma_0^2 \mathbb{I}_{\mathbb{R}^d} \otimes \mathbb{I}_{\mathbb{R}^d}$  for some  $\sigma_0 > 0$ .

Further let  $\{W_t\}_{t \geq 0}$  be a two-dimensional Brownian motion. Again, we want to discretize the RBM

$$X_t = x + \int_0^t b(X_s) ds + \int_0^t \sigma(X_s) dW_s - \int_0^t \gamma(X_s) d\xi_s$$

where

$$\xi_t = \int_0^t \mathbb{1}_{\{X_s \in \partial D\}} d\xi_s$$

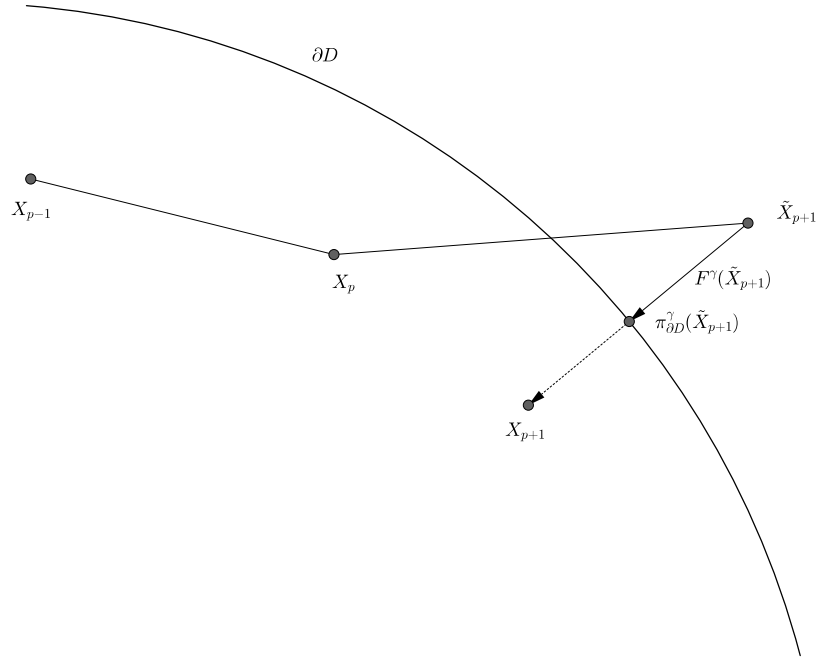


Figure 4: Reflection scheme of the Euler-Maruyama (solid line) and the symmetrized Euler-Maruyama method (dashed line) .

denotes the process which only increases if  $x \in \partial D$ .

We now present the symmetrized Euler scheme. Let again  $h$  be the step size.

- For  $X_0^h = X_0$ ,  $t_p = t_0 + ph$  we set

$$\tilde{X}_{t_{p+1}}^h = X_{t_p}^h + b(X_{t_p}^h)h + \sigma(X_{t_p}^h)(\Delta W_p)$$

- Then

- if  $\tilde{X}_{t_{p+1}}^h \notin \bar{D}$ , we set

$$X_{t_{p+1}}^h = \pi_{\partial D}^\gamma(\tilde{X}_{t_{p+1}}^h) + F^\gamma(\tilde{X}_{t_{p+1}}^h)\gamma(\tilde{X}_{t_{p+1}}^h)$$

for  $F^\gamma \in \mathbb{R}$  the algebraic distance of  $x$  to  $\partial D$  parallel to  $\gamma$  and  $\pi_{\partial D}^\gamma(x)$  the projection of  $x$  onto  $\partial D$  parallel to  $\gamma$ .

- if  $\tilde{X}_{t_{p+1}}^h \in \bar{D}$ , we set

$$X_{t_{p+1}}^h = \tilde{X}_{t_{p+1}}^h$$

- Overall, we obtain

$$X_{t_{p+1}}^h = \tilde{X}_{t_{p+1}}^h + 2[F^\gamma(\tilde{X}_{t_{p+1}}^h)]^+\gamma(\tilde{X}_{t_{p+1}}^h)$$

Bossy, Gobet, and Talay, 2004 derive a convergence result for the above scheme. Therefore, we need one additional assumption:

**Assumption 5.** *The function  $f$  is of class  $C_b^5(\bar{D}, \mathbb{R})$  and satisfies the compatibility condition on  $\partial D$ :  $\forall z \in \partial D$  it holds  $[\nabla f \gamma](z) = [\nabla(Lf)\gamma](z) = 0$ .*

Furthermore, we set  $\|f\|^{(5)} = \sum_{\alpha: |\alpha| \leq 5} \|\partial_x^\alpha f\|_\infty$  for  $f \in C_b^5(\bar{D}, \mathbb{R})$ . This discretization scheme improves the convergence rate towards the solution of the Neumann boundary condition problem:

**Theorem 2.** *Bossy, Gobet, and Talay, 2004*

*Under the above described Assumptions 1-5 holds:*

$$|\mathbb{E}(f(X_T^h)) - \mathbb{E}(f(X_T))| \leq K(T) \|f^{(5)}\| h$$

for some constant  $K(T)$  uniformly in  $x$  and a sufficient function  $f$ . Hereby  $X_T^h$  denotes the solution of the symmetrized discretization scheme and  $X_T$  denotes the solution of the stochastic process.

For the proof of this theorem see (Bossy, Gobet, and Talay, 2004).

#### APPLICATION TO OUR MODEL FORMULATION

We want to use the discretization scheme of Bossy, Gobet, and Talay, 2004 for the two-dimensional case due to its better convergence properties. We adjust the above described scheme by leaving out the drift term, because we want the bat to fly completely randomly over the attraction zone without any preferences towards special parts of the zone. This means that we consider the adjusted SDE

$$X_t = X_0 + \int_0^t \sigma(X_s) dW_s - \int_0^t \gamma(X_s) d\xi_s.$$

Furthermore, we set  $\gamma = n$  such that the reflection direction is always the unit outward normal vector  $n$ . This is biologically induced, because if the bat leaves the zone and notices it, it would fly on the shortest way back to the zone in order to save energy costs. That makes the normal vector the best choice for the reflection vector field. We define the attraction zone  $K$  as a random convex polygon in  $\mathbb{R}^2$ . Then  $X_0 \in K$  is the point where the bat enters the polygon  $K$ . This point is the starting point for the following simulation. The bat flies for a predefined number of time steps over the attraction zone. This happens in a random way until a step tends to leave the zone  $K$ . Then the bat is reflected back to the zone parallel to the unit outward normal vector  $n$ .

The adapted symmetrized Euler-Maruyama scheme is defined as follows:

- Again we start at the point  $X_0$ .

- We discretize the time interval  $[0, T]$  with time step  $h = \frac{T}{N}$ . For a better understanding, we set  $X_{t_p} = X_p$  with  $t_p = t_0 + ph$  again.
- Then for the  $t + 1$ st step we calculate the following approximation:

$$\tilde{X}_{p+1} = X_p + \sigma(X_p)\Delta W_p$$

- We check whether  $\tilde{X}_{p+1}$  is in our polygon:
  - if  $\tilde{X}_p \notin \bar{K}$ , we set

$$X_{p+1} = \pi_{\partial D}^n(\tilde{X}_{p+1}) - F^n(\tilde{X}_{p+1})n(\tilde{X}_{p+1})$$

where  $F^n \in \mathbb{R}(x)$  denotes the algebraic distance of the point  $x \in \mathbb{R}^2$  to the point  $\pi_{\partial K}^n(x)$  with  $\pi_{\partial K}^n(x)$  being the projection of  $x$  onto  $\partial K$  parallel to the vector  $n$ . Again we set  $n(x) = n(\pi_{\partial K}^n(x))$  for points in a surrounding of  $D$ . Of course we have to restrict this to the parts of  $\partial K$  where the normal vector is defined. For all other points, we set projection  $\pi_{\partial K}^n(x) = V$  where  $V$  denotes the closest vertex of the polygon.

- if  $\tilde{X}_p \in \bar{K}$ , we set

$$X_{p+1} = \tilde{X}_{p+1}$$

- Overall we obtain

$$X_{p+1} = X_p + \sigma(X_p)\Delta W_p - 2[F^n(\tilde{X}_{p+1})]^+ n(\tilde{X}_{p+1}).$$

Whether the bat ends its activity after arriving at the roost or whether it starts a new flight is determined by the number of path points that were already visited. For reasons of practicability, we define a maximum amount of steps which can be seen as an equivalent of the maximum time of a bat's activity per night. If the bat has already covered this number, it finishes the activity. If not, it starts a new flight. The steps that the bat covers within the attraction zones are of course added to the total number. On the one hand, this number acts as an indicator for the distance the bat has already covered and thus for the effort it has already taken; on the other hand, it also represents the foraging success of the night, because usually a large portion of path points are located within the attraction zones which supply a high amount of prey.

We want to verify whether we can fulfil the Assumptions 1-5 for the convergence result.

- Assumption 1:  
We want to assume the two-dimensional attraction zones as



polygonally structured. Unfortunately, this is a contradiction to assumption 1. We refer to the work of Costantini, Pacchiarotti, and F., 1998, who were able to show convergence for polygons as well. Although we have not shown the result of Bossy, Gobet, and Talay, 2004 for polygonal structures domains we are optimistic, that it is possible to combine the two approaches and to obtain a good convergence results for the symmetrized Euler-Maruyama scheme for polygons as well.

- Assumption 2:  
We set the vectorfield  $\gamma$  equal to the outward normal vector field  $n$ . Therefore, it holds  $n(s)n(s) \geq 0 \forall s \in \partial D$  and  $n(s)n(s) = 0 \Leftrightarrow n(s) = 0$ .
- Assumption 3:  
In our case  $b = 0$  and  $\sigma = (\sigma_1, \sigma_2)$  is constant, so assumption 3 is fulfilled.
- Assumption 4:  
Since we set the constant parameters  $\sigma_1 > 0$  and  $\sigma_2 > 0$  we can find  $\sigma_0 > 0$  such that

$$\sigma\sigma^T = \begin{pmatrix} \sigma_1^2 & \sigma_1\sigma_2 \\ \sigma_1\sigma_2 & \sigma_2^2 \end{pmatrix} \geq \begin{pmatrix} \sigma_0^2 & \sigma_0^2 \\ \sigma_0^2 & \sigma_0^2 \end{pmatrix}$$

is fulfilled.

- Assumption 5:  
We can chose the function  $f$  in the way, that assumption 5 is fulfilled as well.

We only have a contradiction to assumption 1. However, we remember the approach of Costantini, Pacchiarotti, and F., 1998. There, they have shown a convergence result for a piecewise  $C^1$  domain. It may be possible to show the improved convergence result of Bossy, Gobet, and Talay, 2004 for piecewise  $C^1$  domains as well. Nevertheless, we leave this open for further research and have a closer look on other special behaviour characteristics of bats.

#### 4.3 VORONOI DIAGRAM

In our model, we include the opportunity of simulating territorial behaviour by different preference values. However, we want to include a second possibility into the model for simulating this kind of behaviour inside the colony. The bats therefore prefer regions of the habitat especially inside attraction zones that are not occupied by other members of their population or which are only frequented by a few other bats. Depending on the bat species, this territorial

behaviour is more or less adopted. We achieve this territorial behaviour for small zones by using highly different preference values. For large attraction zones it is possible to divide them into several smaller zones, such that the different individuals can occupy these smaller zones. Hence, we have to divide several attraction zones into different subregions to define the territories of the different individuals.

We do not want to define every subregion manually because this would produce a very high effort for every large attraction zone. Instead of defining every subpolygon, we only define center points and build the subregions by using Voronoi diagrams. This method is used to split regions into a predefined number of subregions. Usually it is used for open domains so we have to adjust the general method for our purpose.

We now explain the different steps of the Voronoi separation for a polygon  $K \in \mathbb{R}^2$ :

- We start by choosing  $N - l$  random points  $C_i, i = 1, \dots, N - l$  inside the attraction zone  $K$ . These are called center points. Here  $N$  is the number of simulated bats and  $0 \leq l \leq N$ . So  $N - l$  is the number of bats that are supposed to fly to the attraction zone or the necessary number of subpolygons respectively.
- The chosen points  $C_i$  then define the center points of the subpolygons inside the Voronoi diagram. We use the euclidean metric. That means the Voronoi separation decides for every point inside the large zone which center point is the nearest. Consequently, every point  $x \in K$  is connected to the center point  $C_i$ , such that  $\text{dist}(x, C_i) \leq \text{dist}(x, C_j) \forall j = 1, \dots, N - l, j \neq i$ . The points which are equally distanced to more than one center point form the boundaries of the new subpolygons  $\bar{V}_i, i = 1, \dots, N - l$ .
- In general, the Voronoi separation is used for open domains. It does not consider the boundaries of the large polygon. Therefore, we have to take the intersections of the Voronoi polygons and the boundaries of the attraction zone to get our wanted subpolygons  $V_i = \bar{V}_i \cap K$ .
- In a last step, we choose a random order of polygons and relate to each polygon  $V_i$  one or several bats which are supposed to fly to this subpolygon. For simulating the territorial behaviour, we decrease the attraction value  $a_i$  of the subpolygon  $V_i$  by multiplying it with a factor  $r \ll 1$  for every other individual. For every new bat that flies to the same zone the attraction value is further reduced. This means that for  $m$  bats flying to zone  $i$ , the attraction value of this zone is  $r^m a$ . This value tends to zero for increasing  $m$  and  $r < 1$ . Therefore, it is unlikely that many bats fly to the same subpolygon which is exactly the territorial behaviour we want to simulate.
- Now every bat that is used to fly to the large zone, enters it and moves by a biased random walk to its own subregion. When the predefined amount of time over the attraction zone is reached, it leaves the zone again by a biased random walk. Thereby,

the behaviour over the subpolygons is simulated as in the non-Voronoi case. So the behaviour over the subpolygon is comparable to a zone without any separation.

**Remark 6.** *This Voronoi separation is possible for every two-dimensional attraction zone but only meaningful for those that are large enough for such a separation. This means that it has to be biologically induced either by the behaviour type of the simulated bat species or by a very high food supply.*

For an illustration of the implementation of the Voronoi separation of an arbitrary two-dimensional polygon see Figure 5. There we can see the separation of one large polygon into seven subpolygons with randomly chosen center points. The behaviour of the bats inside a zone with a Voronoi separation is shown in the numerical results of this chapter.

#### 4.4 ALGORITHM

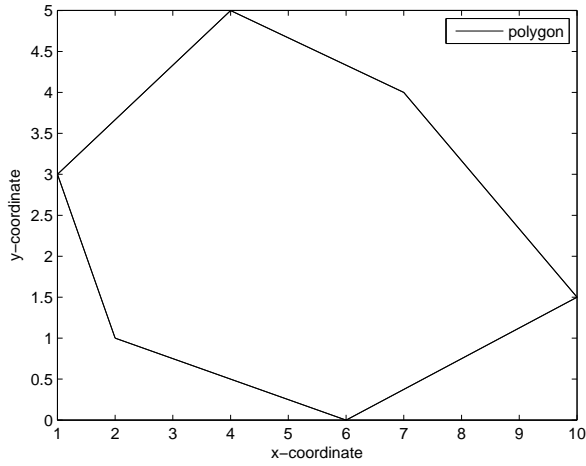
The program for our IBM is very complex and includes many subroutines. Hence, it is not meaningful to show the complete program code in detail in this thesis. For getting a better overview of the main steps we forgo having a detailed description and only present in Algorithm 1 a simplified version with the main steps of our algorithm.

---

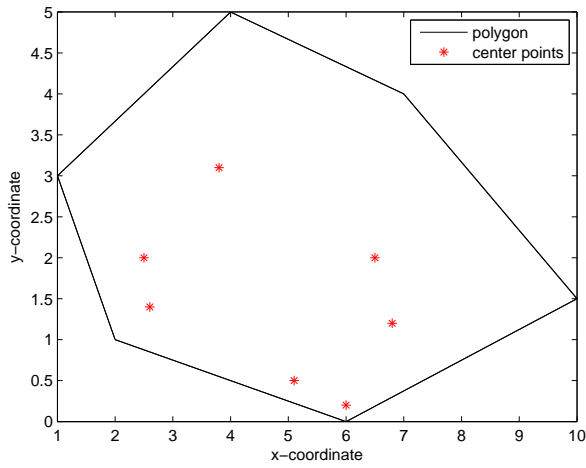
#### Algorithm 1 Pseudocode for IBM

---

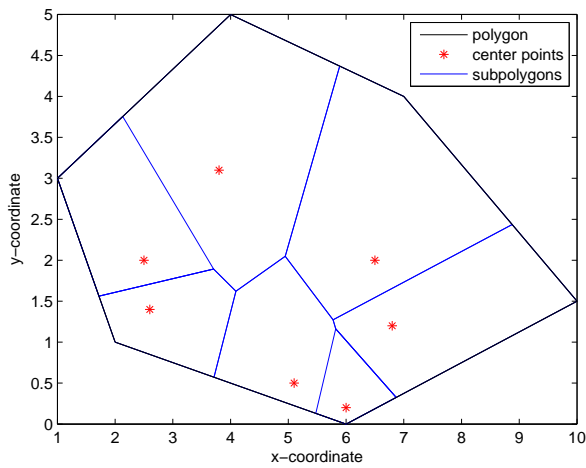
- 1: By using the preference values  $\rho_{i,j}$ , the program chooses the attraction zones which the bat should visit for this flight and defines the visit order randomly.
  - 2: The bat starts in the roost and chooses the sample path that leads to the first attraction zone  $P_1$ .
  - 3: **while** The maximum flight distance is not reached **do**
  - 4:     **while** The bat has not reached all chosen attraction zones **do**
  - 5:         It follows the current sample path  $S_i$ .
  - 6:         **if** It reaches a crossing of two or more sample paths **then**
  - 7:             It chooses the sample path that leads to the wanted attraction zone.
  - 8:         **end if**
  - 9:         **if** It reaches an attraction zone **then**
  - 10:             It spends the defined time on flying above the attraction zone or on its Voronoi section respectively. Then it leaves the zone and chooses the sample path that leads to the next attraction zone.
  - 11:         **end if**
  - 12:     **end while**
  - 13:     It flies to the roost (randomly or on the shortest way).
  - 14: **end while**
-



(a) Polygon



(b) Polygon with randomly chosen center points



(c) Polygon with center points and the corresponding Voronoi-separation

Figure 5: Voronoi separation scheme. We defined the large polygon Figure 5a and the 7 center points Figure 5b. Then the Voronoi theory gives us the separation of the large polygon into 7 subpolygons Figure 5c.

## 4.5 MONTE-CARLO SIMULATION

In the previous sections we have built a model to simulate single trajectories of each individual bat. This is meaningful to get an idea of how our model simulates the night activity of a single bat and to generate trajectories of single individuals. In Chapter 7 we want to fit this model to a real data set in order to choose the right parameters for the model. However, because of the high number of stochastic variables in the program, e.g. the random choice of paths, the random choice of zones and the random order of attraction zones, the generated trajectories have different occurrence probabilities. This means that if we look at one trajectory it is possible that the considered bat would fly this trajectory only once in a lifetime and if we consider this trajectory as possible as every other trajectory we would make a big error in evaluating dangerous positions for wind turbines. Hence, we have to generate an average behaviour of the bat population to estimate each trajectory in the right way and to avoid under- or over-estimation of certain trajectories.

For generating an average occurrence map of the considered habitat  $D \in \mathbb{R}^2$ , we include a Monte-Carlo simulation into our program. Therefore, we divide the habitat into a grid with rectangular subregions  $A_i$ ,  $i = 1, \dots, I$  such that:

$$D = \bigcup_{i=1}^I A_i$$

and repeat the simulation  $M$  times. Each time our process  $\{X_t^m\}_{t=1}^{T_m}$  crosses a grid point, the pass is counted by the characteristic function  $\chi_{A_i}$ . Thereby,  $X_t^m$  denotes the position of the process at time point  $t$  in simulation  $m$  and the number of time steps  $T_m$  is dependent on simulation  $m$ . By normalising these numbers, we obtain a density profile of the bats' occurrence probability. Hence, we sum up all simulations and all time points and divide the sums by the number of simulations  $M$  and the number of time points  $T_m$  respectively and we obtain the corresponding two-dimensional occurrence profile

$$p_{MC}(x, y) = \frac{1}{M} \sum_{m=1}^M \frac{1}{T_m} \sum_{t=1}^{T_m} \chi_{A_i}(X_t^m).$$

This function gives us the average flight behaviour of the bat and shows how intensely each bat visits specific areas in the concerning habitat. Therefore,  $p_{MC}$  can be interpreted as a kind of density distribution function that describes the activity of the simulated bat population. Hence, we obtain an average occurrence indicator for every position in the habitat and therefore an indicator for the danger of every position of a potential or existing wind turbine.

It is well known that the Monte-Carlo simulation converges with a factor of  $\mathcal{O}(1/\sqrt{M})$  where  $M$  is the number of simulations. Hence, a very high number of simulations is necessary in order to obtain a valuable result. Therefore, the method evokes a high computational effort.

#### 4.6 NUMERICAL RESULTS

We now present the numerical results of this first approach and the Monte-Carlo simulation. Therefore, we implement a model landscape, where we present every landscape structure we described above: roost, sample paths, one- and two-dimensional attraction zones. We show different behaviour types by simulating two individuals with different preferences. Further more we present the effect of the variance parameter to the flight behaviour.

After the results of the IBM we show the results of the Monte-Carlo simulation. Again we show the differences between single individuals with different preferences.

Figure 6 shows our model area which we use for illustrating the

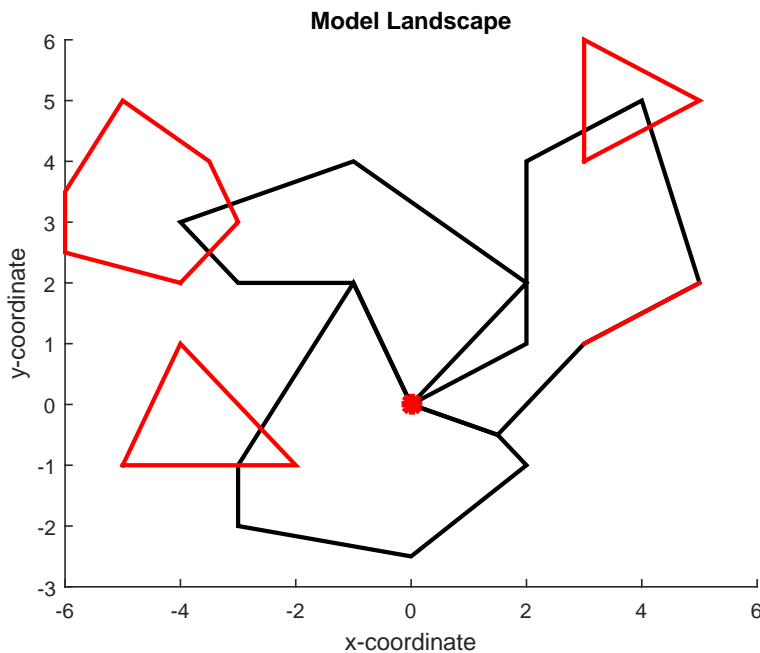
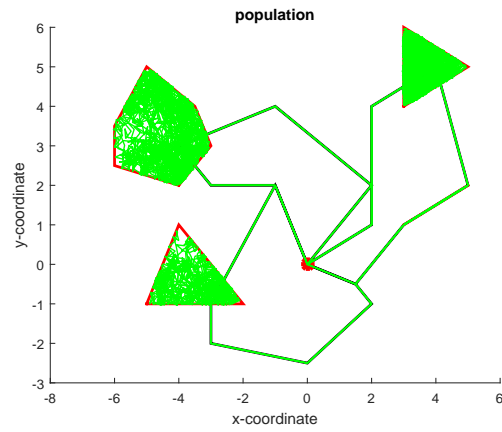


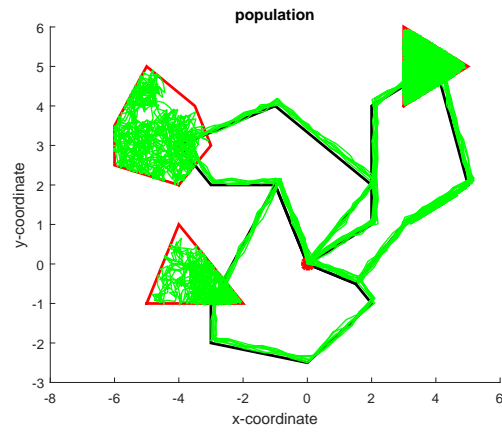
Figure 6: Model area

model results. The map contains the defined sample paths (black lines), the one-dimensional attraction zone (red line) and the two-dimensional attraction zones (three red polygons) and the roost (set in  $(0,0)$ , red dot).

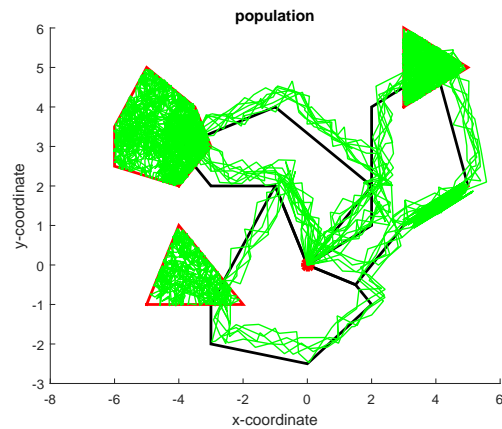
In Figure 7 the behaviour of several simulated individuals ( $N_{ind} = 4$ )



(a) IBM for four individuals with variance parameter  $\sigma_1 = \sigma_2 = 0$ .



(b) IBM for four individuals with variance parameter  $\sigma_1 = \sigma_2 = 0.2$ .



(c) IBM for four individuals with variance parameter  $\sigma_1 = \sigma_2 = 0.7$ .

Figure 7: Behaviour for four individuals with different variance parameters.



is illustrated. In the first picture (Figure 7a), the variance coefficient is equal to zero. This means that all individuals stick close to the paths. In the second picture (Figure 7b) the individuals tend to leave the path and fly in larger distance to it and in the last one (Figure 7c) the individuals leave the path and fly in a very large distance to it. The larger the variance parameter gets, the more landscape is covered by the simulated bats. Hence, this variance parameters have to be set carefully, because the effect on the visit probabilities of special areas is very high.

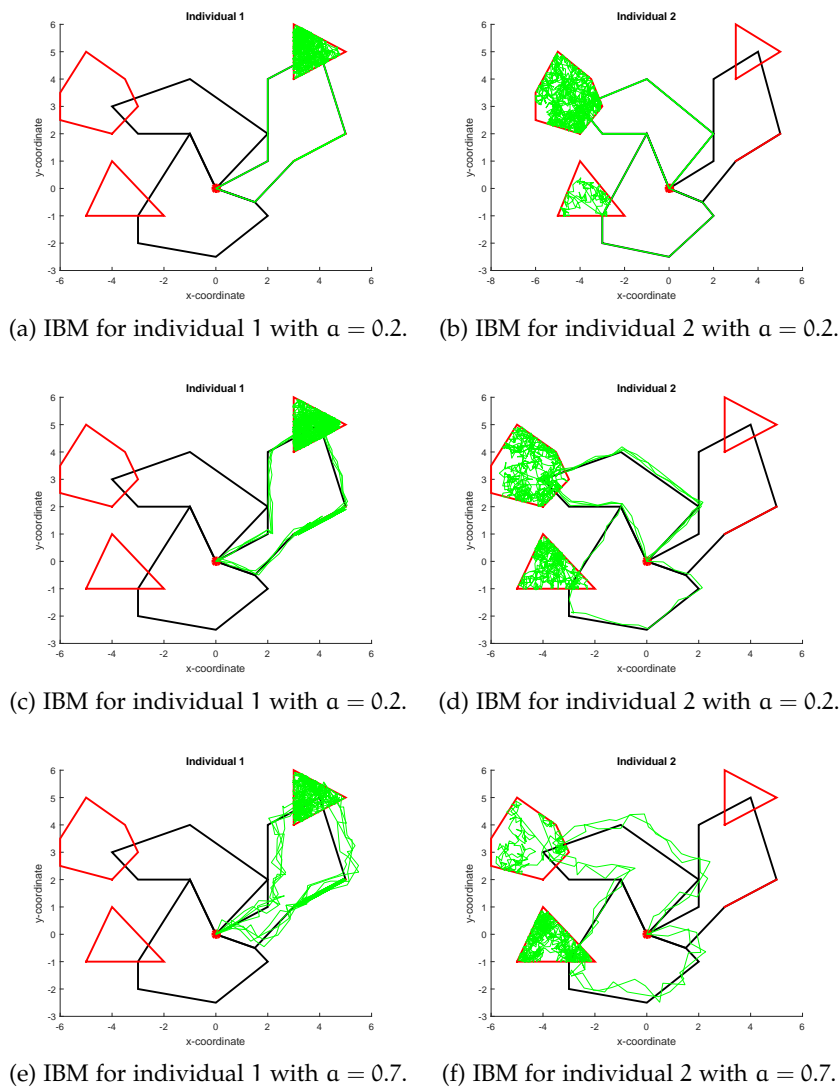


Figure 8: Two individuals with different preferences and three different variance parameters.

Figure 8 shows the different behaviours of two individuals with different preference values. Again, we show the resulting movement

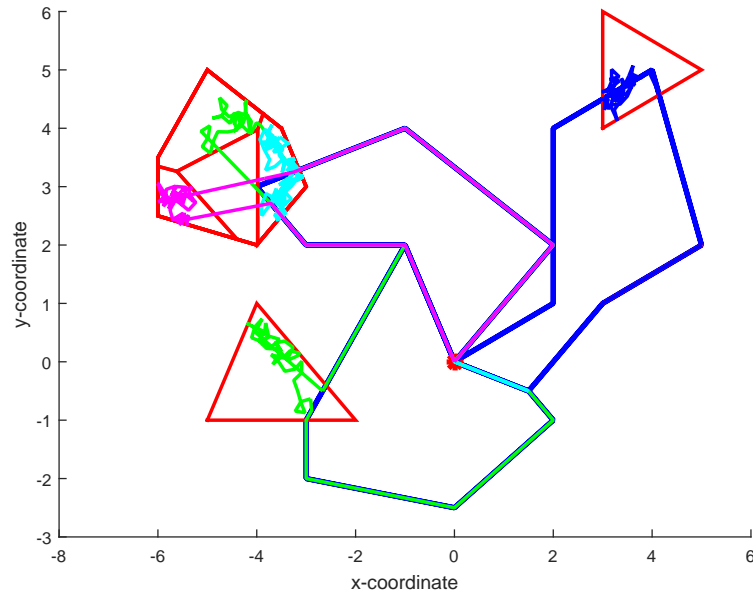


Figure 9: Effect of a Voronoi separation of a zone.

behaviours for three different variance parameters  $\alpha = 0$  (Figure 8a, Figure 8b),  $\alpha = 0.2$  (Figure 8c, Figure 8d) and  $\alpha = 0.7$  (Figure 8e, Figure 8f). The pictures on the left side show an individual preferring a path on the right side of the habitat whereas the individual simulated in the pictures on the right side prefers to fly to the left side and the centre of the habitat. This is the numerical implementation of territorial behaviour inside the colony and can be fitted to the behaviour of the considered bat species.

Figure 9 shows the effect of a Voronoi separation of one large priority zone. The zone is divided in four subzones, three of them are frequented by one bat each, which is illustrated by different colours. This model property is useful to generate territorial behaviour as well. Again, this has to be fitted to the behaviour characteristics of the local bat colony.

The results of the Monte-Carlo simulation for  $M = 10000$  show the average number of passes per flight event of one individual in one round (see Figure 11) and the accumulated behaviour for four individuals (see Figure 10). In all pictures the sample paths, the attraction zones, the edge of the forest and the roost are clearly silhouetted against the sections which are not passed by the bats' flight. The sample paths are not as highly frequented as for example the one-dimensional attraction zone because the bat uses them only as a corridor to get from one foraging area to another but not for foraging itself.

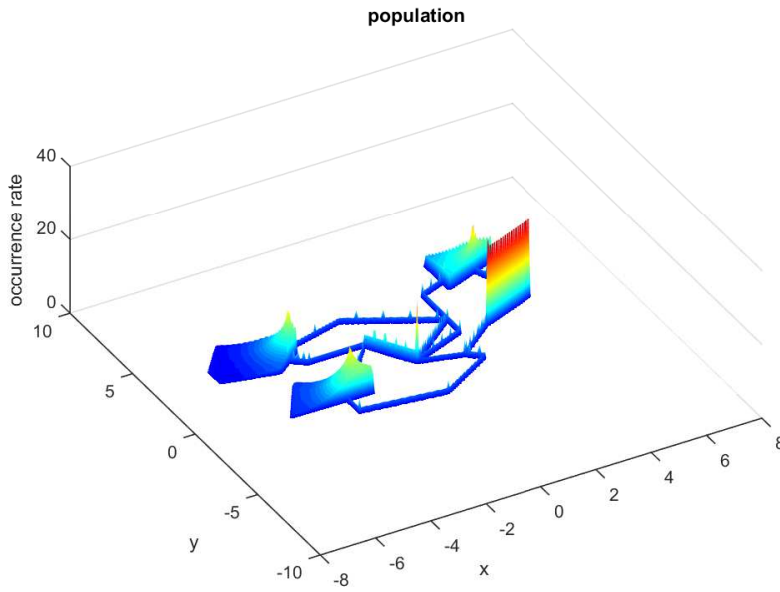
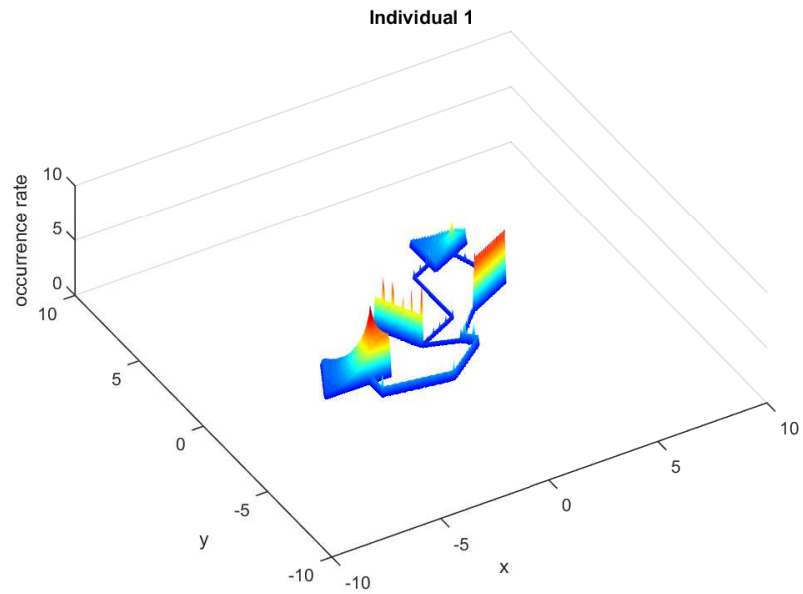
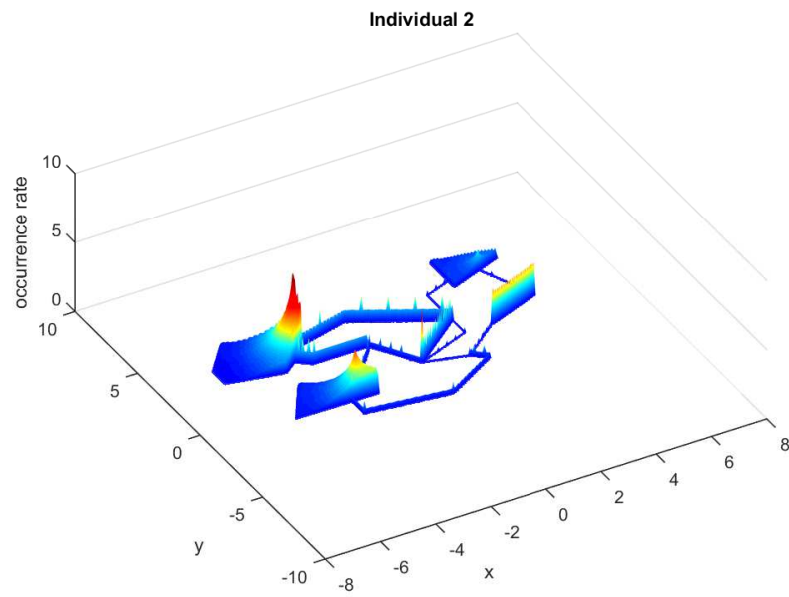


Figure 10: Monte-Carlo simulation for four individuals and  $M = 10000$ .

In Figure 11 we can again observe different preferences of two individuals. It is obvious that the individuals frequent different paths and attraction zones as in the result of the IBM. In Figure 11a, the individual frequents not all paths but mainly the paths and attraction zones on the right side of the habitat. In Figure 11b, the individual frequents all paths and all attraction zones, but mainly on zone on the left side of the habitat.



(a) MCS for individual 1



(b) MCS for individual 2

Figure 11: Monte-Carlo simulation for two individuals with different preferences and  $M = 10000$ .

## APPLICATION

The numerical results in the last chapter represent the behaviour of a bat in an artificial landscape. In this chapter, we want to illustrate the result of the individual based model for a real landscape example. Therefore, we choose the village Lettweiler in Rhineland-Palatinate. This village is suitable for our purpose as a colony of common pipistrelle (*Pipistrellus pipistrellus*) has several nursery colonies around the village. Additionally, C. Lindemann does her research within her PhD in this village and she makes her data available for us. Hence, we can implement the model area and can illustrate a first result of the program for a realistic landscape structure.

In the following figures we can see the behaviour for different

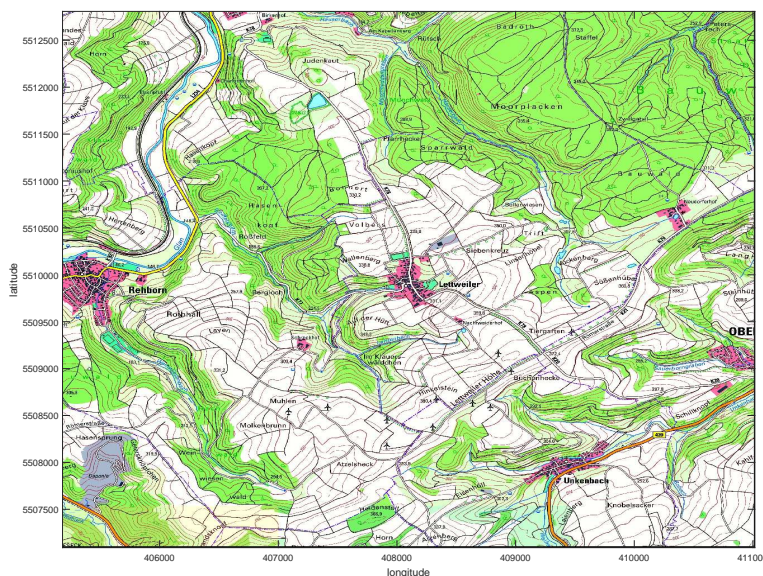


Figure 12: Example for a pipistrelle habitat

parameter settings which correspond to different behaviour characteristics. We have to admit that these results are only a first attempt of implementing a real landscape area and the results have to be fitted to real empirical data sets in the future. However, these results give a good idea of how the program works and how it can be used in future applications.

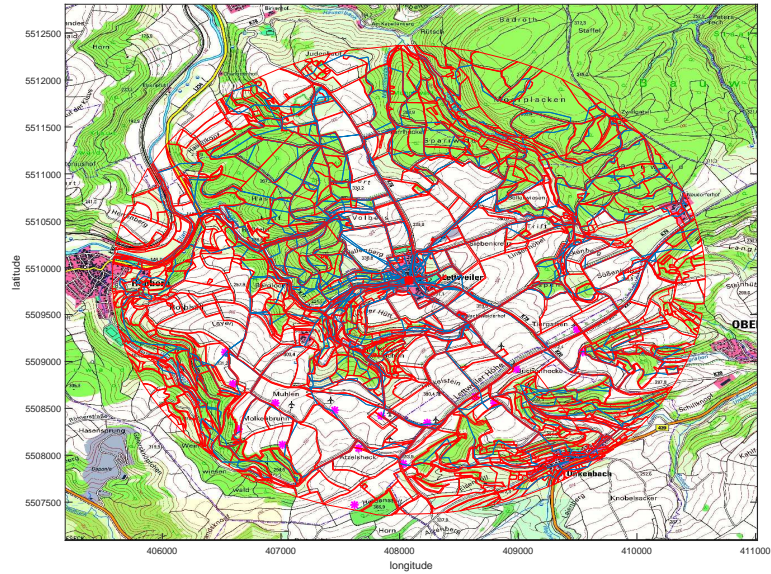


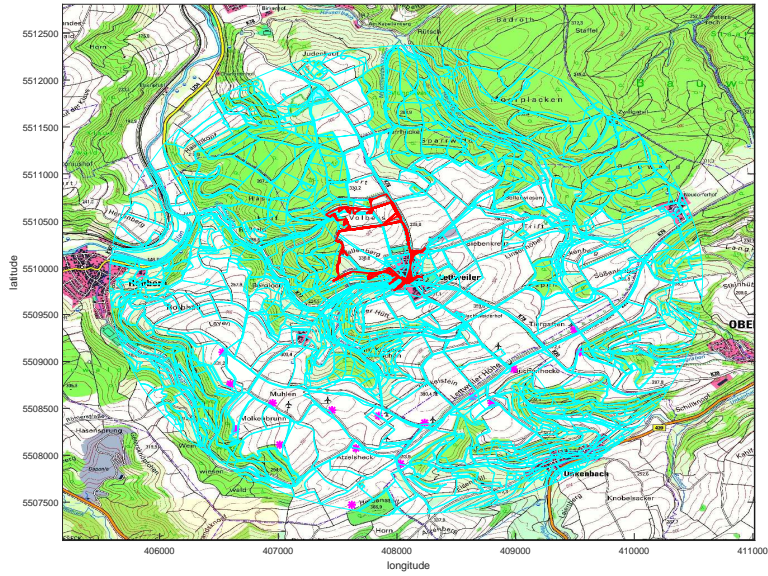
Figure 13: Habitat example with sample paths (blue lines), attraction zones (red lines), a roost (red dot) and several wind turbine locations (magenta dots).

In Figure 12 we present the habitat example which is the area around the village Lettweiler. There are many different landscape structures around the village, e.g. water bodies, rivers, forest patches as well as cultivated areas. C. Lindemann implemented 30 sample paths, 5263 one-dimensional attraction zones and 1055 two-dimensional attraction zones, which are illustrated in Figure 13. The paths are represented by blue lines, the attraction zones by red lines and the roost is the red dot in the middle of the map. The magenta dots represent 16 locations of wind turbines.

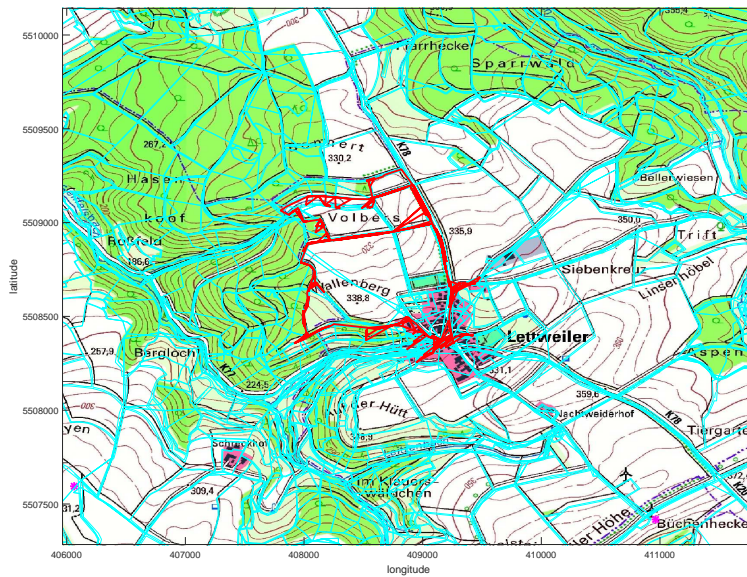
However, we change the colour scheme in the next illustrations to improve the visibility of the bat's trajectories. We represent the attraction zones and the sample paths by cyan lines. The simulated trajectories of the bats are now represented by red lines. In Figure 14, the behaviour of one bat is illustrated and in Figure 14b the trajectory is shown in detail. It is easy to see that the individual follows certain sample paths, but also frequents some zones around the sample paths.

In Figure 15, we show the flight behaviour of four different individuals during one night.

In order to illustrate the effect of different preferences, we show in Figure 16 the behaviour of two individuals which frequent different



(a)



(b) Detail of Figure 14a

Figure 14: Behaviour of one bat for  $\sigma = 0.1$ .

parts of the habitat. In Figure 16a, the individual mainly frequents the northern part of the habitat and in Figure 16b, the individual tends to fly to the eastern part of the habitat.

In Figure 17 - Figure 19, we illustrate the effect of the variance pa-

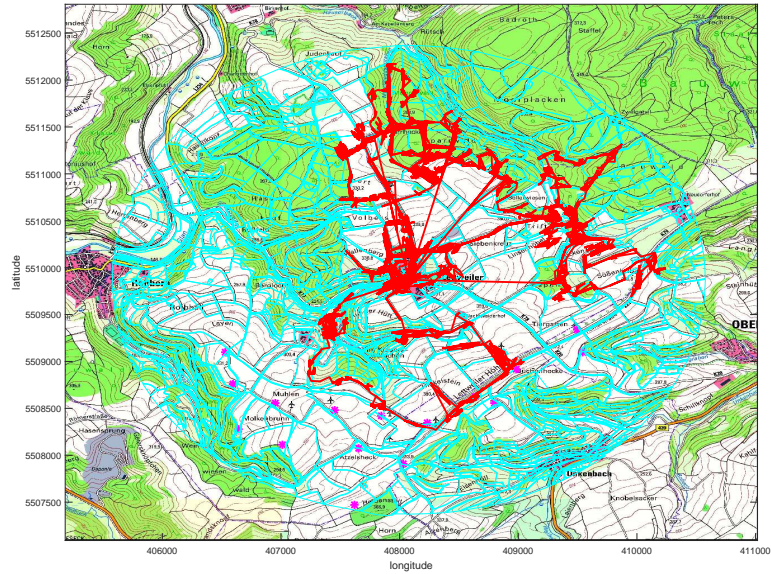
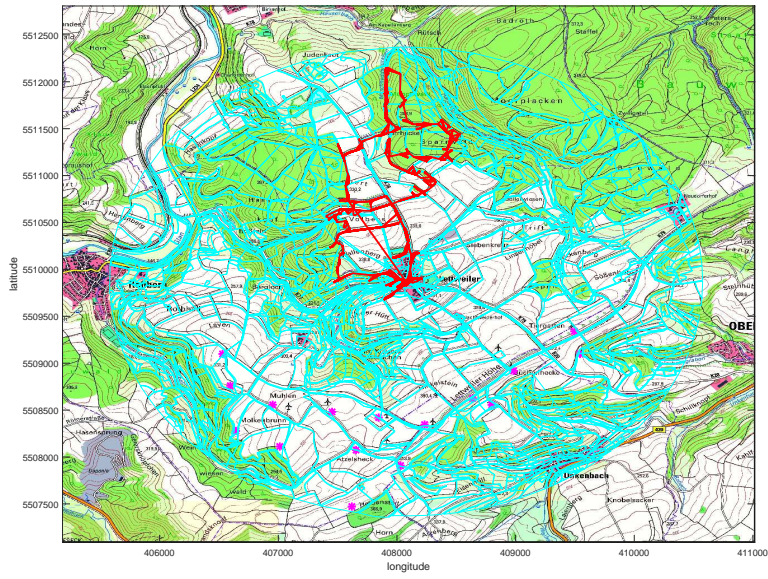


Figure 15: Behaviour of four bats for  $\sigma = 0$ .

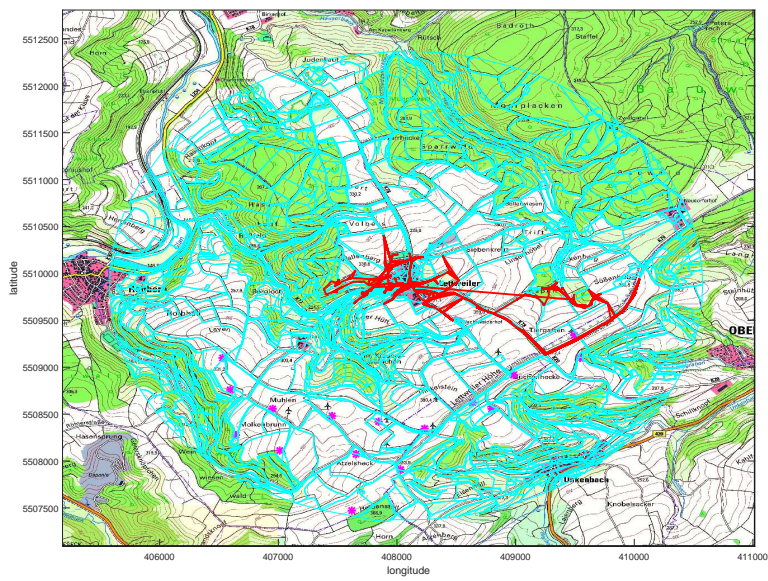
parameter on the trajectories of an individual. Therefore we change the variance parameter from 2 to 5 to 7 and show the resulting flight trajectories. In the detail pictures it becomes obvious how the variance parameter affects the flight behaviour. The larger the variance parameter gets, the more the bat stays around the roost. For a smaller variance parameter the bat tends to fly a higher distance to the roost but on a more direct way.

As mentioned above several parameters have to be fitted in order to get a realistic result. One of them is the flight distance  $D$ . We have to analyse the trajectories of the program and compare them with the empirical data sets of C. Lindemann. With the fitted parameters, it will be possible to generate artificial bat trajectories and use them for several research purposes.



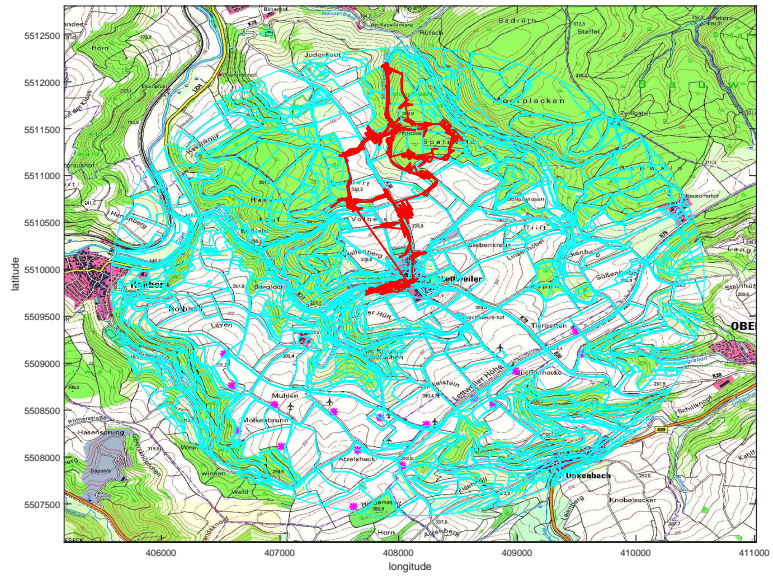


(a) Behaviour of one bat for  $\sigma = 0$ , which tends more to the north of the habitat

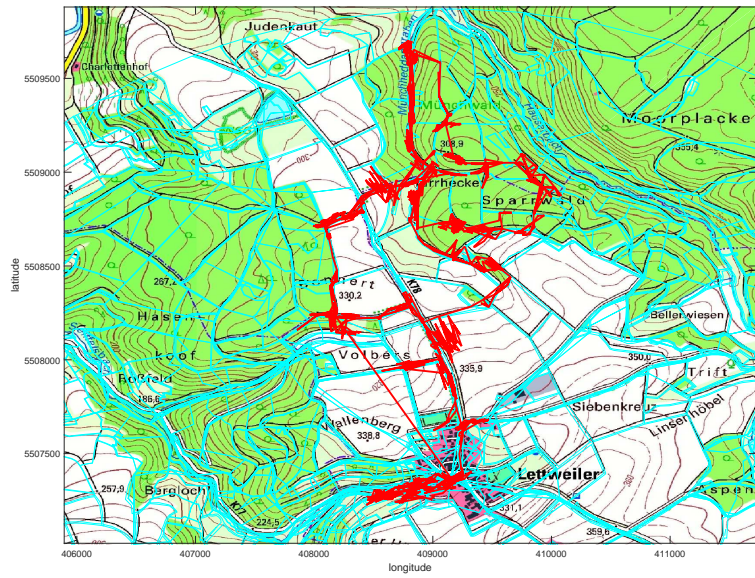


(b) Behaviour of one bat for  $\sigma = 0$ , which tends more to the east of the habitat

Figure 16: Behaviour of two bats for  $\sigma = 0$  with different preferences.

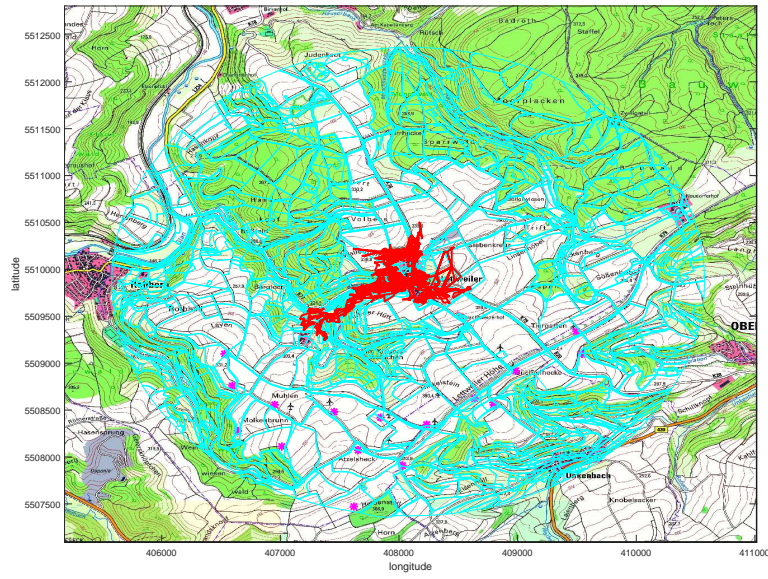


(a)

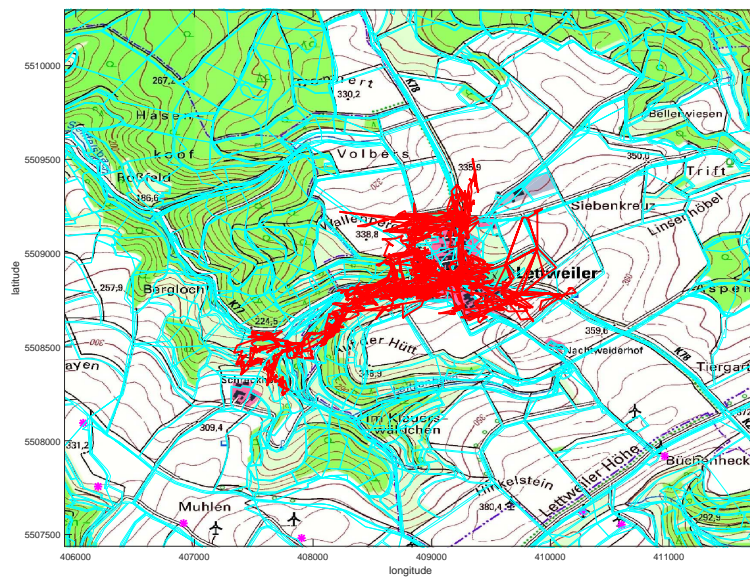


(b) Detail of Figure 17a

Figure 17: Behaviour of one bat for  $\sigma = 2$ .

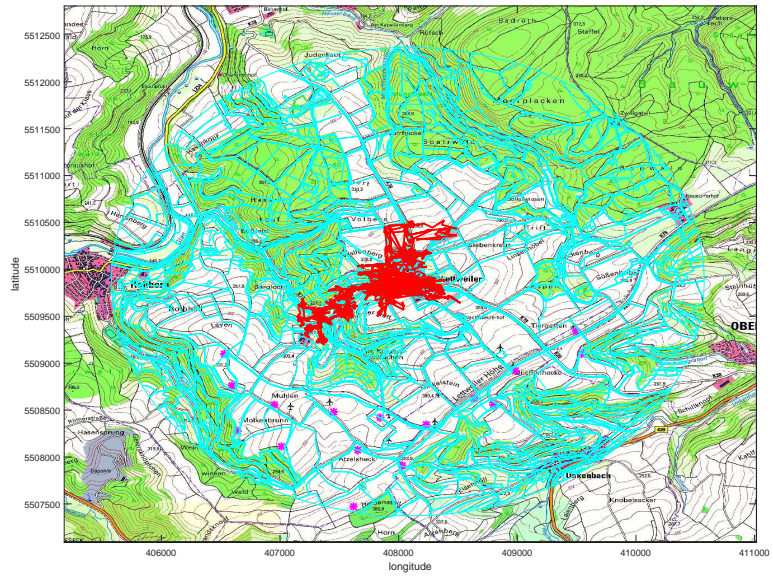


(a)

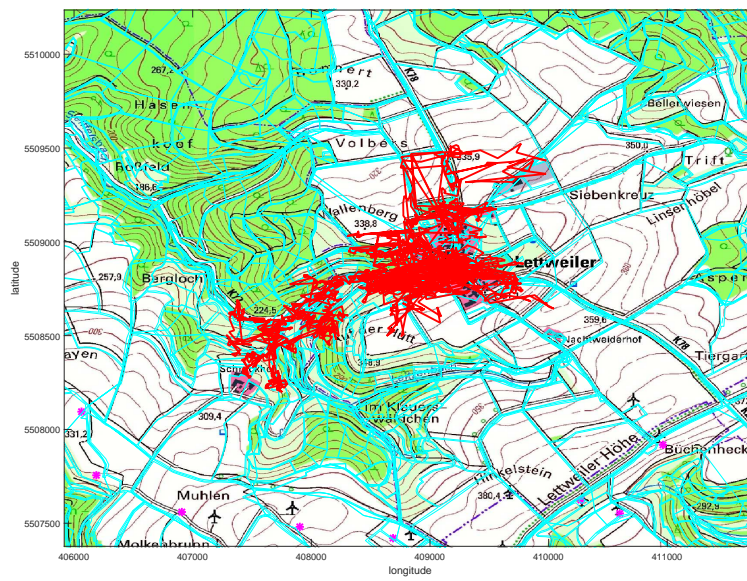


(b) Detail of Figure 18a

Figure 18: Behaviour of one bat for  $\sigma = 5$ .



(a)



(b) Detail of Figure 19a

Figure 19: Behaviour of one bat for  $\sigma = 7$ .

## SECOND APPROACH: PARTIAL DIFFERENTIAL EQUATION MODEL

---

In the past chapter we have presented an individual based model (IBM) approach with a Monte-Carlo simulation to model the foraging behaviour of a local bat population. A main problem of this individual based modelling is the high computational effort of the model approach. The Monte-Carlo simulation is well known for its time-consuming implementation and slow convergence rate as well. Therefore, we want to look at another common approach for simulating animal behaviour. In this chapter we build a PDE based model to simulate the behaviour of a homogeneous bat population.

For this approach we assume that each individual in the population has the same preferences. This means the same attraction zones are preferred and the same sample paths are frequented by each individual. The result of this model is an occurrence profile of the model area. That means we do not have to make a second step like in the first approach (first IBM result, than Monte-Carlo simulation). This is less time-consuming, but, on the other hand, it is neither possible to simulate different preferences within the population with this approach nor to reproduce trajectories of single animals. It strongly depends on the intended use of the model results which of the two approaches is more suitable. Therefore, we finish this chapter by discussing the different characteristics of the results of both models in a more detailed way.

We start this chapter by introducing the respective PDE models for the different movement types of the bats. The most challenging part of the model is the two-dimensional attraction zone. Here we have to derive the general connection between the SDE and PDE formulation. In physics this connection is well known for the Fokker-Planck and the Langevin equations (Risken, 1984). In finance applications it is also known as theorem of Feynman-Kac (Paul and Baschnagel, 1999). But the equivalent PDE based formulation for a reflected Brownian motion is a boundary value problem. Therefore, we need to derive the suitable boundary conditions in this chapter.

### 6.1 TRANSFER TO OUR MODEL

The behaviour of bats is very complex, therefore it is not possible to describe it by only one PDE formulation but we have to divide our

model again in three main parts which depend on the habitat type: sample paths, one- and two-dimensional attraction zones. We now derive the PDE models for these three different habitat types which correspond to the stochastic process formulations in the IBM approach.

### 6.1.1 Sample path and one-dimensional attraction zone

As mentioned above, we assume that, in general, the bats follow certain sample paths. In addition we assume that the bats do not exactly stick to the sample path all the time. Instead, we assume again some kind of slight variation around the given path. Therefore, we generate a normally distributed stochastic component  $W_t$  in each step and add  $\alpha W_t$  to the corresponding coordinates of the sample path. Here  $\alpha \geq 0$  is defined as a small constant which guarantees a limitation of variation such that the bats do not lose sight of the original sample path.

We obtain a normal distribution for the occurrence profile along the sample path where the variance  $\sigma^2$  is a constant value and can be adjusted to simulate the specific behaviour of the concerning bat species. The mean  $\mu$  is the  $x$ -value of the concerning sample path coordinate, except the sample path is parallel to the  $y$ -axis, then we chose the  $y$ -coordinate. So we can define the behaviour along the path as follows.

#### **Definition 9.** PDE approach for the path sections

Let  $p : \mathbb{R} \times [0, T] \rightarrow [0, 1]$  and  $(x_t, y_t)$  be the space coordinate of the sample path at time  $t$ . Then the following equation describes the density distribution of the bat's position at time  $t$ , if the path section is not parallel to the  $y$ -axis

$$p(x, t) = \frac{1}{\sigma\sqrt{2\pi}} e^{-\frac{1}{2}\left(\frac{x-\mu_t}{\sigma}\right)^2},$$

where  $\mu_t = y_t$  and

$$p(y, t) = \frac{1}{\sigma\sqrt{2\pi}} e^{-\frac{1}{2}\left(\frac{y-\mu_t}{\sigma}\right)^2}$$

represents the density distribution along the path if the path is parallel to the  $y$ -axis, where  $\mu_t = x_t$ .

#### **Remark 7.**

Both equations are the same, we only use different coordinate for the mean of the distribution function.

A boundary of the forest or a clearing are exceptional cases of an attraction zone because it is defined as a one-dimensional line instead of a two-dimensional polygon. Hence, the bat flies along the boundary and in each time step it decides whether it continues flying in the same direction or whether it rather turns around and flies in the opposite direction. We can describe this behaviour in a similar way as

the behaviour along the path. The main difference in the behaviour of the animals is the number of flights along the zone per night. The path sections are only visited a few times per night whereas the one-dimensional attraction zones are higher frequented because they are not only used as corridors but as hunting zones. However, the density profile is the same as for the sample path.

### 6.1.2 Two-dimensional attraction zone

Now we look at the most challenging part in the habitat: the two-dimensional attraction zone. Here the bats are supposed to fly randomly over the zone for a fixed amount of time. In the IBM we have simulated this behaviour with a two-dimensional RBM. But we have assumed that the bats fly completely randomly over the zone without any drift effect, so we have adjusted the standard SDE formulation. Hence, we can describe the behaviour of the bat over the two-dimensional attraction zone in the IBM with the adjusted RBM process of Chapter 4:

$$X_t = X_0 + \int_0^t \sigma(X_s) dB_s - \int_0^t n(X_s) d\xi_s. \quad (3)$$

Here  $\sigma \in \mathbb{R}^2$  is constant, that means it is set independently from location  $X$  and time  $t$ . The last term guarantees that the process stays inside the bounded domain.  $n(X, t)$  is a vector field on the boundary of the domain in the direction of the outward normal vectors and  $\xi(t)$  is only increasing if the process leaves the domain. For a more detailed explanation please see Chapter 4.

In this section we want to present the connection between the above described process and the following PDE based model for the two-dimensional attraction zone. We want to simulate the above described behaviour by a parabolic partial differential equation with Neumann boundary conditions. Therefore, we introduce the definition of Neumann boundary conditions:

**Definition 10.** *Neumann boundary condition (Tveito and Winther, 2006)*  
Let  $\Omega$  be a domain. Then

$$\frac{\partial y(x)}{\partial \mathbf{n}} = f(x), \quad \forall x \in \partial\Omega$$

denote a Neuman boundary condition, where  $\mathbf{n}$  denotes the outward normal vector to the boundary  $\partial\Omega$  and  $f$  is a given scalar function.

We want to use the following theorem to link a suitable PDE formulation to our IBM approach formulation Equation 3.

**Theorem 3.** *Langevin and Fokker-Planck equation (Gardiner, 2009; Paul and Baschmagel, 1999; Risken, 1984)*

Let  $X(t)$  be a stochastic variable and  $p(X, t|X_0, t_0)$  the transition probability. For  $t \leq 0$ , the SDE

$$dX_t = \int_0^t F(X, t)dt + \int_0^t B(X, t)dW(t), \quad t \in [0, \infty), X \in \mathbb{R}^n$$

denotes the Langevin equation. Then  $p(X, t)$  is a solution of the parabolic PDE

$$\frac{\partial p(X, t)}{\partial t} = \frac{1}{2} \sum_{ij=1}^n \frac{\partial^2}{\partial X_i \partial X_j} D_{ij} p(X, t) - \sum_{i=1}^n \frac{\partial}{\partial X_i} F_i p(X, t), \quad (4)$$

$$t \in [0, \infty), X \in \mathbb{R}^n,$$

with drift term  $F(X, t)$  and diffusion coefficient  $D(X, t)$  such that  $D = BB^T \in \mathbb{R}^{n \times n}$ . Equation 4 is also called Fokker-Planck equation.

This theorem gives us the theoretical link between our two different approaches: the IBM with its RBM formulation and the PDE approach which we want to derive in the following. Therefore, we only consider the non-reflecting part of Equation 3:

$$X_t = X_0 + \int_0^t \sigma(X_s)dB_s \quad (5)$$

We now derive the corresponding PDE formulation. The main connection is between the coefficients of the SDE and PDE. By Theorem 3, the equivalent PDE is given by the following formulation:

$$\frac{\partial p(X, t)}{\partial t} = \frac{1}{2} \sum_{i,j=1}^2 \frac{\partial^2}{\partial X_i \partial X_j} D_{ij} p(X, t), \quad t \in [0, \infty), X \in \mathbb{R}^2, \quad (6)$$

with  $D = \sigma\sigma^T \in \mathbb{R}^{2 \times 2}$  the diffusion coefficient. So Equation 6 is the corresponding PDE formulation to the non-reflecting part of our IBM approach Equation 5.

We have to add boundary and initial conditions to the above PDE for obtaining the equivalent formulation to our SDE. In analogy to the work of Bossy et al. (Bossy, Gobet, and Talay, 2004), we use Neumann boundary conditions and a delta function as initial condition. Then we obtain the following boundary value problem for the two dimensional attraction zones:

**Definition 11.** *PDE approach for the two-dimensional attraction zones*

Let  $K \in \mathbb{R}^2$  be a polygon. Further let  $D = \begin{pmatrix} \sigma_1^2 & \sigma_1 \sigma_2 \\ \sigma_1 \sigma_2 & \sigma_2^2 \end{pmatrix}$  be the



diffusion coefficient and  $\delta$  be the dirac measure. Let  $x \in K$  be the two-dimensional space-coordinate and  $t \in [0, T]$  the time-coordinate. Then the parabolic PDE

$$\frac{\partial p(x, t)}{\partial t} = \frac{1}{2} \sum_{i,j=1}^2 D_{ij} \left( \frac{\partial^2 p_2(x, t)}{\partial x_i \partial x_j} \right),$$

$$t \in [0, T], x \in K$$

with initial condition

$$p(x, 0) = \delta(x)$$

and Neumann boundary condition

$$\frac{\partial p}{\partial n} = 0 \quad \forall x \in \partial K, t \in (0, T]$$

describes the behaviour of the bats over the two-dimensional attraction zone.

The magnitude of  $D$  determines the spread velocity of the bat. If  $D$  is large, the diffusion of the flight is also high and the bat is likely to fly a high distance in short time. If  $D$  is low, the bat stays close to its starting point. This fits perfectly the meaning of the coefficient matrix  $\sigma$  in the IBM (see Chapter 4).

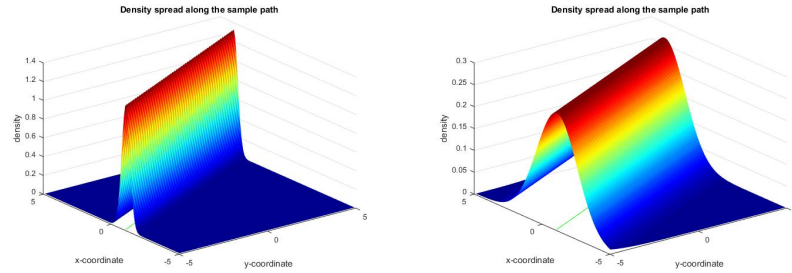
**Remark 8. Extension**

A possible extension of the model is a space dependent diffusion coefficient  $D(x)$  such that we can simulate a more complex behaviour inside the attraction zones. The individuals would not disperse evenly to all directions, but they would prefer special regions inside the attraction zones. This can happen if the preferences of the bat concerning the zone are not uniformly distributed, e.g. if a special part of the zone has an especially high amount of prey insects. Then the bat would concentrate on this special part of the zone.

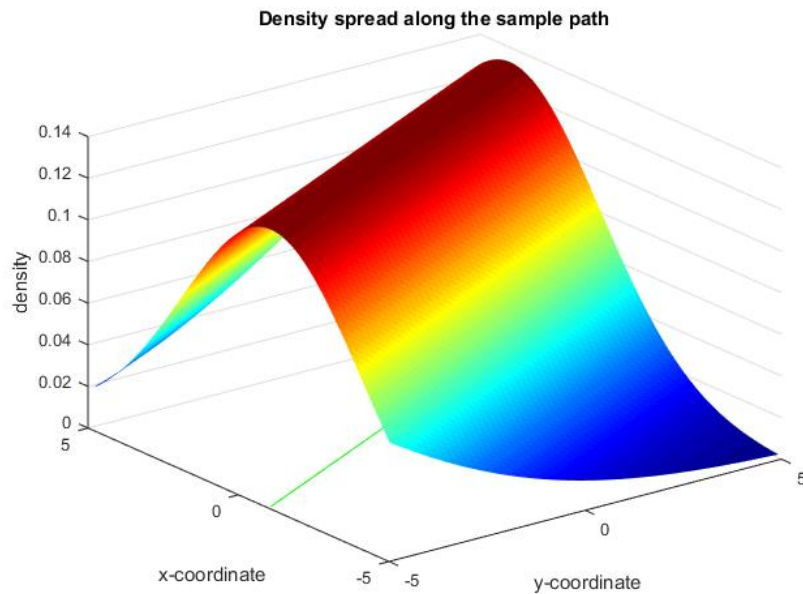
## 6.2 NUMERICAL RESULTS OF THE PDE MODEL

Just as in the first approach we want to show the numerical results for this model. Hence, we consider the same model area as in the first approach and present the results for representative parts of the model area, before we finish the chapter by comparing the results of this model to the results of the Monte-Carlo simulation.

The PDE approach along the sample path is just the normal distribution that is shifted along the path. The form of the distribution depends on the variance parameter. For a larger variance parameter the curve is more spread out, for a small variance parameter the curve is narrower. This fits the corresponding behaviour of the bats. A big variance parameter represents a more loose connection to the path



(a) PDE approach for the path with variance  $\sigma = 0.3$ . (b) PDE approach for the path with variance  $\sigma = 1.5$ .



(c) PDE approach for the path with variance  $\sigma = 3$ .

Figure 20: PDE model for the path with three different variance parameters.

and the bat tends to fly in a higher distance to the path coordinates. Therefore, the probability of leaving the path is higher. A small variance parameter describes exactly the opposite behaviour. Then the bat sticks closely to the path. Hence, the probability besides the path declines very fast.

In Figure 20 we can see an example for the path (green line) and the corresponding density profile with the effect of the different variance parameters: small ( $\sigma = 0.3$ ), midsize ( $\sigma = 1.5$ ) and large ( $\sigma = 3$ ).

In Figure 21 we can see the PDE approach for a one-dimensional attraction zone. Again the green line represents the attraction zone. It is the same distribution as over the paths such that different vari-

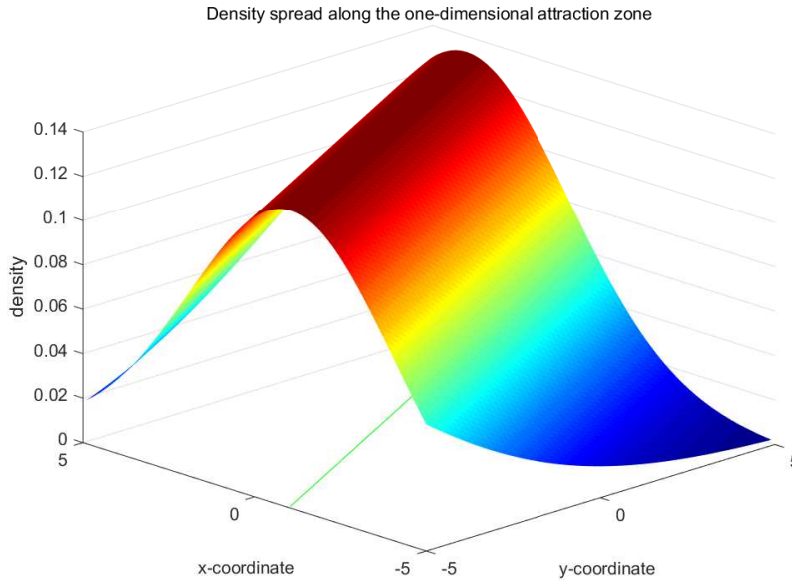


Figure 21: PDE model for the one-dimensional attraction zone.

ance parameters have the same effect on the density profile.

In Figure 22 we show the result for a two-dimensional attraction zone. The highest density peaks occur at the entering points and then the profile flattens to the other directions of the zone. The diffusion is, as mentioned before, space independent. So the curve flattens equally distributed to all boundaries.

### 6.3 COMPARISON OF THE TWO APPROACHES

In the literature the most mentioned problem of an IBM is the high computational effort (see e.g. Grimm et al., 2006) and therefore the necessity of reducing the number of simulated individuals. A PDE model is usually more efficient and it is possible to simulate the behaviour of a whole population in a very short time horizon, but we can not generate trajectories of single individuals. Although in Chapter 2 we have presented various PDE approaches for simulating different types of complex animal behaviour patterns, it is not possible to apply one general PDE approach to simulate all three behaviour types of our bat population.

We finish this chapter by presenting a short comparison of the previously discussed approaches to simulate bat's movement behaviour: the Monte-Carlo simulation and the PDE-based model. We illustrate the comparison of the two approaches by presenting the numerical

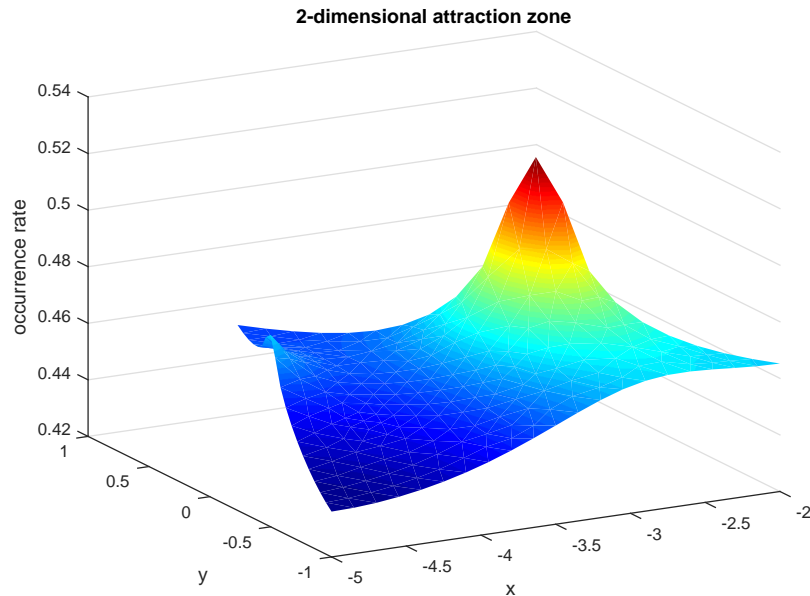


Figure 22: PDE model for the two-dimensional attraction zone.

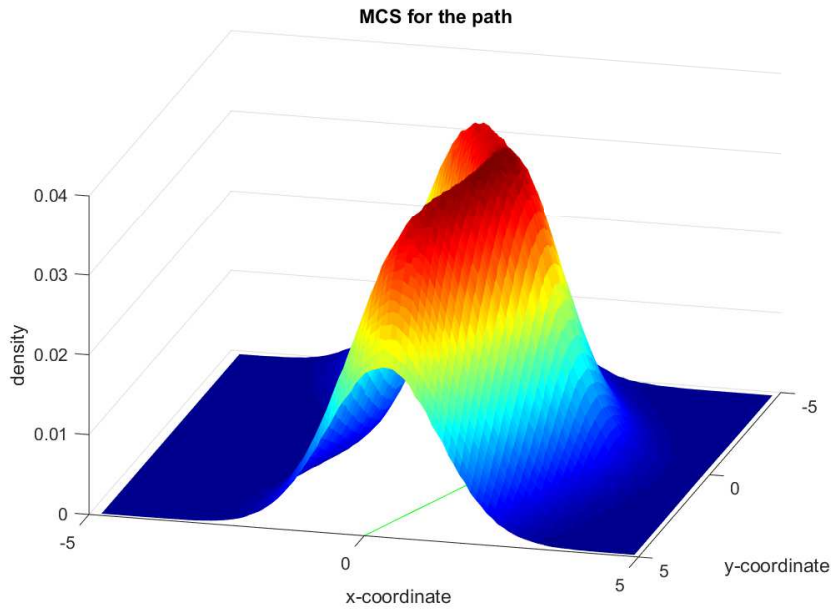
results for a path section and two different two-dimensional attraction zones.

In Figure 23 we compare the results of the two approaches for the sample path. In Figure 23a we show the result of the Monte-Carlo simulation and in Figure 23b we show the result of the the PDE model for the same part of sample path. The results are very similar to one another.

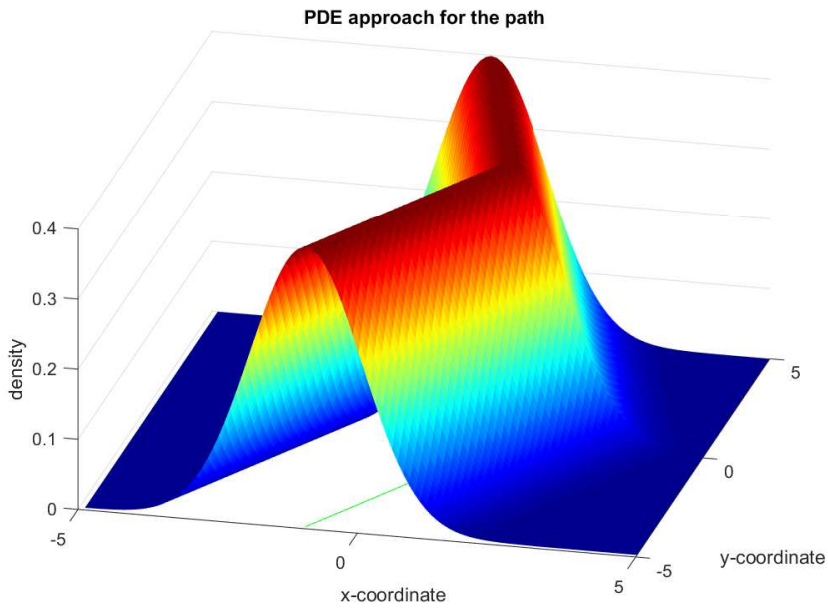
The model of the one-dimensional attraction zone is nearly the same as the one of the sample path. That is the reason why we will not represent this case here in detail. Instead, we show the comparison for the two-dimensional attraction zones. In Figure 24 and Figure 25 we show both models for two different attraction zones and compare the results of the two approaches.

By comparing the density profiles of the Monte Carlo simulation and the PDE approach for a given section of the habitat, it becomes obvious that the two models again generate similar occurrence profiles for the bat behaviour. We can see the peaks of occurrence at the same edges of the attraction zones.

The main difference of the two approaches is the loss of information in the PDE approach. In the Monte-Carlo simulation it is possible to show a density profile for the bats occurrence probabilities, but it is also possible to generate average visit numbers to show how often bats frequent a special region in the habitat in one night. This is especially relevant for the evaluation of the danger caused by wind

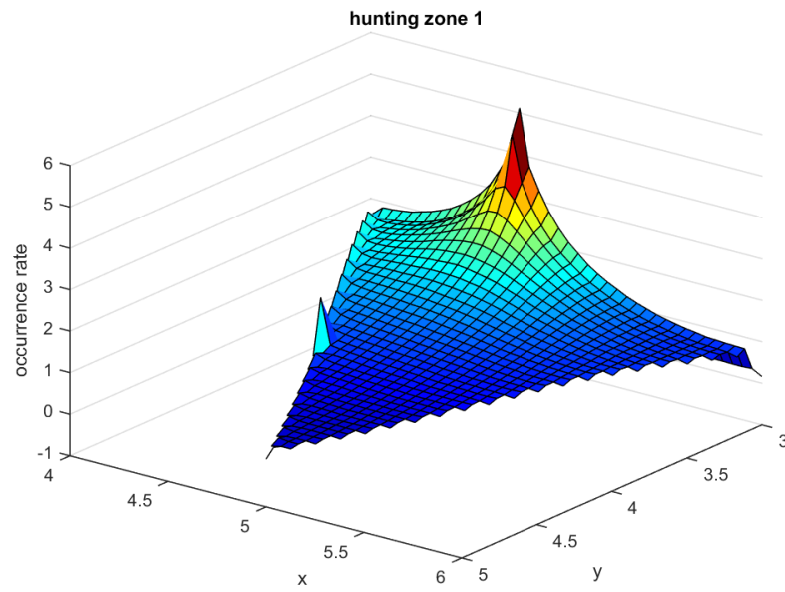


(a) Monte-Carlo simulation for the path for  $\sigma_1 = \sigma_2 = 1$  and  $N = 10,00000$  simulations.

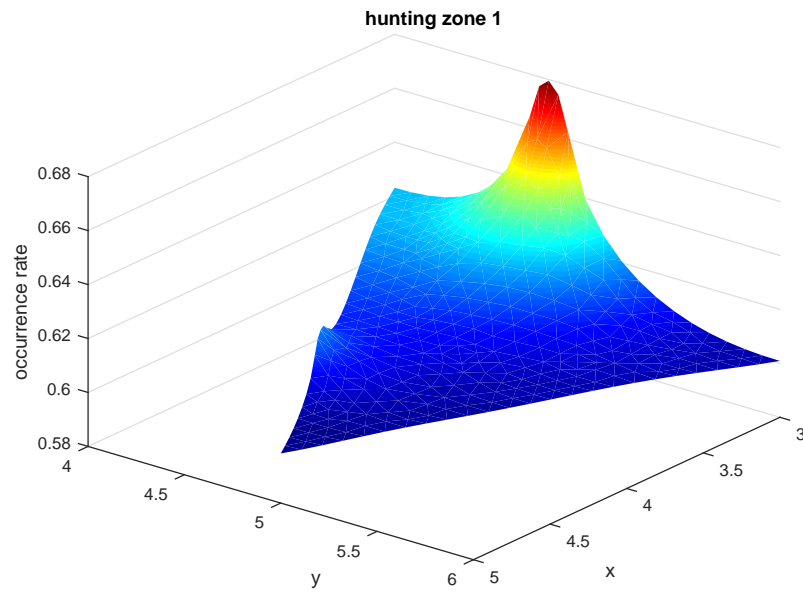


(b) PDE model for the path for  $\sigma = 1$ .

Figure 23: Comparison of the two models for the path.

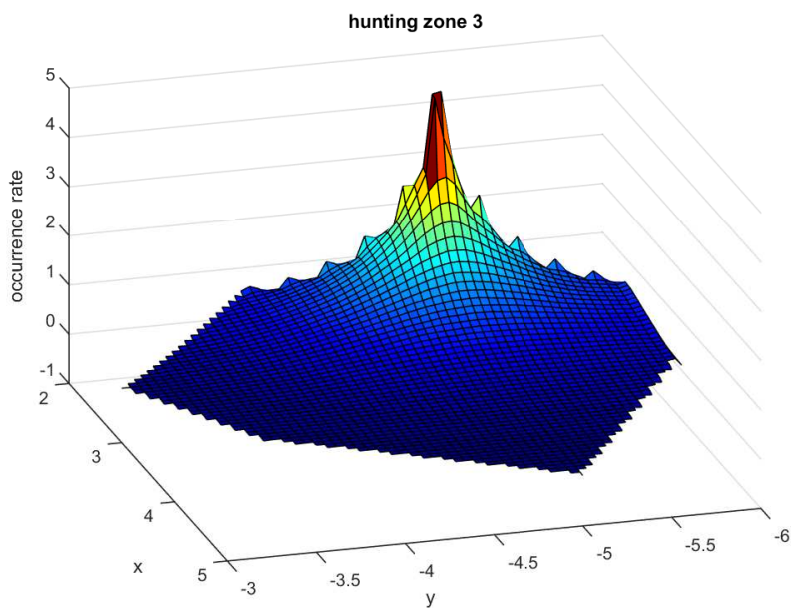


(a) Monte-Carlo simulation for hunting zone one and  $M = 10,000$  simulations.

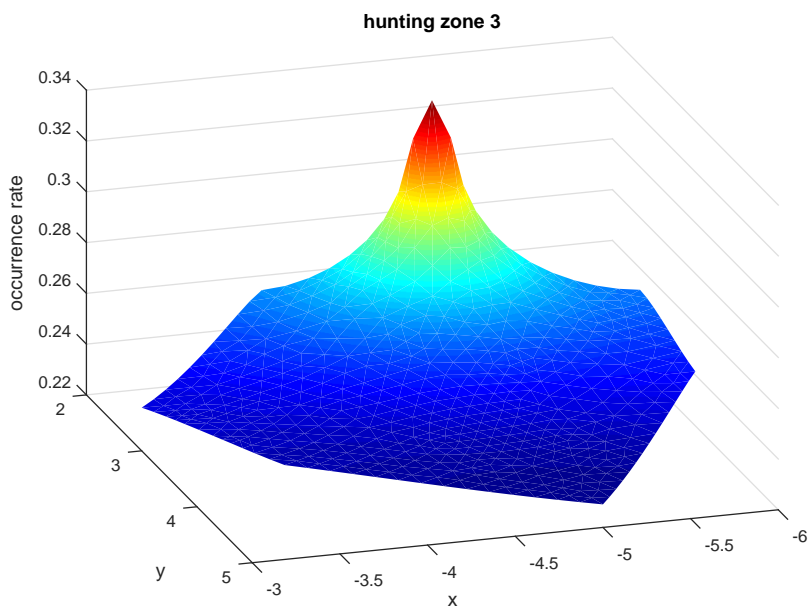


(b) PDE approach for hunting zone one.

Figure 24: Comparison for zone 1



(a) Monte-Carlo simulation for hunting zone two and  $M = 10,000$  simulations.



(b) PDE approach for hunting zone two.

Figure 25: Comparison for zone 2

turbines. For highly frequented places it is possible that a bat visits the place several times each night and therefore the danger of a wind turbine in that region would highly increase. Unfortunately, it is not possible to generate these numbers with the PDE based approach, because we do not know in advance how often one animal frequents one special path. The PDE approach only tells us what the density profile looks like if the bat visit this path but not how often this actually happens. This is one reason for us to prefer the IBM approach for our later risk estimation.

Another reason for preferring the IBM based approach is the ability to build trajectories. This can be used to extend empirical data sets if this is too expensive or time consuming to do it by empirical studies. Hence, it can be a huge improvement of the planning process for new wind turbines or other projects evoking human wildlife conflicts.



## MODEL CALIBRATION USING THE ADJOINT EQUATION

---

In the previous chapters, we have presented our model assumptions, the out coming models (IBM and PDE based approach) and the resulting occurrence profiles of one bat and finally of the local population. In this chapter, we want to explain the theoretical methods to fit these model results to empirical data sets. This model calibration is absolutely necessary for validating the model results and identifying the optimal parameter values in the model. Another useful idea is to test which assumptions effect the model results in a relevant way or which additional assumptions we should make to get a more realistic model result.

We start this chapter by introducing the general theory of numerical calibration methods. We first introduce the general numerical method for solving a calibration problem, the Gauß-Newton method.

Then we extend the general framework and introduce the adjoint equation. These method was first introduced by Giles and Glasserman (Giles and Glasserman, 2006) and is mainly used for financial market model calibration (see e.g. Kaebe, Maruhn, and Sachs, 2009). We adjust this method to our special model properties and point out the advantages of this method.

### 7.1 GENERAL CALIBRATION MODEL

The goal of solving calibration problems is always to fit a model to empirical or synthetical data sets. Hence, we have a model function  $f : \mathbb{R}^l \rightarrow \mathbb{R}^n \times \mathbb{R}^m$  that depends on a vector  $x \in \mathbb{R}^l$  of variables which determines the result of the model. Additionally, we have a set of empirical data  $y \in \mathbb{R}^n \times \mathbb{R}^m$ .

Now we want to find the set of variables  $x_i$ ,  $i = 1, \dots, l$ , such that the model result is as close as possible to the empirical data set  $y$ . This can be described by a least squares problem:

**Definition 12.** *Least squares problem:*

*With the parameter set  $y \in \mathbb{R}^n \times \mathbb{R}^m$  and the model function  $f : \mathbb{R}^l \rightarrow$*

$\mathbb{R}^n \times \mathbb{R}^m$  and  $x \in \mathbb{R}^l$ , we define the non-linear least squares problem as follows:

$$\min_x \frac{1}{2} \left\| \sum_{i,j} y_{ij} - f(x)_{ij} \right\|^2 =: r(x)$$

In our case, the function  $f$  can be either the model equation of our IBM approach or the formulation of our PDE based approach. In both cases, it is reasonable to split the habitat again in the three sub models: sample path, one- and two-dimensional attraction zones, and to derive the calibration problem for every sub model. A very challenging characteristic of the model are the transitions between the different zones.

First, we present the general numeric theory to treat the above described problem.

## 7.2 GAUSS-NEWTON METHOD

A general method for solving a non-linear least squares problem is the Gauß-Newton method (see e.g. Björck, 1996). Instead of solving the original problem we solve a linear approximation,

$$\min_p \|r(x_k) + J(x_k)p\|_2.$$

Here  $r(x_k)$  defines the residual in step  $k$  and  $J$  defines the Jacobi matrix of  $r$ .

Let  $p_k$  be the solution of the optimization problem above, then we obtain the new step of the method as

$$x_{k+1} = x_k + p_k.$$

By iterating these two steps, we get an approximation of the exact solution of the least squares problem.

There exist many of approved methods like the damped Gauß-Newton or the Levenberg Marquard method, which fasten the convergence of this method. However, the main challenge of all mentioned methods is to compute the derivative  $J$ . In our case, this derivative cannot be calculated analytically, so we have to approximate it by using numerical methods. The most common method to compute a derivative is the finite differences scheme, but this method causes a high computational effort. We want to present a method to compute  $J$  with much lower computational effort in the next section.

## 7.3 ADJOINT EQUATION

Adjoint based methods have been successfully used to fit financial market models to market data (Kaebe, Maruhn, and Sachs, 2009). The big advantage of this method is, that the result is an exact calculation of the derivative. Therefore, it is preferable over any finite difference method which only gives us an approximation of the derivative  $J$ . Additionally, it reduces the computational effort such that it is preferable concerning other methods which give us an exact derivative but cause a high computational effort, e.g. the sensitivity equation.

We want to adjust this method to our flight behaviour model. In our IBM and in the PDE model we always identify three different behaviour types depending on the landscape structure. The behaviour of the bats are highly dependent on these three sub models and each model has other parameters which we want to fit in the calibration method.

We want to focus on fitting the model equations of the IBM to an empirical data set in the following sections. For the PDE model the problem can be treated analogously.

7.3.1 *Model characteristics of the IBM*

Every night each bat flies over different landscape structures, e.g. it flies from the roost via a sample path to a lake, then via another sample path to a forest and finally via a third sample path back to the roost again. This behaviour differs in every flight and between the individuals as well. For this special model, it is necessary to merge our three different sub models to one model equation, depending on the order of each bat flight. Therefore, we summarize the different model properties of each of the three sub models:

## PATH

We start with the model for the sample path. Let  $X_t \in \mathbb{R}^2$  be the position at time  $t \in [0, T_m]$ , then the behaviour over the path in simulation  $m$  is described recursively by

$$X_{t+1}^m = X_t^m + h d^m(X_{t+1}) + \sigma_0 \Delta W_t^m.$$

Here,  $h \in \mathbb{R}$  is the constant step size,  $d^m(X_t + 1) \in \mathbb{R}^2$  is the corresponding constant path direction, the coefficient  $\sigma_0$  regulates the effect of the normal distributed stochastic term  $W_t \in \mathbb{R}^2$  with  $\mu = 0$  and variance  $\hat{\sigma}^2 = 1$ .  $m$  is the number of the corresponding Monte-Carlo simulation and the above equation holds for every simulation  $m = 1, \dots, M$ .

In each night, the bat spends several time intervals over different path

sections. Therefore, we describe the time steps in which the bat flies over the path through the index set

$$T_0 = \{T_{0_p} = \{t_{p_1}, \dots, t_{p_{k(p)}}\}, p = 1, \dots, P\}.$$

Here  $P$  is the number of path sections and  $k(p)$  is the number of steps in path section  $p$ .

#### ONE-DIMENSIONAL ATTRACTION ZONE

Now, we describe the behaviour over the one-dimensional attraction zone. Let  $Y_t \in \mathbb{R}^2$  be the position at time  $t$ , then the behaviour over the one-dimensional attraction zone is described recursively by

$$Y_{t+1}^m = F_B + \delta_{t+1}^m d_1 + \sigma_1 \Delta W_t^m.$$

Here,  $\delta_t^m \in [0, 1]$  denotes the random step size for the time step  $t$ ,  $d_1 = (F_E(1) - F_B(1), F_E(2) - F_B(2))^T \in \mathbb{R}^2$  is the corresponding direction of the zone with beginning point  $F_B \in \mathbb{R}^2$  and ending point  $F_E \in \mathbb{R}^2$ , which is the same for all steps over the zone,  $\sigma_1$  is the regulation coefficient of the normal distributed stochastic term  $W_t \in \mathbb{R}^2$  with mean  $\mu$  and variance  $\hat{\sigma}^2$ .  $m = 1, \dots, M$  is again the number of the Monte-Carlo simulation.

Then we define the time steps which the bat spends over the one-dimensional attraction zones by the index set

$$T_1 = \{T_{1_f} = \{t_{f_1}, \dots, t_{f_{k(f)}}\}, f = 1, \dots, F\}.$$

Here  $F$  is the number of one-dimensional attraction zone sections and  $k(f)$  is the number of steps in section  $f$ .

#### TWO-DIMENSIONAL ATTRACTION ZONE

Finally, we consider the model for the two-dimensional attraction zone. Let  $K \in \mathbb{R}^2$  be a convex Polygon which represents the two-dimensional attraction zone and  $Z_t \in \mathbb{R}^2$  be the position at time  $t$ . The behaviour over the two-dimensional attraction zone is described recursively by

$$Z_{t+1}^m = \tilde{Z}_{t+1}^m + 2[G^n(\tilde{Z}_{t+1}^m)]^+ n(\tilde{Z}_{t+1}^m),$$

with  $\tilde{Z}_{t+1}^m = Z_t^m + \sigma_2 \Delta W_t^m$ . Here  $\sigma_2$  is the regulation coefficient of the normal distributed stochastic term  $\Delta W_t \in \mathbb{R}^2$  with mean  $\mu$  and variance  $\hat{\sigma}^2$ .  $G^n$  is the distance between  $\tilde{Z}_{t+1}^m$  and its projection on  $K$ :  $\pi_{\partial K}^n(\tilde{Z}_{t+1}^m)$  parallel to the outward normal vector  $n$ :  $G^n(\tilde{Z}_{t+1}^m) = \|\tilde{Z}_{t+1}^m - \pi_{\partial K}^n(\tilde{Z}_{t+1}^m)\|_2$ .

Then the time steps in which the bat stays over the two-dimensional attraction zones are described through the index set

$$T_2 = \{T_{2_l} = \{t_{l_1}, \dots, t_{l_{k(l)}}\}, l = 1, \dots, L\}.$$

Here  $L$  denotes the number of two-dimensional attraction zone sections and  $k(l)$  is the number of steps in section  $l$ .

Now we combine all three sub models and obtain the flight behaviour of one bat for one night by the following definition:

**Definition 13.** *Combined flight behaviour*

Let  $B_t^m$  be the position of the bat at time  $t \in [0, T_m]$  in Monte-Carlo simulation  $m$ . Further let  $B_0^m = R = B_{T_m}^m \forall m = 1, \dots, M$ , where  $R \in \mathbb{R}^2$  is the position of the roost. Then

$$B_t^m = \begin{cases} X_t^m, & t \in T_{0,p}, \text{ for one } p \in \{1, \dots, P\} \\ Y_t^m, & t \in T_{1,f}, \text{ for one } f \in \{1, \dots, F\} \\ Z_t^m, & t \in T_{2,l}, \text{ for one } l \in \{1, \dots, L\} \end{cases}$$

$$t = 0, \dots, T_m \quad m = 1, \dots, M$$

denotes the stochastic process which represents the movement of the bat in simulation  $m$ . Here  $T_m$  is the point in time when the bat stops its activity in simulation  $m$ .

This equation holds for every bat in every simulation. We can calibrate the behaviour of each bat in an own calibration model which is useful for the IBM because there, we simulate every bat on their own with different behaviour types.

Therefore, we need to define the function  $g$ , the control parameter  $u$  and the matrix  $B$ :

The function  $g$  consists of the model equations:

$$g(B_{t+1}^m) = \begin{cases} X_{t+1}^m - X_t^m - \text{hd}(X_{t+1}) - \sigma_0 \Delta W_t^m, & t \in T_{0,p}, \text{ for one } p \in \{1, \dots, P\} \\ Y_{t+1}^m - F_B - \delta_{t+1}^m d_1 - \sigma_1 \Delta W_t^m, & t \in T_{1,f}, \text{ for one } f \in \{1, \dots, F\} \\ Z_{t+1}^m - Z_t^m - \sigma_2 \Delta W_t^m - 2[G^n(\check{Z}_{t+1}^m)]^+ n(\check{Z}_{t+1}^m), & t \in T_{2,l}, \text{ for one } l \in \{1, \dots, L\} \end{cases}$$

$$\forall t = 1, \dots, T_m \quad m = 1, \dots, M$$

In the calibration problem, this function has to be equal zero such that the model equations are fulfilled.

$u$  denotes the control parameter and consists of the parameters  $\sigma_0$ ,  $\sigma_1$  and  $\sigma_2$ :

$$u = \begin{pmatrix} \sigma_0 \\ \sigma_1 \\ \sigma_2 \end{pmatrix}$$

By changing these parameters, we later fit the model result to the empirical data set.

The matrix  $B^m$  consists of the coordinates of the stochastic process of the simulated bat in simulation  $m$ .

$$B^m = \begin{pmatrix} B_1^m \\ \vdots \\ B_{T_m}^m \end{pmatrix}$$

### 7.3.2 Transitions between different parts

Additionally, we need initial and in some cases also ending conditions. We assume that every bat is starting and ending its activity in the roost  $R \in \mathbb{R}^2$ . Therefore, we have the following condition:

$$B^m(1) = R = B^m(T_m), \quad \forall m = 1, \dots, M$$

Besides this, we have initial and in some cases even ending values for every transition between the zones. All path sections have a fixed starting and ending points. For the attraction zones we only define starting points. Over these zones the bat has a clearly defined starting point but it moves randomly over the zone. If it has reached the predefined step number of the zone it just jumps to the starting point of the next section.

It is a complex situation, because we cannot identify the exact time points, when the transitions between the zones take place, in advance. Hence, let  $S^m = \{i_1, \dots, i_S\} \subset \{1, \dots, T_m\}$  be the index set of the transition points and let  $\bar{B}_{i_1}^m, \dots, \bar{B}_{i_S}^m$  be the corresponding starting and ending values in simulation  $m$ . Then we can define the function  $h: \mathbb{R}^2 \rightarrow \mathbb{R}$  as

$$h(B_t^m) = \begin{cases} B_t^m - \bar{B}_t^m, & \text{if } t \in S \\ 0, & \text{if } t \notin S \end{cases}$$

In the calibration problem, this function has to be equal zero, like the function  $g$ , to guarantee that the starting and ending conditions are fulfilled.

### 7.3.3 Calibration model for bats flight behaviour

With these functions we can now describe the calibration problem for our IBM:

**Definition 14.** *Calibration problem*

Let  $B_{\text{obs}}$  be an empirical data set,  $B^m$  and  $u$  are given as above. Further,

let  $A_i$  be the sub regions of our model landscape and  $\chi_{A_i}(B_t^m)$  the function which counts the crosses of the bats for section  $A_i$  for each  $i = 1, \dots, I$ . That means, if  $B_t^m$  is inside  $A_i$  then  $\chi_{A_i}(B_t^m) = 1$  otherwise  $\chi_{A_i}(B_t^m) = 0$ . Then

$$\begin{aligned} \min \frac{1}{2} \left\| \sum_{i=1}^I \frac{1}{M} \sum_{m=1}^M \frac{1}{T_m} \sum_{t=1}^{T_m} \chi_{A_i}(B_t^m) - B_{\text{obs}_i} \right\|^2 &:= R(\chi_A) \\ \text{s.t. } g(B_t^m, \mathbf{u}) = 0, \quad \forall m = 1, \dots, M, \quad t = 1, \dots, T_m & \quad (7) \\ h(B_t^m) = 0, \quad \forall m = 1, \dots, M, \quad t = 1, \dots, T_m & \end{aligned}$$

denotes the calibration problem for our model. Here  $B_{\text{obs}_i}$  is the value of the empirical data set for section  $A_i$ .

**Remark 9.** Differentiability of  $\chi_{A_i}$

It is obvious that  $\chi_{A_i}$  is not differentiable for any subregion  $A_i$ . Therefore, we use a smooth approximation  $\tilde{\chi}_{A_i}$ ,  $i = 1, \dots, I$  of the original function. For notational reasons we denote this smooth version in the following with  $\chi_{A_i}$ . Then the derivative of  $\chi_{A_i}$  with respect to  $B_t^m$  exists and we denote it with  $\chi'_{A_i}$ ,  $\forall i = 1, \dots, I$ .

#### 7.3.4 Lagrange function and necessary first order conditions

We define the corresponding Lagrange function for the as described before minimization problem Equation 7. For solving the optimization problem we derive the Lagrange function:

**Definition 15.** Lagrange function

Let the calibration problem be given as above, then we can define the corresponding Lagrange function

$$\mathcal{L}(B^m, \mathbf{u}) = R(\chi_A) + \lambda^m g(B^m, \mathbf{u}) + \mu^m h(B^m), \quad \forall m = 1, \dots, M,$$

depending on simulation  $m$ .

Next, we derive the necessary first order conditions for the Lagrange function.

**Definition 16.** Necessary first order conditions

The necessary first order conditions for the above defined Lagrangian are described by the derivative with respect to the control parameter  $\mathbf{u}$

$$\frac{\partial \mathcal{L}}{\partial \mathbf{u}} = \lambda^m g_{\mathbf{u}}(B^m, \mathbf{u}) = \sum_{t=1}^{T_m} \lambda_t^m g_{\mathbf{u}}(B_t^m, \mathbf{u}) \stackrel{!}{=} 0, \quad \forall m = 1, \dots, M \quad (8)$$

to be equal to zero and the derivative with respect to  $B_t^m$

$$\frac{\partial \mathcal{L}}{\partial B_t^m} = R_{B_t^m}(\chi_A(B_t^m), \mathbf{u}) + (\lambda_t^m g_{B_t^m}(B_t^m, \mathbf{u}) + \mu^m h_{B_t^m}(B_t^m)) \stackrel{!}{=} 0, \quad (9)$$

$$\forall t = 1, \dots, T_m, \quad \forall m = 1, \dots, M$$

to be equal to zero.

We want our model to fulfil these two conditions for all simulations. In the following we check them for our specified model equations. Therefore, we have to consider again our three cases. For simplification, we assume in each case that the bat only stays over the corresponding part: path, one- and two-dimensional attraction zone such that there are no transitions between these zones.

We now derive the Lagrange parameters for the three cases. In each case we have to guess  $\lambda(0, \cdot)$  and we have to choose  $\lambda(N, \cdot)$  such that the ending condition is fulfilled if it exists.

#### PATH

We start by reformulating the Lagrange function for the path. Let  $B_0$  be the initial value, then

$$\begin{aligned} \mathcal{L}(B_t^m, \mathbf{u}) = & \frac{1}{2} \sum_{i=1}^I \left( \frac{1}{M} \sum_{m=1}^M \frac{1}{T_m} \sum_{t=1}^{T_m} \chi_{A_i}(B_t^m) - B_{\text{obs}_i} \right)^2 \\ & + \lambda_t^m (B_t^m - B_{t-1}^m - \text{hd}(X_t) - \sigma_0 \Delta W_{t-1}^m) \\ & \forall t = 1, \dots, T_m + 1, \quad \forall m = 1, \dots, M \end{aligned}$$

holds. Although we usually only consider the time points until  $T_m$ , we here include additionally the time point  $T_m + 1$  because the path section has an ending condition, such that we have an additional Lagrange parameter, which we have to choose later. Then the Lagrange parameter for the path fulfils the following theorem.

#### **Theorem 4.** *Lagrange parameter for the path*

*The Lagrange parameter for the path section  $\lambda_0$  is given by:*

$$\begin{aligned} \lambda_{0_t}^m = & \lambda_{0_{t+1}}^m - \sum_{i=1}^I \left( \frac{1}{M} \sum_{m=1}^M \frac{1}{T_m} \sum_{t=1}^{T_m} \chi_{A_i}(B_t^m) - B_{\text{obs}_i} \right) \chi'_{A_i}(B_t^m) \\ & \forall m = 1, \dots, M \quad \forall t = T_m, \dots, 2. \end{aligned} \tag{10}$$

*Proof.*

We calculate the derivative of  $\mathcal{L}$  with respect to  $B_t^m$ :

$$\begin{aligned} \mathcal{L}_{B_t^m}(B_t^m, \mathbf{u}) = & \sum_{i=1}^I \left( \frac{1}{M} \sum_{m=1}^M \frac{1}{T_m} \sum_{t=1}^{T_m} \chi_{A_i}(B_t^m) - B_{\text{obs}_i} \right) \chi'_{A_i}(B_t^m) \\ & + \lambda_t^m - \lambda_{t+1}^m, \quad \forall t = 1, \dots, T_m, \quad \forall m = 1, \dots, M. \end{aligned}$$



So we obtain for our necessary first order condition Equation 9:

$$\begin{pmatrix} \sum_{i=1}^I \left( \frac{1}{M} \sum_{m=1}^M \frac{1}{T_m} \sum_{t=1}^{T_m} \chi_{A_i}(B_t^m) - B_{\text{obs}_i} \right) \chi'_{A_i}(B_1^m) + \lambda_1^m - \lambda_2^m \\ \vdots \\ \sum_{i=1}^I \left( \frac{1}{M} \sum_{m=1}^M \frac{1}{T_m} \sum_{t=1}^{T_m} \chi_{A_i}(B_t^m) - B_{\text{obs}_i} \right) \chi'_{A_i}(B_{T_m}^m) + \lambda_{T_m}^m - \lambda_{T_m+1}^m \end{pmatrix} = 0, \quad \forall m = 1, \dots, M.$$

By solving this equation, we obtain a recursion formula for the Lagrange parameter  $\lambda_t$ :

$$\begin{pmatrix} - \sum_{i=1}^I \left( \frac{1}{M} \sum_{m=1}^M \frac{1}{T_m} \sum_{t=1}^{T_m} \chi_{A_i}(B_t^m) - B_{\text{obs}_i} \right) \chi'_{A_i}(B_1^m) \\ \vdots \\ - \sum_{i=1}^I \left( \frac{1}{M} \sum_{m=1}^M \frac{1}{T_m} \sum_{t=1}^{T_m} \chi_{A_i}(B_t^m) - B_{\text{obs}_i} \right) \chi'_{A_i}(B_{T_m}^m) \end{pmatrix} = \begin{pmatrix} \lambda_1^m - \lambda_2^m \\ \vdots \\ \lambda_{T_m}^m - \lambda_{T_m+1}^m \end{pmatrix}, \quad \forall m = 1, \dots, M$$

□

We can solve the above problem by calculating  $B_1^m, \dots, B_{T_m}^m$  pathwise via the system equations:

$$\begin{aligned} B_1^m &= B_0^m + \text{hd}(X_1) + \sigma_0 \Delta W_1^m, & m &= 1, \dots, M \\ &\vdots \\ B_{T_m}^m &= B_{T_m-1}^m + \text{hd}(X_{T_m}) + \sigma_0 \Delta W_{T_m}^m, & m &= 1, \dots, M \end{aligned}$$

for every  $m$ .

Then we guess  $\lambda_{T_m+1}^m$  and determine the other Lagrange parameters pathwise backwards  $(\lambda_{T_m}, \dots, \lambda_1)$  by using the recursion formula Equation 10 for every  $m$ .

By the derivative with respect to  $u$ , we here only consider the derivative with respect to  $\sigma_0$  since the derivatives with respect to  $\sigma_1$  and  $\sigma_2$  are equal to zero. So

$$\mathcal{L}_{\sigma_0}(B_t^m, \sigma_0) = \sum_{t=1}^{T_m+1} -\lambda_t^m \Delta W_t^m, \quad \forall m = 1, \dots, M$$

denotes the derivative of  $\mathcal{L}$  with respect to the control parameter.

## ONE-DIMENSIONAL ATTRACTION ZONE

In this case, we have an initial value problem. Let  $B_0$  be the initial value. Then we derive the Lagrange function in analogy to the path:

$$\begin{aligned} \mathcal{L}(B_t^m, u) = & \frac{1}{2} \sum_{i=1}^I \left( \frac{1}{M} \sum_{m=1}^M \frac{1}{T_m} \sum_{t=1}^{T_m} \chi_{A_i}(B_t^m) - B_{\text{obs}_i} \right)^2 \\ & + \lambda_t^m (B_t^m - F_B - \delta_t^m d_1 - \sigma_1 \Delta B_{t-1}^m) \\ & \forall t = 1, \dots, T_m, \quad \forall m = 1, \dots, M. \end{aligned}$$

Then the Lagrange parameter fulfils the following theorem.

**Theorem 5.** *Lagrange parameter for the one-dimensional attraction zone*  
For the one-dimensional attraction zone the Lagrange parameter  $\lambda_1$  is given by:

$$\begin{aligned} \lambda_{1_t}^m = & - \sum_{i=1}^I \left( \frac{1}{M} \sum_{m=1}^M \frac{1}{T_m} \sum_{t=1}^{T_m} \chi_{A_i}(B_t^m) - B_{\text{obs}_i} \right) \chi'_{A_i}(B_t^m), \\ & \forall m = 1, \dots, M \quad t = T_m, \dots, 1. \end{aligned}$$

*Proof.*

We calculate the derivative of  $\mathcal{L}$  with respect to  $B_t^m$  and obtain:

$$\begin{aligned} \mathcal{L}_{B_t^m}(B_t^m, u) = & \sum_{i=1}^I \left( \frac{1}{M} \sum_{m=1}^M \frac{1}{T_m} \sum_{t=1}^{T_m} \chi_{A_i}(B_t^m) - B_{\text{obs}_i} \right) \chi'_{A_i}(B_t^m) + \lambda_t^m \\ & \forall t = 1, \dots, T_m, \quad \forall m = 1, \dots, M \end{aligned}$$

So we obtain for our necessary first order condition Equation 9:

$$\begin{aligned} \left( \begin{array}{c} \sum_{i=1}^I \left( \frac{1}{M} \sum_{m=1}^M \frac{1}{T_m} \sum_{t=1}^{T_m} \chi_{A_i}(B_t^m) - B_{\text{obs}_i} \right) \chi'_{A_i}(B_1^m) + \lambda_1^m \\ \vdots \\ \sum_{i=1}^I \left( \frac{1}{M} \sum_{m=1}^M \frac{1}{T_m} \sum_{t=1}^{T_m} \chi_{A_i}(B_t^m) - B_{\text{obs}_i} \right) \chi'_{A_i}(B_{T_m}^m) + \lambda_{T_m}^m \end{array} \right) = 0, \\ \forall m = 1, \dots, M \end{aligned}$$

This condition holds if for every  $m = 1, \dots, M$  yields:

$$\left( \begin{array}{c} - \sum_{i=1}^I \left( \frac{1}{M} \sum_{m=1}^M \frac{1}{T_m} \sum_{t=1}^{T_m} \chi_{A_i}(B_t^m) - B_{\text{obs}_i} \right) \chi'_{A_i}(B_1^m) \\ \vdots \\ - \sum_{i=1}^I \left( \frac{1}{M} \sum_{m=1}^M \frac{1}{T_m} \sum_{t=1}^{T_m} \chi_{A_i}(B_t^m) - B_{\text{obs}_i} \right) \chi'_{A_i}(B_{T_m}^m) \end{array} \right) = \left( \begin{array}{c} \lambda_1^m \\ \vdots \\ \lambda_{T_m}^m \end{array} \right)$$

□

Again, we can solve the optimization problem by using the system equations (for explanation see paragraph path).

Now we calculate the derivative with respect to the control parameter. Therefore, we only consider the derivative with respect to  $\sigma_1$ . Then

$$\mathcal{L}_{\sigma_1}(B_t^m, \sigma_1) = \sum_{t=1}^{T_m} -\lambda_t^m \Delta W_t^m, \quad \forall m = 1, \dots, M$$

denotes the derivative of  $\mathcal{L}$  with respect to the control parameter.

#### TWO-DIMENSIONAL ATTRACTION ZONE

Again, we have an initial value problem, because there is no ending value given. We obtain the Lagrange function in analogy to the path:

$$\begin{aligned} \mathcal{L}(B_t^m, u) = & \frac{1}{2} \sum_{i=1}^I \left( \frac{1}{M} \sum_{m=1}^M \frac{1}{T_m} \sum_{t=1}^{T_m} \chi_{\Lambda_i}(B_t^m) - B_{\text{obs}_i} \right)^2 \\ & + \lambda_t^m (B_t^m - B_{t-1}^m - \sigma_2 \Delta W_{t-1}^m - 2[G^n(\tilde{B}_t^m)]^+ n(\tilde{B}_t^m)) \\ & \forall t = 2, \dots, T_m, \quad \forall m = 1, \dots, M. \end{aligned}$$

Then the Lagrange parameter fulfils the following theorem.

**Theorem 6.** *Lagrange parameter for the two-dimensional attraction zone*  
The Lagrange parameter for the two-dimensional attraction zone  $\lambda_2$  is given by the recursion formula

$$\begin{aligned} \lambda_{2t}^m = & \lambda_{2t+1}^m (1 + G_{B_t^m}(t+1)) \\ & - \sum_{i=1}^I \left( \frac{1}{M} \sum_{m=1}^M \frac{1}{T_m} \sum_{t=1}^{T_m} \chi_{\Lambda_i}(B_t^m) - B_{\text{obs}_i} \right) \chi'_{\Lambda_i}(B_t^m), \\ & \forall m = 1, \dots, M \quad t = T_m - 1, \dots, 1, \end{aligned}$$

where  $G_{B_t^m}$  denotes the derivative of  $[G^n(\tilde{B}_t^m)]^+ n(\tilde{B}_t^m)$  with respect to  $B_t^m$ .

*Proof.*

We calculate the derivative of  $\mathcal{L}$  with respect to  $B_t^m$ :

$$\begin{aligned} \mathcal{L}_{B_t^m}(B_t^m, u) = & \sum_{i=1}^I \left( \frac{1}{M} \sum_{m=1}^M \frac{1}{T_m} \sum_{t=1}^{T_m} \chi_{\Lambda_i}(B_t^m) - B_{\text{obs}_i} \right) \chi'_{\Lambda_i}(B_t^m) \\ & + \lambda_t^m - \lambda_{t+1}^m - 2\lambda_{t+1}^m G_{B_t^m}(t+1), \\ & \forall m = 1, \dots, M, \quad \forall t = 1, \dots, T_m - 1. \end{aligned}$$

We have a closer look on the last term of the derivative. Here we have to determine the derivative of the projection rule of the symmetrized Euler-Maruyama scheme with respect to  $B_t^m$ . We remember that there where two cases in this projection rule. The first one is simple, if  $\tilde{B}_t^m \in K$  the term is equal to zero and the derivative is zero as well. The second case is much more challenging. For  $\tilde{B}_t^m \notin K$ , the projection is unequal zero and we have to calculate its derivative. This problem

has been subject of many research papers (see e.g. Fitzpatrick and Phelps, 1982; Haraux, 1977; Shapiro, 1994). If we consider our special case, the projection in direction of the outward normal vector  $\mathbf{n}$  on a convex Polygon  $K$ , we have to distinguish between two different cases. The normal vector  $\mathbf{n}$  does not exist and we project the point  $\tilde{B}_t^m \notin K$  on the nearest vertex. Let  $(V_1, V_2)$  be the coordinates of this vertex, then holds for the length of the projection:

$$G^n \mathbf{n} = \tilde{B}_t^m - (V_1, V_2)^T,$$

where

$$\tilde{B}_t^m = B_{t-1}^m + \sigma_2 \Delta W_t^m.$$

The derivative of  $[G^n(\tilde{B}_t^m)]^+ \mathbf{n}(\tilde{B}_t^m)$  with respect to  $B_t^m$  is therefore given by 1.

For the second case,  $\mathbf{n}$  exists, we construct a line through the side of the polygon which contains the solution of the projection  $\pi_{\partial K}^n(\tilde{B}_t^m)$ . Then every point of this line fulfils the equation

$$y = mx + b, \tag{11}$$

where  $(x, y)$  are the coordinates of the points,  $m$  denotes the slope and  $b$  the intercept of the line. We can then describe the solution of the projection  $\pi_{\partial K}^n$  by the solution of the following optimization problem:

$$\begin{aligned} & \min_{x, y \in \partial K} \frac{1}{2} \left| \sqrt{(x - \tilde{B}_1)^2 + (y - \tilde{B}_2)^2} \right|^2 \\ & = \min_{x \in \mathbb{R}} \frac{1}{2} ((x - \tilde{B}_1)^2 + (mx + b - \tilde{B}_2)^2). \end{aligned}$$

For solving this minimization problem, we determine the derivative with respect to  $x$  and set it equal to zero:

$$\begin{aligned} 0 &= \frac{1}{2} (2(x - \tilde{B}_1) + 2m(mx + b - \tilde{B}_2)) \\ x + m^2 x &= \tilde{B}_1 - bm + m\tilde{B}_2 \\ x^* &= \frac{1}{1 + m^2} (\tilde{B}_1 + m\tilde{B}_2 - bm). \end{aligned}$$

Then we obtain  $y^*$  by plugging  $x^*$  into Equation 11:

$$y^* = \frac{m}{1 + m^2} (\tilde{B}_1 + m\tilde{B}_2 - bm) + b$$

In our case  $G^n$  is given by the Euclidean distance between  $\tilde{B}_t^m$  and  $(x^*, y^*)^T$  and the normal vector  $\mathbf{n}$  is the vector from the point  $(x^*, y^*)^T$  to the point  $\tilde{B}_t^m$  and therefore it holds:

$$G^n \mathbf{n} = \begin{pmatrix} \tilde{B}_1 - x^* \\ \tilde{B}_2 - y^* \end{pmatrix}.$$

We get for the derivative

$$G_{B_t^m} = \begin{pmatrix} 1 - \frac{1}{1+a^2} & -\frac{a}{1+a^2} \\ -\frac{a}{1+a^2} & 1 - \frac{a^2}{1+a^2} \end{pmatrix}.$$

Now we can summarize the three results:

$$G_{B_t^m} = \begin{cases} 0, & \tilde{B}_t^m \in K \\ 1, & \tilde{B}_t^m \notin K \text{ and } n \text{ does not exist} \\ \begin{pmatrix} 1 - \frac{1}{1+a^2} & -\frac{a}{1+a^2} \\ -\frac{a}{1+a^2} & 1 - \frac{a^2}{1+a^2} \end{pmatrix} & \tilde{B}_t^m \notin K \text{ and } n \text{ exists} \end{cases}.$$

We obtain for our necessary first order condition Equation 9 for each  $t = 1, \dots, T_{m-1}$ :

$$\sum_{i=1}^I \left( \frac{1}{M} \sum_{m=1}^M \frac{1}{T_m} \sum_{t=1}^{T_m} \chi_{A_i}(B_t^m) - B_{obs_i} \right) \chi'_{A_i}(B_t^m) + \lambda_t^m - \lambda_{t+1}^m (1 + G_{B_t^m}) = 0, \quad \forall m = 1, \dots, M$$

This condition holds if for every  $m = 1, \dots, M$  yields:

$$\begin{pmatrix} -\sum_{i=1}^I \left( \frac{1}{M} \sum_{m=1}^M \frac{1}{T_m} \sum_{t=1}^{T_m} \chi_{A_i}(B_t^m) - B_{obs_i} \right) \chi'_{A_i}(B_1^m) \\ \vdots \\ -\sum_{i=1}^I \left( \frac{1}{M} \sum_{m=1}^M \frac{1}{T_m} \sum_{t=1}^{T_m} \chi_{A_i}(B_t^m) - B_{obs_i} \right) \chi'_{A_i}(B_{T_m}^m) \end{pmatrix} = \begin{pmatrix} \lambda_1^m - \lambda_2^m (1 + G'(1)) \\ \vdots \\ \lambda_{T_{m-1}}^m - \lambda_{T_m}^m (1 + G'(T_m)) \end{pmatrix}.$$

By solving this equation, we again obtain the recursion formula for the Lagrange parameter  $\lambda_t$ .  $\square$

Now, we calculate the derivative with respect to the control parameter  $\sigma_2$ . Again the most challenging part is the derivative of the projection. In analogy to the derivative with respect to  $B_t^m$ , we denote with  $G_{\sigma_2}$  the derivative of  $[G^n(\tilde{B}_t^m)]^+ n(\tilde{B}_t^m)$  with respect to  $\sigma_2$  and it holds:

$$G_{\sigma_2}(t) = \begin{cases} 0, & \tilde{B}_t^m \in K \\ \Delta W_t^m, & \tilde{B}_t^m \notin K \text{ and } n \text{ does not exist} \\ \begin{pmatrix} 1 - \frac{1}{1+a^2} & -\frac{a}{1+a^2} \\ -\frac{a}{1+a^2} & 1 - \frac{a^2}{1+a^2} \end{pmatrix} \text{diag}(\Delta W_t^m) & \tilde{B}_t^m \notin K \text{ and } n \text{ exists} \end{cases}$$

For a better notation, we denote the term with

$$\mathcal{L}_{\sigma_2}(B, d_{2_t}^m) = \sum_{t=1}^{T_m} -\lambda_t^m \Delta W_t^m - 2\lambda_{t+1} G_{\sigma_2}(t), \quad \forall m = 1, \dots, M.$$

#### MIXED MODEL

In the preceding paragraphs, we have calculated the Lagrange parameter for each habitat zone: sample path, one- and two-dimensional attraction zone. Finally, we define the Lagrange parameter for our mixed model:

**Definition 17.** *Lagrange parameter for the mixed model*

Let  $\lambda_0$ ,  $\lambda_1$  and  $\lambda_2$  be given as above defined, then the Lagrange Parameter for the whole model is given by the following formulation:

$$\lambda^m(t, \cdot) = \begin{cases} \lambda_0^m(t, \cdot), & t \in T_{0_p}, \text{ for one } p \in \{1, \dots, P\} \\ \lambda_1^m(t, \cdot), & t \in T_{1_f}, \text{ for one } f \in \{1, \dots, F\} \\ \lambda_2^m(t, \cdot), & t \in T_{2_l}, \text{ for one } l \in \{1, \dots, L\} \end{cases},$$

$$t = 1, \dots, T_m, \quad m = 1, \dots, M.$$

In order to derive the Lagrange parameter for our whole calibration model we have to calculate the Lagrange parameter for every sub model and then we can arrange them in the suitable order.

Within this chapter, we managed to derive the calibration problem for our special model characteristics. With a suitable data set it is now possible to fit the model parameters to this empirical data. With the calibration it also possible to evaluate the model and to estimate the difference between the model prediction and empirical data. If this difference is too high, it is useful to add or to change some model assumptions in order to get a more realistic result. Additionally, we can justify our model assumptions with a good calibration result and make it applicable to many biologically induced questions.

## MODEL OF THE ADDITIONAL DEATH RISK CAUSED BY WIND TURBINES

---

In the previous chapters of this thesis we managed to derive an occurrence map of each bat or the local bat population, respectively. This map tells us how often the bats frequent special regions in the considered habitat. We now wonder what happens if we put several wind turbines into this habitat. It is obvious that not every bat which reaches a wind turbine is killed by it. In this chapter we want to derive a formula which gives us the risk for the bat being killed, depending on the type of the wind turbine and the wind velocity. This risk is varying between the simulated bat species, because every bat species has special movement behaviours, concerning the flight height. However, for most bat species, a wind turbine poses an attraction because they consider them as trees or are simply curious and explore the wind turbine by flying up and down the tower.

### 8.1 MODEL STRUCTURE

Let  $W \in \mathbb{R}^2$  be the position of the wind turbine which we consider in this chapter. In our previous chapters we have already built models which give us an occurrence map of the activity of our bat population. For calculating the number of bats reaching the considered wind turbine, we determined a radius  $r$  around the wind turbine, if the bat flies into this radius it is attracted by it (tallest tree hypothesis (Cryan et al., 2014)) with probability  $p_r \in [0, 1]$ . This gives us the number of bats reaching this special wind turbine position. Hereby  $p_r$  is not only dependent on the radius  $r$ , but it is also based on the type of the wind turbine, the landscape structure around the wind turbine (forest, field, etc.) and it has to be fitted to the simulated bat species.

Now, we want to calculate the probability of the bat actually being killed. This happens if the bat is hit by one of the three blades or if it suffers from barotrauma. This means that the dangerous zone for the bats is the area around the turning blades and where barotrauma can occur. The extent of this dangerous zone depends on various factors, e.g. the height of the wind turbine  $h$ , the rotor radius of the wind turbine  $b$  or the velocity of the turbine blades  $v$ , which itself depends on the prevailing wind intensity.

## 8.2 PROBABILITY DENSITY FUNCTIONS

For estimating the number of individuals that reach the dangerous circ area of the wind turbine (see Figure 27), we need occurrence functions for the distribution of flight height and for the vertical spread of the flight behaviour near the wind turbine. In the application of this model we would like to derive the density function for the flight height based on an empirical study which focusses on the flight height of bats near similar objects like wind turbines. But until we have these data we assume the following probability density functions:

### HEIGHT

For the height we assume a normal distribution. The mean  $\mu_1$  of the normal distribution is set to the average height of the crest level of the surrounding trees. This is especially meaningful for species which are used to hunting at this height.

$$\rho(x) = \frac{1}{\sigma_1 \sqrt{2\pi}} e^{-\frac{1}{2} \left( \frac{x-\mu_1}{\sigma_1} \right)^2}. \quad (12)$$

It is possible to fit the variance parameter  $\sigma_1$  to empirical data in order to obtain a realistic result.

### WIDTH

For the width along the wind turbine we also assume a normal distribution with mean  $\mu_2$  set on the position of the middle of the rotor. This is biologically meaningful because the bat is attracted by the tower of the wind turbine (highest tree hypothesis). Therefore, they are most attracted by the tower and then the attraction value flattens to the sides.

$$\theta(x) = \frac{1}{\sigma_2 \sqrt{2\pi}} e^{-\frac{1}{2} \left( \frac{x-\mu_2}{\sigma_2} \right)^2}. \quad (13)$$

The variance parameter  $\sigma_2$  also has to be fitted to empirical data.

## 8.3 KILLING RATE

We now derive the formula to calculate the number of fatalities for the population for one wind turbine.

We first need the visit number of one bat at the wind turbine location. This average number is given by the result of the Monte-Carlo simulation or of the PDE based approach and we denote it with  $N_{\text{position}}$ .

Then we need the number of bats flying to the dangerous circ area of



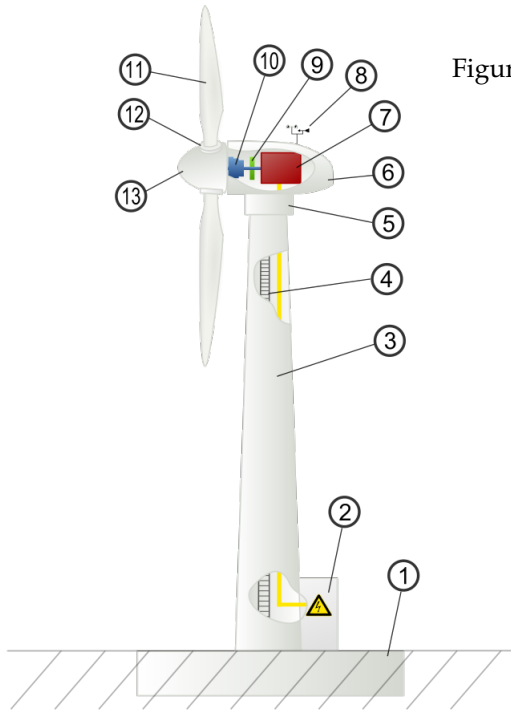


Figure 26: Technical description of a wind turbine:

- 1 foundation
  - 2 connection to electric grid
  - 3 tower
  - 4 access ladder
  - 5 wind orientation control
  - 6 nacelle
  - 7 generator
  - 8 anemometer
  - 9 brake
  - 10 gear box
  - 11 rotor blade
  - 12 blade pitch control
  - 13 rotor hub
- source: Arne Nordmann (commons.wikimedia.org)

the wind turbine. We can calculate this number by integrating over the circ area using the corresponding occurrence functions:

$$P_{\text{circ}}(h, b, \theta, \rho) = \int_{h-b}^{h+b} \int_{-\sqrt{b^2-(h-k)^2}}^{\sqrt{b^2-(h-k)^2}} \theta(y) dy \rho(k) dk,$$

where  $\rho$  is the occurrence function for the flight height (see Equation 12) and  $\theta$  is the occurrence function for the spatial flight distribution (see Equation 13).  $[h-b, h+b]$  denotes the integration domain for the flight height,  $h-b$  is the lowest point of the circ area and  $h+b$  is the highest point.

$[-\sqrt{b^2-(h-k)^2}, \sqrt{b^2-(h-k)^2}]$  denotes the dangerous spatial area, which we derive by using the Pythagorean theorem (for explanation see Figure 27). It is possible to include the density functions based on empirical data here.

Finally the rate of actual hitting the blades is given by the following formula:

$$P_{\text{blades}} = \begin{cases} 3 \frac{t}{s}, & \text{if } 3 \frac{t}{s} \leq 1 \\ 1, & \text{if } 3 \frac{t}{s} > 1 \end{cases},$$

where  $s$  is the time that one blade needs to go round and  $t$  is the time that a bat needs to cross the dangerous sector. If the bat needs more time to cross the dangerous section than one blade need to finish one-third of a round ( $t \geq \frac{1}{3}$ ), it is definitely hit by a blade and so

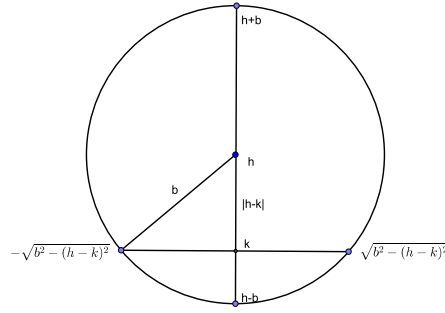


Figure 27: Integration scheme: circ area generated by the wind turbine blades with rotor height  $h$  and blade radius  $b$ .

the killing rate will be one.

**Definition 18.** *Killing rate*

The killing rate of one wind turbine for the considered bat population is given by:

$$R = N_{\text{position}} P_{\text{circ}} P_{\text{blades}}. \quad (14)$$

#### 8.4 NUMERICAL IMPLEMENTATION

It is very challenging to solve the integral term for  $P_{\text{circ}}$  analytically. Especially for the use of discrete empirical occurrence functions it is impossible to get an analytical solution. Therefore, we will use a numerical approximation to calculate the value of this integral term.

We apply the Simpson rule to the above integral term. For an interval  $[a, b]$  we obtain the approximation:

$$S(f) = \frac{b-a}{6} \left( f(a) + 4f\left(\frac{a+b}{2}\right) + f(b) \right)$$

for the integral term  $\int_a^b f(x) dx$ .

The approximation error of this rule is  $\frac{1}{90} \left(\frac{b-a}{2}\right)^5 |f^{(4)}(\xi)|$ , with  $\xi$  between  $a$  and  $b$  (Deuffhard and Hohmann, 2008).

In order to get a better approximation result we want to apply the composite Simpson rule. Therefore, we split the interval  $[a, b]$  into  $N/2$  subintervals  $[x_{2i}, x_{2i+2}]$ ,  $i = 0, \dots, N/2 - 1$  with  $N$  even, such that

each subinterval has the same length  $h$ . Then we obtain the composite Simpson rule:

$$S_N(f) = \frac{h}{3} \left( \sum_{i=0}^{N/2-1} f(x_{2i}) + 4f(x_{2i+1}) + f(x_{i+1}) \right) \quad (15)$$

Here the approximation error can be estimated by:

$$\begin{aligned} \left| \int_a^b f(x) dx - S_N(f) \right| &\leq \sum_{i=0}^{N/2-1} \left| \int_{x_{2i}}^{x_{2i+2}} f(x) dx - \frac{h}{3} (f(x_{2i}) + 4f(x_{2i+1}) + f(x_{i+1})) \right| \\ &\leq \sum_{i=0}^{N/2-1} \left| \frac{h^5}{90} f^{(4)}(\xi_i) \right| \\ &\leq \frac{N h^5}{2 \cdot 90} \|f^{(4)}(\xi)\|_\infty \\ &= \frac{b-a}{180} h^4 \|f^{(4)}(\xi)\|_\infty, \end{aligned}$$

where  $\xi_i \in [x_{2i}, x_{2i+2}] \forall i = 0, \dots, N/2 - 1$ .

Applying this to our integral term  $P_{\text{circ}}$ , we obtain the following approximation.

**Lemma 1.** *Numerical approximation of the death rate*

*Using the composite Simpson rule, the approximation for Equation 14 is given by:*

$$\begin{aligned} S_M(I_2) &= \frac{b}{3M} \sum_{j=0}^{M-1} \left( \rho(k_j) + 4\rho\left(\frac{k_j + k_{j+1}}{2}\right) + \rho(k_{j+1}) \right) \\ &\quad * \left( \frac{\sqrt{b^2 - (h-k)^2}}{3N} \left[ \sum_{i=0}^{N-1} \theta(y_i) + 4\theta\left(\frac{y_i + y_{i+1}}{2}\right) + \theta(y_{i+1}) \right] \right) \end{aligned}$$

*Proof.* We start by approximating the inner integral term, which we denote with:

$$I_1 = \int_{-\sqrt{b^2 - (h-k)^2}}^{\sqrt{b^2 - (h-k)^2}} \theta(y) dy.$$

Then it follows with Equation 15 for  $y_0 = -\sqrt{b^2 - (h-k)^2}, y_1 = -\sqrt{b^2 - (h-k)^2} + \bar{h}, \dots, y_N = \sqrt{b^2 - (h-k)^2}$  with step size  $\bar{h} = \frac{2\sqrt{b^2 - (h-k)^2}}{N}$ :

$$S_N(I_1) = \frac{\sqrt{b^2 - (h-k)^2}}{3N} \left[ \sum_{i=0}^{N-1} \theta(y_i) + 4\theta\left(\frac{y_i + y_{i+1}}{2}\right) + \theta(y_{i+1}) \right].$$

For the second integral

$$I_2 = \int_{h-b}^{h+b} \text{Int}_1 \rho(k) dk$$

we set  $k_0 = h - b, k_1 = h - b + \tilde{h}, \dots, k_M = h + b$  for stepsize  $\tilde{h} = \frac{2b}{M}$ . Then we obtain the approximation:

$$S_M(I_2) = \frac{b}{3M} \sum_{j=0}^{M-1} \left( \rho(k_j) + 4\rho\left(\frac{k_j + k_{j+1}}{2}\right) + \rho(k_{j+1}) \right) \left( \frac{\sqrt{b^2 - (h - k_j)^2}}{3N} \left[ \sum_{i=0}^{N-1} \theta(y_i) + 4\theta\left(\frac{y_i + y_{i+1}}{2}\right) + \theta(y_{i+1}) \right] \right).$$

□

This numerical framework makes it possible to calculate the number of bat fatalities caused by one or by several wind turbines. We want to use this extra mortality for estimating the effect of the wind turbines for our local bat population. Therefore, we have a look at the theory of population size modelling in the next chapter.

## POPULATION GROWTH MODELS WITH APPLICATION TO A LOCAL BAT POPULATION

---

### 9.1 INTRODUCTION

Growth or decay of population sizes has been the issue of research since the 18th century. Thereby lots of different effects on the development of a population were examined, e.g. different growth rates, carrying capacity of the natural habitat (Verhulst, 1845; Vogels et al., 1975), interaction between different species (see e.g. Lotka, 1925; Volterra, 1927) and age effects (Leslie, 1945).

One of the first mathematical models to describe population dynamics with differential equations was proposed by Malthus. In the 18th century, he described population growth by the following linear ordinary differential equation

$$\frac{d}{dt}P(t) = \alpha P(t) - \mu P(t) = \delta P(t),$$

which is also called Malthus' Law (Malthus, Winch, and James, 1992). The parameter  $\delta = \alpha - \mu$  is called Malthusian parameter of the population. In this model the population size increases without any restrictions and independent on the population size which is certainly a very hard assumption and nearly never fulfilled in a real population. Therefore, Pierre Francois Verhulst considered a different approach (Verhulst, 1845, 1847; Vogels et al., 1975). He assumed that not arbitrary many individuals can survive together in the same habitat, so he derived the logistic function:

$$\frac{dN(t)}{dt} = rN(t) \left(1 - \frac{N(t)}{K}\right)$$

Here  $N(t)$  is the number of individuals at time  $t$ ,  $r$  is the intrinsic growth rate of the population and  $K$  is the carrying capacity of the environment. This means that only  $K$  individuals can survive in the considered habitat. A reason for this restriction can be for example a finite amount of food resources.

The logistic equation can be solved explicitly and has the solution

$$N(t) = \frac{K}{1 + CKe^{-rt}}$$

with  $C$  given through the initial condition such that:  $C = 1/N(0) - 1/K$  where  $N(0)$  is the initial number of individuals. In this model

the population grows until it reaches the carrying capacity, independent on other influence factors like age effects or predators. Verhulst extends Malthus' Law by introducing this carrying capacity and this results in a more realistic model for population growth. However, the growth or decay of population size is certainly not just dependent on a constant growth rate and a carrying capacity.

Another extension of population growth model is the assumption of more than one species. One of the most famous models of this type is the Lotka-Volterra model (Lotka, 1925; Volterra, 1927) which treats the interaction between two species. Here the growth rate of the predator population is proportional to the population size of prey individuals and vice versa. The food supply for the prey population is assumed unlimited and the predator population is dependent on the prey population. The equation for the prey population is of the following form:

$$\frac{dx}{dt} = \alpha x - \beta xy, \quad (16)$$

where  $x$  is the number of prey individuals and  $y$  is the number of predator individuals,  $\alpha$  is the growth rate of the prey population and  $\beta$  is the decay rate of prey individuals due to being killed by the predators. In the case of  $y = 0$  the prey population growth is unlimited and we obtain again Malthus' Law.

For the predator population yields

$$\frac{dy}{dt} = \delta xy - \gamma y, \quad (17)$$

where  $\delta$  is the growth rate for the predator population and  $\gamma$  represents the decay of individuals due to emigration or death. Equation 16 and Equation 17 are also called Predator-Prey equations. The solutions of this model is often of periodic type.

In 1945 Patrick Leslie extended the work of Lotka. He introduced life tables and presented age-structured models (Leslie, 1945). With this models it is possible to represent different effects during a life cycle on the individual. The individuals are separated in different age classes and every age class can have different birth and death rates. This is especially meaningful for species with a high life expectancy.

In this chapter we present the general theory of modelling population developments. We introduce several approaches for modelling population size over a fixed time horizon. We start with a simple discrete model which describes the population size development by the difference between the number of births and the number of deaths. Thereby we include a carrying capacity for the habitat. Then we derive an ordinary differential equation model for simulating the effect

of time dependent birth and death rate. Again we include a carrying capacity.

Moreover, we introduce age-dependent population models. In the discrete case we present matrix population models which make it possible to describe different fertility and death rates for predefined age classes inside the population. The most challenging part is the inclusion of the carrying capacity which is valuable for the cumulative population size, because we do not want to define a carrying capacity for each age class but only one for the whole population size. We again derive the continuous version, a hyperbolic PDE model, for this age-dependent case and include the carrying capacity into the model equation as well.

Finally we fit every model to our considered bat species and we include the danger of wind turbines into the models. For this purpose we add the above calculated additional death risk (caused by the considered wind turbines) and evaluate the effects for the local bat population.

## 9.2 TIME-DEPENDENT POPULATION MODELS

### 9.2.1 Discrete model

We start with the discrete version similar to Malthus Law. We can describe the general development of the population size as follows:

$$\begin{aligned}n(t+1) &= n(t) + B(t) - D(t) + I(t) - E(t), \quad t = 0, \dots, T \\n(0) &= n_0\end{aligned}$$

Here  $n(t)$  is the number of individuals at time  $t$ ,  $B$  is the number of births,  $D$  is the number of deaths,  $I$  is the number of immigrants,  $E$  is the number of emigrants and  $n_0$  is the initial number of individuals at time  $t = 0$ .

**Remark 10.**

*I is the only number which can exceed the population size  $n(t)$ . The number of immigrants is not dependent on  $n(t)$ .*

Usually, the carrying capacity of the considered environment is limited. That means that the maximum number of individuals is determined by the available resources. So there is a need to reduce the number of individuals if there are too many offsprings. This can happen by a reduced birth rate, an increased death rate or the offsprings have to migrate to another habitat until only the number of individuals is left that can survive with the available resources. Hence, we want to include a carrying capacity  $K$  as first introduced by Verhulst.

**Definition 19.** *Carrying capacity  $K$*

For the population size  $n$  and carrying capacity  $K$  hold:

$$n(t) \leq K \quad \forall t = 0, \dots, T.$$

This carrying capacity is dependent on the natural habitat (food resources, water supply, roost opportunities, etc.) and on the considered species.

Additionally we introduce birth, death, immigration and emigration rate.

**Definition 20.** *Rates*

For all  $t \in [0, T]$  we define the following rates:

- Birth rate  $b(t) = \frac{B(t)}{n(t)} \in [0, 1]$
- Death rate  $d(t) = \frac{D(t)}{n(t)} \in [0, 1]$
- Immigration rate  $i(t) = \frac{I(t)}{n(t)} \in [0, \infty]$
- Emigration rate  $e(t) = \frac{E(t)}{n(t)} \in [0, 1]$

By using the two Definitions 19 and 20, we can define a discrete population model with carrying capacity using the logistic function of Verhulst.

**Definition 21.** *Discrete population model with carrying capacity*

We describe the population development by:

$$n(t+1) = n(t) + (b(t) - d(t) + i(t) - e(t))n(t) \left(1 - \frac{n(t)}{K}\right)$$

$$n(0) = n_0$$

where  $K$  is the carrying capacity,  $n_0$  is the initial number of individuals and the other terms are as defined in Definition 20.

**Remark 11.**

The last term of the equations causes a population decrease if  $n(t) > K$  and a population increase if  $n(t) < K$ .

For constant functions  $e$ ,  $i$ ,  $d$  and  $b$  we introduce the following lemma for the long-time behaviour of  $n$ :

**Theorem 7.** *Long-time behaviour (discrete case)*

For constant  $e$ ,  $i$ ,  $d$ ,  $b$  such that  $b - d - i + e \neq 0$  and  $t \rightarrow \infty$  the solution of

$$n(t+1) = n(t) + (b - d + i - e)n(t) \left(1 - \frac{n(t)}{K}\right)$$

$$n(0) = n_0$$

converges to  $K$  or to  $0$ .



*Proof.* We can say that

$$\lim_{t \rightarrow \infty} n(t+1) = \lim_{t \rightarrow \infty} n(t)$$

therefore follows

$$\begin{aligned} \lim_{t \rightarrow \infty} n(t+1) &= \lim_{t \rightarrow \infty} \left( n(t) + (b-d+i-e)n(t) \left( 1 - \frac{n(t)}{K} \right) \right) \\ \Leftrightarrow \lim_{t \rightarrow \infty} n(t+1) &= \lim_{t \rightarrow \infty} n(t) + \lim_{t \rightarrow \infty} \left( (b-d+i-e)n(t) \left( 1 - \frac{n(t)}{K} \right) \right) \\ &\Leftrightarrow 0 = \lim_{t \rightarrow \infty} \left( (b-d+i-e)n(t) \left( 1 - \frac{n(t)}{K} \right) \right) \\ &\Leftrightarrow 0 = (b-d+i-e) \lim_{t \rightarrow \infty} n(t) \left( 1 - \frac{\lim_{t \rightarrow \infty} n(t)}{K} \right) \\ &\Leftrightarrow 0 = (b-d+i-e) \lim_{t \rightarrow \infty} n(t) \quad \vee \quad 0 = 1 - \frac{\lim_{t \rightarrow \infty} n(t)}{K} \\ &\Leftrightarrow 0 = \lim_{t \rightarrow \infty} n(t) \quad \vee \quad 1 = \frac{\lim_{t \rightarrow \infty} n(t)}{K} \\ &\Leftrightarrow 0 = \lim_{t \rightarrow \infty} n(t) \quad \vee \quad K = \lim_{t \rightarrow \infty} n(t) \end{aligned}$$

□

For the non constant case, we can not clearly determine whether the population size converge to zero, to the carrying capacity  $K$  or if there is another long-time behaviour like a periodic solution. This depends on the development of the growth rate  $b-d+i-e$ .

### 9.2.2 ODE model

Now we want to transfer our discrete model to an ordinary differential equation model. By using a Taylor expansion we can define the following initial value problem.

**Definition 22.** *ODE model for population size*

*With the above used notation, the population size satisfies*

$$\frac{\partial n(t)}{\partial t} = (b(t) - d(t) + i(t) - e(t))n(t) \left( 1 - \frac{n(t)}{K} \right), \quad t \in [0, \infty), \quad (18)$$

with

$$n(0) = n_0, \quad (19)$$

where  $n_0$  again is the initial number of individuals.

For constant birth, death, immigration and emigration rates,

$$n(t) = \frac{n_0 K e^{rt}}{K + n_0 (e^{rt} - 1)}$$

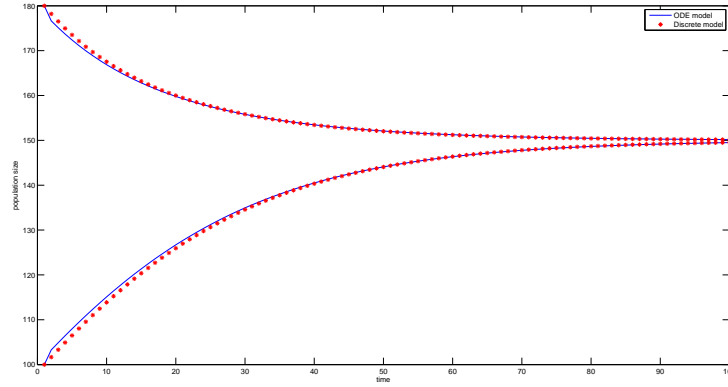


Figure 28: Effect of the carrying capacity. Population model for  $K = 150$  and two different initial population sizes. For  $n_0 = 180$  the population size decreases until it reaches the carrying capacity and for  $n_0 = 100$  the population size increases until it reaches the carrying capacity. The solution of the ODE model (blue line) and the solution of the discrete model (red dots) converge to each other with increasing  $t$ .

denotes an analytical solution for Equation 18 with initial condition Equation 19 (Murray, 2011) and  $r = b - d + i - e$  (Murray, 2011).

Again we can analyse the behaviour for  $t \rightarrow \infty$ .

**Theorem 8.** *Long-time behaviour (continuous case)*

For constant  $e, i, d, b$  such that  $r = b - d - i + e \neq 0$  and  $t \rightarrow \infty$  holds

$$\lim_{t \rightarrow \infty} n(t) = \lim_{t \rightarrow \infty} \frac{n_0 K e^{rt}}{K + n_0 (e^{rt} - 1)} = \begin{cases} 0, & \text{if } r < 0 \\ K, & \text{if } r > 0 \\ n_0, & \text{if } r = 0 \end{cases}$$

*Proof.* For  $r = 0$  we can simply calculate the solution and obtain

$$n(t) = \frac{n_0 K}{K} = n_0,$$

for  $r > 0$  follows with L'Hôpital's rule

$$\begin{aligned} \lim_{t \rightarrow \infty} n(t) &= \lim_{t \rightarrow \infty} \frac{n_0 K e^{rt}}{K + n_0 (e^{rt} - 1)} \\ &= \frac{\lim_{t \rightarrow \infty} n_0 r K e^{rt}}{\lim_{t \rightarrow \infty} n_0 r e^{rt}} \\ &= K \end{aligned}$$

and for the last case  $r < 0$  holds:

$$\begin{aligned}\lim_{t \rightarrow \infty} n(t) &= \lim_{t \rightarrow \infty} \frac{n_0 K e^{rt}}{K + n_0 (e^{rt} - 1)} \\ &= \frac{0}{K - n_0} = 0\end{aligned}$$

□

**Remark 12.**

For  $t \rightarrow \infty$  and  $r > 0$  this solution converges to  $K$ . The population grows until it has reached the carrying capacity  $K$  and then its size stays constant. For  $r < 0$  this solution converges to  $0$ . That means that the population becomes extinct.

We illustrate the effect of the carrying capacity for the discrete and the continuous model in Figure 28. Therefore, we start with one initial population size above and one under the defined carrying capacity. We can see for both cases that the population size converges to the carrying capacity  $K$ .

We have introduced the basic idea of population growth. Now we want to transfer this to our special model species.

### 9.2.3 Age-independent models for a local bat population

In the last section we have presented the general theory of population size modelling. In our case we have some specific properties which we want to consider in the following sections. Therefore, we set  $e(t) = -i(t)$ , because it is very difficult to find data for emigration or immigration rates for a specific bat colony.

#### 9.2.3.1 Discrete model

We divide our considered time period into summer and winter time, which is useful because bats hibernate and their behaviour depend therefore strongly on the prevailing season. We start with the summer period. Although the reproduction takes place in winter, we attach the birthrate to the summer season because the offsprings are not born until spring.

We assume an initial number  $n_0$  of individuals. Furthermore, we assume that every individual is female, because we only consider the nursery colony. We ignore the male individuals by assuming that enough male individuals are there to guarantee a maximum reproduction.

We split our model as above mentioned into two periods. Summer is our initial season and we start our model with  $n_0$  individuals. Birth

takes only place in the summer period. Furthermore, we exclude multiple births in our model such that  $b \in [0, 1]$ .

We assume an average death rate of  $d_s \in [0, 1]$  in summer and  $d_w \in [0, 1]$  in winter. For the summer period in year  $t + 1$ , we then obtain

$$n_s(t+1) = n_w(t) + (b - d_s)n_w(t) \left(1 - \frac{n_w(t)}{K}\right),$$

where  $n(t)$  is the number of individuals that are alive at the beginning of the summer period of year  $t + 1$ .

For the winter period we obtain respectively

$$n_w(t+1) = n_s(t+1) - d_w n_s(t+1).$$

In winter there is only a decrease in population size possible, so we do not need to include the carrying capacity into our model.

For the number of individuals at the end of the time period  $t + 1$  we obtain

$$\begin{aligned} n_w(t+1) &= n_w(t) + (b - d_s)n_w(t) \left(1 - \frac{n_w(t)}{K}\right) \\ &\quad - d_w \left( n_w(t) + (b - d_s)n_w(t) \left(1 - \frac{n_w(t)}{K}\right) \right) \\ &= n_w(t) + (b - d_s - d_w(1 + b - d_s))n_w(t) \left(1 - \frac{n_w(t)}{K}\right) \end{aligned}$$

Besides the carrying capacity  $K$  which influences the size of the population, the second term determines whether the population increases ( $b - d_s - d_w(1 - b - d_s) > 0$ ) or decreases ( $b - d_s - d_w(1 + b - d_s) < 0$ ).

The increase of wind energy production affects the bat populations. Many bats die by collision or by the turbulences of the wind turbines. But how big is this effect and causes it a decrease of bat populations? We want to answer this question with our model. Therefore, we identify the added death rate  $d_a \in [0, 1]$  which is caused by the wind turbines. We obtain the new population model by simply adding the additional death rate to the summer period

$$n_s(t+1) = n_w(t) + (b - d_s - d_a)n_w(t) \left(1 - \frac{n_w(t)}{K}\right)$$

The general population size development can be defined as follows:

**Definition 23.** *Discrete population size model for a local bat population*  
The population size development fulfils

$$\begin{aligned} n(t+1) &= n(t) \\ &\quad + (b - d_s - d_a - d_w(1 + b - d_s - d_a))n(t) \left(1 - \frac{n(t)}{K}\right) \end{aligned}$$

for every  $t \geq 0$ .

For the long term behaviour of the population size we have to examine the term  $b - d_s - d_t - d_w(1 + b - d_s - d_a)$ . We have to decide whether this term is positive or negative. This result leads to a population growth to the carrying capacity or to zero, respectively.

### 9.2.3.2 ODE model

For fitting the ODE model to our specific model characteristics, we do not have to split the model into two periods. We only have to define the time-dependent death rate  $d(t)$ , the time-dependent birth rate  $b(t)$  and the time-dependent additional death rate caused by the wind turbine  $d_a(t)$ . Furthermore let  $K > 0$  be again the carrying capacity. Then we obtain the following definition.

**Definition 24.** *ODE model for population size of local bat population*  
Let  $n_0$  be the initial number of individuals at time  $t = 0$ . Then the initial value problem

$$\begin{aligned} \frac{\partial n(t)}{\partial t} &= (b(t) - d(t) - d_a(t))n(t) \left(1 - \frac{n(t)}{K}\right), \quad t \in [0, \infty) \\ n(0) &= n_0 \end{aligned}$$

*describes the population development of our local bat population.*

For this time-dependent case it is not possible to solve the above equation analytically, so we need to use numerical methods to approximate the solution. However, we can say that if  $b(t) > d(t) - d_a(t)$  for all  $t$  the population size increases and if  $b(t) < d(t) - d_a(t)$  for all  $t$  the population size decreases. In all other cases the population size oscillates and we have to do further examinations to estimate the long term behaviour.

For piecewise constant birth and death rates (as in the discrete case) we obtain the following initial value problem:

$$\begin{aligned} \frac{\partial n(t)}{\partial t} &= (b - d_s - d_a - d_w(1 + b - d_s - d_a))n(t) \left(1 - \frac{n(t)}{K}\right), \\ & \quad t \in [0, \infty) \\ n(0) &= n_0. \end{aligned}$$

For this formulation we can again present an analytical solution

$$n(t) = \frac{n_0 K e^{rt}}{K + n_0 (e^{rt} - 1)}$$

for  $r = b - d_s - d_a - d_w(1 + b - d_s - d_a)$ . Again the sign of  $r$  indicates whether the population grows until the carrying capacity or whether it became extinct. The effect of this term is illustrated in Figure 29 for the discrete and the continuous model. Here we can see that it strongly depends on the growth rate  $r$  whether the population has a chance to survive in the future.

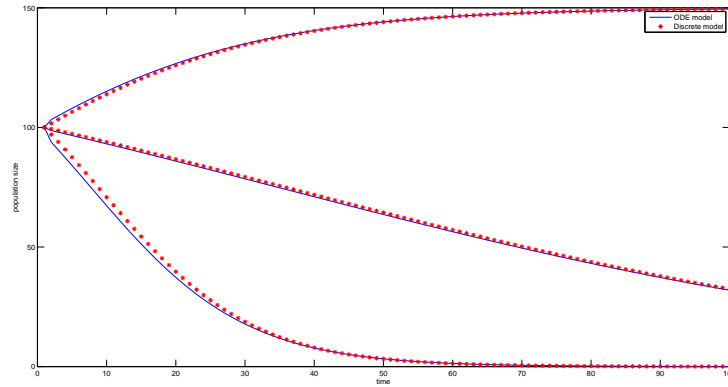


Figure 29: Effect of birth rate. Population model for carrying capacity  $K = 150$ , initial population size  $n_0 = 100$ , three different birth rates  $b = 0.6, 0.7, 0.9$  and death rates  $d_w = 0.3$ ,  $d_s = 0.2$ ,  $d_a = 0.2$ . Only for the highest birth rate the population grows. For the other two birth rates the population decays. The ODE (blue line) and the discrete solution (red dots) again converge to each other.

### 9.3 AGE-DEPENDENT POPULATION MODELS

Another type of population models considers age-dependent processes, e.g. age-dependent fertility or death rates. So it is possible to assume different properties for an individual during its life cycle. This is especially useful for species with a long life expectation.

#### 9.3.1 Discrete age-dependent model: the Leslie matrix

We start by considering a discrete version of age-structured population models. In the introduction we have mentioned the work of Leslie. He introduced matrices in population growth theory to describe the population size in certain age classes. These matrices are also called Leslie matrices.

The Leslie model or matrix is one common technique to model an age-structured population. Therefore, we have to define a discrete set of age classes  $i = 1, \dots, I$ . An individual belongs to class  $i$  if  $i - 1 \leq x < i$  holds for the age of the individual. Then we project the population from time point  $t$  to the next time point  $t + 1$ , such that the surviving individuals of age class  $i$  belong to age class  $i + 1$  in time point  $t + 1$ . Therefore let  $n(t) \in \mathbb{R}^I$  be a vector and its elements  $n_i(t)$  define the number of individuals in each age class  $i$  at time  $t$ . Let  $P_i \in [0, 1]$  be the surviving probability of an individual of age class  $i = 1, \dots, s - 1$  at time point  $t$ . To complete the model we set  $P_s = 0$ , i.e. the individuals of age class  $s - 1$  have no chance to survive and achieve age

$s + 1$ . This simply means that we define a maximum age that the individuals can achieve.

Then we describe the projection to the next time period by the following rule:

$$n_{i+1}(t + 1) = P_i n_i(t), \quad i = 1, \dots, s - 1 \tag{20}$$

An exception of this rule is of course the first age class, because it can not be achieved by projection. For  $i = 1$  the number of individuals  $n_1(t + 1)$  origins from the reproduction of all other classes. Hence, let  $F_i(t)$  be the per capita fertility of age class  $i \forall i = 1, \dots, s$  at time point  $t$ . Then yields for  $i = 1$  naturally:

$$n_1(t + 1) = \sum_{i=1}^s F_i n_i(t) \tag{21}$$

With Equation 20 and Equation 21 we can define the projection matrix.

**Definition 25.** *Projection matrix*

Let  $F_i$  be the fertility rates for age class  $i$  at time period  $t$  for  $i = 1, \dots, s$  and  $P_i$  be the survival rates for age class  $i = 1, \dots, s - 1$ . We set  $P_s = 0$ . This simply means that no individual can survive the last age class. Then we can define the projection matrix  $A$ :

$$A = \begin{pmatrix} F_1 & \dots & \dots & F_s & \\ P_1 & 0 & \dots & & 0 \\ 0 & P_2 & 0 & \ddots & 0 \\ \ddots & & \ddots & & \vdots \\ 0 & \dots & 0 & P_{s-1} & 0 \end{pmatrix}$$

such that we can describe the projection of the population to the next time period by the following projection rule:

$$n(t + 1) = An(t), \quad t = 0, \dots, T$$

The definition above gives us the population development for the constant case, i.e. the birth and the survival rates stay constant for the whole time horizon. Of course we can include a time or/and population dependent matrix  $A$ . Then we obtain the following cases:

**Remark 13.** *Different cases for the projection matrix  $A$*

- *Linear case:  $A$  is time dependent*

$$n(t + 1) = A_t n(t)$$

- *Non-linear case:  $A$  is dependent on the population size*

$$n(t + 1) = A_n n(t)$$

- *Inhomogeneous non-linear case: A depends on time and on the population size*

$$n(t+1) = A_{n,t}n(t)$$

*It depends on the assumptions concerning the population dynamics, which of the four cases is most suitable. The more variables we include, the more realistic the resulting model gets. However, we also need very detailed information about the considered species to identify the matrix A and a very detailed data set to calibrate the model.*

### 9.3.1.1 Birth and population increase

Now we want to identify conditions in the matrix model that cause birth and therefore population increase. For this purpose we take a closer look to the previously defined age-structured population model. We again consider the projection matrix A, the population vector  $n(t)$  and the corresponding model equation:

$$n(t+1) = An(t)$$

Then we can describe the population size by using the eigenvalues  $\lambda_i$  of the matrix A.

#### **Theorem 9.**

*Let  $\lambda_i$ , where  $i = 1, \dots, s$ , be the eigenvalues of matrix A and  $w_i$  the corresponding eigenvectors. Then we can describe the population size at time t by*

$$n(t) = \sum_{i=1}^s c_i \lambda_i^t w_i. \quad (22)$$

*Proof.*

Let  $w$  be the right eigenvector of A and the scalar  $\lambda$  the corresponding eigenvalue if

$$Aw = \lambda w.$$

This implies that  $(A - \lambda I)w = 0$ , where I is here the identity matrix. General linear algebra theory tells us that a nonzero solution for  $w$  only exists if  $(A - \lambda I)$  is singular, i.e. if

$$\det(A - \lambda I) = 0.$$

Additionally the vector  $v$  is called left eigenvector if for the complex conjugate transpose  $v^*$

$$v^*A = \lambda v^*$$

holds.

For a  $s$ -dimensional matrix A we will have  $s$  eigenvalue-eigenvector



pairs and the characteristic equation is a polynomial of order  $s$ . We assume that all eigenvectors are linearly independent.

We now describe the initial population  $n_0$  as a linear combination of the right eigenvectors  $w_i$ :

$$\begin{aligned} n_0 &= c_1 w_1 + \dots + c_s w_s \\ &= \begin{pmatrix} w_1 & \dots & w_s \end{pmatrix} \begin{pmatrix} c_1 \\ \vdots \\ c_s \end{pmatrix} \\ &= Wc \end{aligned}$$

with coefficients  $c_i$  and  $W$  the matrix whose columns are the right eigenvectors  $w_i$ . We apply this to our projection rule and obtain for  $t = 1$

$$n(1) = An_0 = \sum_{i=1}^s c_i Aw_i = \sum_{i=1}^s c_i \lambda_i w_i.$$

Then yields for  $t = 2$

$$\begin{aligned} n(2) &= An(1) = AAn_0 = A \sum_{i=1}^s c_i Aw_i = A \sum_{i=1}^s c_i \lambda_i w_i \\ &= \sum_{i=1}^s c_i \lambda_i Aw_i \\ &= \sum_{i=1}^s c_i \lambda_i^2 w_i. \end{aligned}$$

Equation 22 follows by induction. □

**Remark 14. Eigenvalues**

We can see that the long-term behaviour of the population size  $n(t)$  depends on the eigenvalues  $\lambda_i$  of  $A$ .  $n(t)$  is dependent on the term  $\lambda_i^t$ . Therefore, we get exponential growth for  $\lambda_i > 1 \forall i$  and exponential decay for  $0 < \lambda_i < 1 \forall i$ . For other cases we often get oscillations.

9.3.1.2 Asymptotic analysis and strong ergodic theorem

Here we consider the behaviour of the population size for  $t \rightarrow \infty$ . We therefore start with the definitions of asymptotic analysis and ergodicity which are often used in the context of the long time behaviour of population size.

**Definition 26. Asymptotic analysis (Keyfitz and Caswell, 2006)**

Asymptotic analysis describes the behaviour of the population size for a long time horizon. Here we can determine whether a population shrinks, expands or stays stable in the future.

**Definition 27.** *Ergodicity (Keyfitz and Caswell, 2006)*

*Ergodicity indicates the model dependence on the initial conditions. A model is called ergodic, if its asymptotic dynamics are independent of initial conditions.*

We want to analyse the behaviour of the matrix  $A$  for different scenarios. Therefore, we need some terms of matrix algebra. Hence, we start with some further definitions, which we later use for proving the behaviour of  $n(t)$  for  $t \rightarrow \infty$ .

**Definition 28.** *Nonnegative/ positive matrix*

*A matrix is called nonnegative if all elements are greater than or equal to zero.*

*A matrix is called positive if all elements are strictly greater than zero.*

**Remark 15.**

*A negative entry in a population projection matrix implies a negative number of individuals. Hence, all population projection matrices are at least nonnegative. However, they are usually not positive.*

**Definition 29.** *Irreducibility (Keyfitz and Caswell, 2006)*

*A nonnegative matrix  $A$  is irreducible if its life cycle graph contains a path from every node to every other node.*

**Definition 30.** *Primitivity (Keyfitz and Caswell, 2006)*

*A irreducible nonnegative matrix  $A$  is primitive if there exists some  $k > 0$  such that  $A^k$  is strictly positive.*

**Remark 16.**

*Since  $P_i > 0 \forall i = 1, \dots, k - 2$ , our projection matrix  $A$  is primitive and irreducible.*

Now we can introduce the well known Perron-Frobenius theorem which we later apply to our projection matrix.

**Theorem 10.** *Perron-Frobenius theorem (Keyfitz and Caswell, 2006; Meyer, 2000)*

*Let  $A$  be a nonnegative, irreducible  $s \times s$  matrix and  $\lambda_1$  denote the greatest eigenvalue of  $A$ . Then holds:*

- $\lambda_1 > 0$  and  $\lambda_1 \in \mathbb{R}$  and  $\lambda_1$  is a simple root of the characteristic equation ( $\text{algmult}_A(\lambda_1) = 1$ ),
- the corresponding eigenvectors  $w_1$  and  $v_1$  are real and  $> 0$  if  $A$  is primitive and  $\geq 0$  if  $A$  is imprimitive.
- there exists no other eigenvalue with nonnegative eigenvectors

For a proof see for example (Meyer, 2000).

Now we consider again the population growth rate and present the strong ergodic theorem which connects the eigenvalue  $\lambda_1$  with the growth rate of the population size.

**Theorem 11.** *Strong ergodic theorem (Cohen, 1979)*  
 Let  $\lambda_1 > |\lambda_i|$  for  $i \geq 2$  be the eigenvalues of matrix  $A$ . Then

$$\lim_{t \rightarrow \infty} \frac{n(t)}{\lambda_1^t} = c_1 w_1$$

holds, where  $c_1$  is a positive constant and  $w_1$  is the eigenvector which corresponds to the biggest eigenvalue  $\lambda_1$ .

**Remark 17.**

Hence, the long-term evolution of the population size  $n(t)$  divided by the population growth rate  $\lambda_1^t$  is equal to a constant vector. Therefore, the population growth rate behaves asymptotically like the biggest eigenvalue  $\lambda_1$  of matrix  $A$ .

*Proof.*

Let  $n_0 = \sum_{i=1}^s c_i w_i$  be the vector that contains the age structure of the initial population. Then we can represent the population size by:

$$\begin{aligned} n(t) &= A n(t-1) = A A n(t-2) = \dots = A^t n_0 \\ &= A^t \sum_{i=1}^s c_i w_i = \sum_{i=1}^s c_i A^t w_i \\ &= \sum_{i=1}^s c_i \lambda_i^t w_i \\ &= \lambda_1^t \left( c_1 w_1 + \sum_{i=2}^s c_i \left( \frac{\lambda_i}{\lambda_1} \right)^t w_i \right) \end{aligned}$$

The assumption that  $\lambda_1$  is the biggest eigenvalue yields  $\left( \frac{\lambda_i}{\lambda_1} \right) < 1$ . Therefore

$$\begin{aligned} \lim_{t \rightarrow \infty} n(t) &= \lambda_1^t (c_1 w_1 + 0) \\ &= \lambda_1^t c_1 w_1. \end{aligned}$$

holds and this completes the proof.  $\square$

### 9.3.1.3 Euler-Lotka equation

We have found out that the biggest eigenvalue of the Leslie matrix is of great importance for the growth or the decay of the population size. Now we take a look at the structure of our matrix  $A$  to find out, if it is possible to compute the eigenvalues.

We again consider the following matrix:

$$A = \begin{pmatrix} F_0 & \cdots & \cdots & F_{s-1} & \\ P_0 & 0 & \cdots & & 0 \\ 0 & P_1 & 0 & \ddots & 0 \\ \ddots & & \ddots & & \vdots \\ 0 & \cdots & 0 & P_{s-2} & 0 \end{pmatrix} \quad (23)$$

with the fertility rate  $F_i$ ,  $i = 0, \dots, s-1$  of age class  $i$  and the survival rates  $P_i$ ,  $i = 0, \dots, s-2$  for age class  $i$ . Additionally, we set  $P_{s-1} = 0$ .

**Theorem 12.** *Population growth rate*

Let  $A \in \mathbb{R}^{s \times s}$  be our population projection matrix as given in Equation 23. Then we can calculate the population growth rate  $\lambda$  by only using the number of births  $b_i$  of age class  $i$  and the probabilities of surviving until age  $i$   $l_i$ :

$$1 = \sum_{k=1}^s \frac{l_k b_k}{\lambda^k}$$

with

$$b_{i+1} = \frac{F_i}{P_i}, \quad i = 0, \dots, s-1 \quad (24)$$

and

$$l_{i+1} = P_i l_i, \quad i = 0, \dots, s-1 \quad (25)$$

where  $l_0 = 1$ .

*Proof.*

For proving the theorem we need that

$$\prod_{k=0}^i P_k = \frac{l_1}{l_0} \frac{l_2}{l_1} \cdots \frac{l_{i+1}}{l_i} = \frac{l_{i+1}}{l_0} = l_{i+1} \quad (26)$$

The last equality holds because  $l_0 = 1$ .

Let  $\lambda$  be an eigenvalue of our matrix, then holds  $n_i(t+1) = P_{i-1} n_{i-1}(t)$  for  $i = 1, \dots, s-1$ . This can simply be seen by Definition 25. Then we can follow with Theorem 11:

$$\begin{aligned} \lim_{t \rightarrow \infty} \frac{n(t)}{\lambda^t} &= \lim_{t \rightarrow \infty} \frac{n(t+1)}{\lambda^{t+1}} = \frac{1}{\lambda} \lim_{t \rightarrow \infty} \frac{An(t)}{\lambda^t} \\ &= \frac{1}{\lambda} \lim_{t \rightarrow \infty} \frac{1}{\lambda^t} \begin{pmatrix} F_0 n_1(t) + \cdots + F_{s-1} n_s(t) \\ P_0 n_1(t) \\ \vdots \\ P_{s-2} n_{s-1}(t) \end{pmatrix} \end{aligned}$$

Hence, for each  $n_i(t)$ ,  $i = 2, \dots, s$ :

$$\begin{aligned} \lim_{t \rightarrow \infty} \frac{n_i(t)}{\lambda^t} &= \frac{1}{\lambda} \lim_{t \rightarrow \infty} \frac{P_{i-2} n_{i-1}(t)}{\lambda^t} = \frac{P_{i-2}}{\lambda} \lim_{t \rightarrow \infty} \frac{n_{i-1}(t)}{\lambda^t} \\ &= \frac{P_{i-2}}{\lambda} \frac{P_{i-3}}{\lambda} \lim_{t \rightarrow \infty} \frac{n_{i-2}(t)}{\lambda^t} = \dots \\ &= \frac{\prod_{k=0}^{i-2} P_k}{\lambda^{i-1}} \lim_{t \rightarrow \infty} \frac{n_1(t)}{\lambda^t} = \frac{l_{i-1}}{\lambda^{i-1}} \lim_{t \rightarrow \infty} \frac{n_1(t)}{\lambda^t} \end{aligned}$$

The last equality follows with Equation 26.

For the first element of  $n(t)$  we have:

$$\begin{aligned} \lim_{t \rightarrow \infty} \frac{n_1(t)}{\lambda^t} &= \frac{1}{\lambda} \lim_{t \rightarrow \infty} \frac{1}{\lambda^t} \sum_{i=0}^{s-1} F_i n_{i+1}(t) \\ &= \frac{1}{\lambda} \left( \sum_{i=0}^{s-1} F_i \lim_{t \rightarrow \infty} \frac{n_{i+1}(t)}{\lambda^t} \right) \\ &= \frac{1}{\lambda} \left( \sum_{i=0}^{s-1} F_i \frac{l_i}{\lambda^i} \lim_{t \rightarrow \infty} \frac{n_1(t)}{\lambda^t} \right). \end{aligned}$$

Division by the left hand side yields

$$1 = \frac{1}{\lambda} \sum_{i=0}^{s-1} F_i \frac{l_i}{\lambda^i}.$$

By using Equation 24 we reformulate the equation:

$$1 = \frac{1}{\lambda} \sum_{i=0}^{s-1} b_{i+1} P_i \frac{l_i}{\lambda^i}.$$

Finally we obtain

$$1 = \frac{1}{\lambda} \sum_{i=0}^{s-1} b_{i+1} \frac{l_{i+1}}{l_i} \frac{l_i}{\lambda^i} = \sum_{i=0}^{s-1} b_{i+1} \frac{l_{i+1}}{\lambda^{i+1}} = \sum_{i=1}^s \frac{b_i l_i}{\lambda^i}.$$

by using Equation 25. □

**Remark 18.**

*Unfortunately, the equation above is not only true for the biggest eigenvalue of  $A$  but also for all other eigenvalues.*

9.3.1.4 Carrying capacity

The implementation of a carrying capacity into an age-dependent model is not as simple as in the age independent cases. In the age-dependent case we consider each age class on its own, but we do not want to define a carrying capacity for each age class, because this is not biologically meaningful. Instead we want that the population size  $\sum_{i=1}^s n_i(t)$  converges to a carrying capacity  $K$  as in the age-independent models.

**Definition 31.** *Carrying capacity for the matrix model*

Let  $A$  be the projection matrix as given before and let  $K$  be the carrying capacity. Then

$$\mathbf{n}(t+1) = A \left( \mathbf{n}(t-1) + \mathbf{n}(t) \left( 1 - \frac{\sum_{i=1}^s n_i(t)}{K} \right) \right) \quad (27)$$

denotes the projection rule.

We again have a look at the long-time behaviour of the population size for the above described projection rule.

**Theorem 13.** *Long-time behaviour (matrix model)*

For the above described projection rule,  $\sum_{i=1}^s n_i(t)$  for  $t \rightarrow \infty$  converges to the carrying capacity  $K$  or  $\lim_{t \rightarrow \infty} n_i(t) = 0 \forall i = 1, \dots, s$ .

*Proof.* We reformulate the projection rule Equation 27

$$\begin{aligned} \mathbf{n}(t+1) &= A \left( \mathbf{n}(t-1) + \mathbf{n}(t) \left( 1 - \frac{\sum_{i=1}^s n_i(t)}{K} \right) \right) \\ &= A\mathbf{n}(t-1) + A\mathbf{n}(t) \left( 1 - \frac{\sum_{i=1}^s n_i(t)}{K} \right) \\ &= \mathbf{n}(t) + A\mathbf{n}(t) \left( 1 - \frac{\sum_{i=1}^s n_i(t)}{K} \right) \end{aligned}$$

Consider  $t \rightarrow \infty$ :

$$\begin{aligned}
\lim_{t \rightarrow \infty} n(t+1) &= \lim_{t \rightarrow \infty} n(t) + \lim_{t \rightarrow \infty} An(t) \left( 1 - \frac{\sum_{i=1}^s n_i(t)}{K} \right) \\
\Leftrightarrow \lim_{t \rightarrow \infty} n(t+1) - \lim_{t \rightarrow \infty} n(t) &= \lim_{t \rightarrow \infty} An(t) \left( 1 - \frac{\sum_{i=1}^s n_i(t)}{K} \right) \\
\Leftrightarrow 0 &= A \lim_{t \rightarrow \infty} n(t) \left( 1 - \frac{\lim_{t \rightarrow \infty} \sum_{i=1}^s n_i(t)}{K} \right) \\
\Leftrightarrow 0 &= A \lim_{t \rightarrow \infty} n(t) \quad \vee \quad 1 - \frac{\lim_{t \rightarrow \infty} \sum_{i=1}^s n_i(t)}{K} \\
\Leftrightarrow 0 &= A \lim_{t \rightarrow \infty} n(t) \quad \vee \quad \lim_{t \rightarrow \infty} \sum_{i=1}^s n_i(t) = K \\
\Leftrightarrow 0 &= \lim_{t \rightarrow \infty} \begin{pmatrix} \sum_{i=1}^{s-1} F_i n_i(t) \\ P_1 n_1(t) \\ \vdots \\ P_{s-1} n_{s-1}(t) \end{pmatrix} \quad \vee \quad \lim_{t \rightarrow \infty} \sum_{i=1}^s n_i(t) = K \\
\Leftrightarrow \lim_{t \rightarrow \infty} \sum_{i=1}^{s-1} F_i n_i(t) &= 0 \\
\wedge \quad \lim_{t \rightarrow \infty} P_i n_i(t) &= 0 \quad \forall i = 1, \dots, s-1 \quad \vee \quad \lim_{t \rightarrow \infty} \sum_{i=1}^s n_i(t) = K \\
\Leftrightarrow \lim_{t \rightarrow \infty} n_0(t+1) &= 0 \\
\wedge \quad \lim_{t \rightarrow \infty} n_i(t+1) &= 0 \quad \forall i = 2, \dots, s-1 \quad \vee \quad \lim_{t \rightarrow \infty} \sum_{i=1}^s n_i(t) = K \\
\Leftrightarrow \lim_{t \rightarrow \infty} n_i(t) &= 0 \quad \forall i = 0, \dots, s-1 \quad \vee \quad \lim_{t \rightarrow \infty} \sum_{i=1}^s n_i(t) = K
\end{aligned}$$

□

For the optimal parameter choice the solution of Equation 27 converge to the carrying capacity  $K$ . We can see this in the numerical example in Figure 30. For the same parameters as in the age independent cases (blue line and red dots) the solution of the matrix model (green dots) converges to the same population size. In the other case the number of individuals in each age class converge to zero and the population dies out.

### 9.3.2 Continuous age-dependent models

Again, we want to derive a continuous approach for the easier implementation of time-dependent birth and death rates. We introduce an age variable  $a \in \mathbb{R}_+$ . Then  $n(a, t)$  denotes the age density function at time  $t$ . We can define an upper bound for the age variable  $a$  which we denote by  $\bar{a}$ . This should be the highest age that an individual in

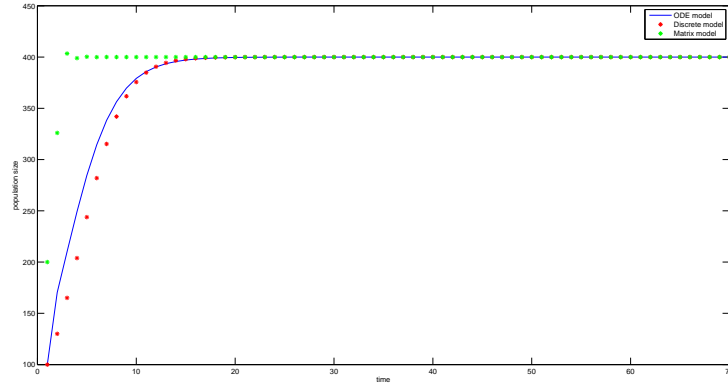


Figure 30: Effect of the carrying capacity for the matrix model.  $K = 400$ ,  $b = 0.7$ ,  $d = 0.3$  and five age classes

the population can achieve and it holds  $a \in [0, \bar{a}]$ . Analogously let  $b(a, t)$  be the age dependent birth rate and  $d(a, t)$  be the age dependent death rate.

Then we can calculate the number of individuals of age between  $a_1$  and  $a_2$  at time  $t$ :

$$n(a_1 : a_2, t) = \int_{a_1}^{a_2} n(s, t) ds$$

Let  $N(t) = \int_0^{\bar{a}} n(a, t) da$  denote the total population size at time  $t$ . Analogously  $B(t) = \int_0^{\bar{a}} b(a, t) n(a, t) da$  denotes the total number of births at time  $t$ . At the same time it is equal to  $n(0, t)$ , the number of individuals at age 0 at time  $t$ . The total number of deaths is defined by  $D(t) = \int_0^{\bar{a}} d(a, t) n(a, t) da$ .

For the next time point we have the following rule

$$n(a+1, t+1) = n(a, t)(1 - d(a, t))$$

gives us the number of individuals in the next age class. This means that the number of individuals of age  $a+1$  at time  $t+1$  is equal to the number of individuals of age  $a$  at time  $t$  and survived until the next time step  $t+1$ .

By using a Taylor expansion we obtain

$$n(a, t) + \frac{\partial n(a, t)}{\partial a} + \frac{\partial n(a, t)}{\partial t} + \mathcal{O}(a^2 + t^2) = n(a, t)(1 - d(a, t)).$$

We can represent this equation by the hyperbolic PDE formulation and therefore define the continuous age-dependent population model:

**Definition 32.** *Continuous age-dependent population size model*

For  $n(a, t)$  the number of individuals at age  $a$  at time  $t$  holds

$$\frac{\partial n}{\partial t} + \frac{\partial n}{\partial a} = -d(a, t)n(a, t), \quad (28)$$



where the first age class is given by:

$$n(0, t) = \int_0^{\bar{a}} b(a, t)n(a, t)da$$

and a given initial population size structure

$$n(a, 0) = n_0(a).$$

### 9.3.2.1 Carrying capacity

We want to include a carrying capacity into this model as well. The population size at time  $t$  is given by the integral term

$$\int_0^{\bar{a}} n(a, t)da.$$

Then we can include the carrying capacity as we did in the age independent case and obtain a PIDE formulation:

**Definition 33.** *Carrying capacity for the continuous age-dependent case*  
Let  $K > 0$  be the carrying capacity of the considered habitat. Then we get

$$\frac{\partial n}{\partial t} = - \left( \frac{\partial n}{\partial a} + d(a, t)n(a, t) \right) \left( 1 - \frac{\int_0^{\bar{a}} n(a, t)da}{K} \right)$$

for the population size development, where the first age class is given by

$$n(0, t) = \int_0^{\bar{a}} b(a, t)n(a, t)da$$

and a given initial population size structure

$$n(a, 0) = n_0(a).$$

**Remark 19.**

*For only one age class, the above described formulation would transform to the age-independent case.*

## 9.3.3 Age-dependent models for a local bat population

### 9.3.3.1 Matrix model

We divide our bat population into  $I$  age classes. Furthermore, we assume constant fertility rates  $F_i, i = 1, \dots, I$ . For the survival probabilities we orientate on the discrete model. The survival rate for age class  $i$  in the summer period is  $1 - d_s(i)$  and in the winter period  $1 - d_w(i)$ , respectively. Hence, the survival rate for age class  $i$  for the total year is  $P_i = (1 - d_s(i))(1 - d_w(i))$ . Then we can describe the matrix model for our bat population as follows.

**Definition 34.** *Matrix model for the bat population*

For the projection equation

$$n(t+1) = A \left( n(t-1) + n(t) \left( 1 - \frac{\sum_{i=1}^s n_i(t)}{K} \right) \right), \quad t = 0, \dots, T$$

holds, where

$$A = \begin{pmatrix} F_1 & \cdots & \cdots & F_I & \\ P_1 & 0 & \cdots & & 0 \\ 0 & P_2 & 0 & \ddots & 0 \\ \ddots & & \ddots & & \vdots \\ 0 & \cdots & 0 & P_{I-1} & 0 \end{pmatrix}$$

with  $P_i = (1 - d_s(i))(1 - d_w(i)) \forall i$ .

Certainly we also want to include the additional danger of wind turbines for the local bat population. We assume this danger to be age independent and only occurring during the summer period. We denote the additional risk for each age class besides the first by  $d_a$ . Then our matrix  $A$  changes into

$$A = \begin{pmatrix} F_1 & \cdots & \cdots & F_I & \\ \hat{P}_1 & 0 & \cdots & & 0 \\ 0 & \hat{P}_2 & 0 & \ddots & 0 \\ \ddots & & \ddots & & \vdots \\ 0 & \cdots & 0 & \hat{P}_{I-1} & 0 \end{pmatrix}$$

with  $\hat{P}_i = (1 - d_s(i) - d_a)(1 - d_w(i)) \forall i$ .

### 9.3.3.2 Continuous age-dependent model

We adjust Equation 28 to our specific model properties:

**Definition 35.** *Continuous age-dependent model for the bat population*

We can represent the age dependent continuous growth model for a local bat population by the following initial value problem:

$$\begin{aligned} \frac{\partial n}{\partial t} &= - \left( \frac{\partial n}{\partial a} + d(a, t)n(a, t) \right) \left( 1 - \frac{\int_0^{\bar{a}} n(a, t)}{K} \right), & t \in (0, T], \\ & & a \in (0, \bar{a}] \\ n(a, 0) &= n_0(a), & a \in (0, \bar{a}] \\ n(0, t) &= \int_0^{\bar{a}} b(a, t)n(a, t) da, & t \in (0, T] \end{aligned}$$

with  $\bar{a}$  being the maximum age of the population and  $d(a, t) = 1 + (1 - d_s(a))(1 - d_w(a))$ .

We now include again the danger of the wind turbines into our model by increasing the death rate  $\hat{d}$ .

**Definition 36.** *Continuous age-dependent model for the bat population with increased death probability*

We can represent the age dependent continuous growth model for a local bat population through the following initial value problem:

$$\begin{aligned} \frac{\partial n}{\partial t} &= - \left( \frac{\partial n}{\partial a} + \hat{d}(a, t)n(a, t) \right) \left( 1 - \frac{\sum_{l=1}^J n(l, i)}{K} \right), & t \in (0, T], \\ & & a \in (0, \bar{a}] \\ n(a, 0) &= n_0(a), & a \in (0, \bar{a}] \\ n(0, t) &= \int_0^{\bar{a}} b(a, t)n(a, t)da, & t \in (0, T] \end{aligned}$$

with  $\bar{a}$  the maximum age of the population and  $\hat{d}(a, t) = 1 + (1 - d_s(a) - d_a)(1 - d_w(a))$ .

For the implementation of the above equation we use the discretization scheme of the Lax-Wendroff method which is a common discretization method for hyperbolic PDEs. We start by deriving this discretization scheme. Therefore, we use the Taylor expansion of the function  $n$ . Let  $\Delta a$  and  $\Delta t$  be the step sizes for the age and time intervals  $[0, \bar{a}]$  and  $[0, T]$ , respectively:

$$n(t + \Delta t, a) = n(t, a) + \Delta t \frac{\partial n(t, a)}{\partial t} + \frac{\Delta t^2}{2} \frac{\partial^2 n(t, a)}{\partial t^2} + \mathcal{O}(\Delta t^3) \quad (29)$$

Now we consider a more simple version of the above hyperbolic PDE:

$$\frac{\partial n(t, a)}{\partial t} = - \frac{\partial n(t, a)}{\partial a} \quad (30)$$

For the second derivative we have

$$\frac{\partial^2 n(t, a)}{\partial t^2} = \frac{\partial^2 n(t, a)}{\partial a^2}. \quad (31)$$

We use Equation 30 and Equation 31 and apply them to Equation 29:

$$n(t + \Delta t, a) = n(t, a) - \Delta t \frac{\partial n(t, a)}{\partial a} + \frac{\Delta t^2}{2} \frac{\partial^2 n(t, a)}{\partial a^2} + \mathcal{O}(\Delta t^3)$$

By using forward differencing for the time derivative and the symmetrized difference quotient for the derivative with respect to  $a$  we obtain the Lax-Wendroff scheme

$$\begin{aligned} n(t + \Delta t, a) &= n(t, a) - \frac{\Delta t}{2\Delta a} (n(t, a + \Delta a) - n(t, a - \Delta a)) \\ &\quad + \frac{\Delta t^2}{2\Delta a^2} (n(t, a + \Delta a) - 2n(t, a) + n(t, a - \Delta a)) \quad (32) \\ &\quad + \mathcal{O}(\Delta t^2) + \mathcal{O}(\Delta a^2). \end{aligned}$$

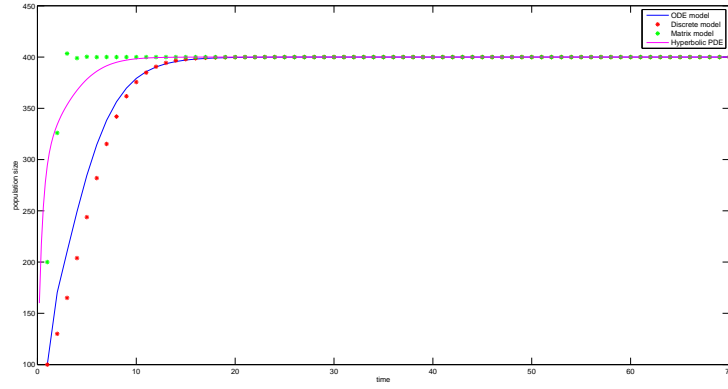


Figure 31: Effect of the carrying capacity for continuous age-dependent approach.  $K = 400$ ,  $b = 0.7$ ,  $\hat{d} = 0.3$ .

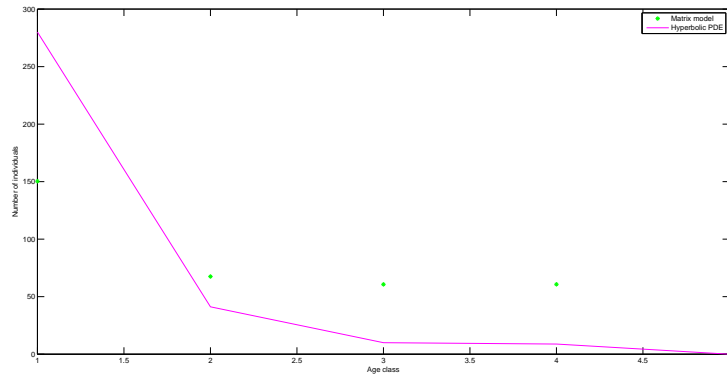


Figure 32: Number of individuals for each age class for the continuous and the discrete approach at time  $T = 70$ .

We now adapt Equation 32 to our hyperbolic equation. Therefore let  $J = \bar{a}/\Delta_a$  and  $I = T/\Delta_t$  be the number of age and of time discretisation steps, respectively. For notation purposes we set  $t_i = i$  and  $a_j = j$ . The integral term is approximated by using a composite trapezoidal rule. Then we obtain

$$\begin{aligned}
 n(j, i + 1) = & n(j, i) - \frac{\Delta t}{2\Delta a} (n(j + 1, i) - n(j - 1, i)) \left(1 - \frac{T_n(i)}{K}\right) \\
 & + \frac{\Delta t^2}{2\Delta a^2} (n(j + 1, i) - 2n(j, i) + n(j - 1, i)) \left(1 - \frac{T_n(i)}{K}\right) \\
 & - \Delta t \hat{d}(j, i) n(j, i) \left(1 - \frac{T_n(i)}{K}\right), \\
 j = & 2, \dots, J - 1, \quad i = 1, \dots, I - 1
 \end{aligned}$$

for each time step  $i = 1, \dots, T$  and each age class  $j = 1, \dots, J - 1$ , where

$$T_n(i) = \Delta_a \left( \frac{1}{2}(n(0, i) + n(J, i)) + \sum_{j=1}^{J-1} n(j, i) \right)$$

denotes the time dependent approximation of the integral term. The effect of the carrying capacity  $K$  to all four models is illustrated in Figure 31. Thereby we use the same parameter settings for all approaches and we can see that all model results converge to the carrying capacity  $K$ . The age-dependent approaches yield a faster convergence rate than the age-independent approaches, such that the population size reaches  $K$  in a shorter time horizon.

In Figure 32 we see the number of individuals for each age class for the discrete and the continuous approach.



## PARTIAL INTEGRO-DIFFERENTIAL EQUATIONS FOR SIMULATING SWARM BEHAVIOUR

---

In the previous chapters of this thesis, we have discussed the danger of wind turbines for a local bat population. Therefore we have simulated the behaviour of the foraging individuals in their habitat. These individuals act on their own most of the time and only adjust their behaviour to other bats when it comes to competitive behaviour, e.g. if there are too many individuals for the food supply in a special region.

Migrating birds or bats tend to fly in special swarm formations. By doing that, they naturally cross regions where wind turbines stand. Considering the effect of swarming to the danger caused by wind turbines is therefore necessary to predict a realistic number of fatalities.

Now, we want to consider these effects of swarm behaviour. In an animal swarm, the individuals not only consider their own preferences when they are moving but they include the behaviour of the individuals surrounding them into their moving decisions. Therefore it is not possible to simulate moving behaviour for each animal without considering the behaviour of the other animals. When we now want to simulate the behaviour of an animal  $x$  we have to include the behaviour of the animals  $y$  in a certain distance  $R$  to it, since their movement decisions depend on each other.

Often, the relevant parameter inside these swarms is the individual density. When this density becomes too high it is not possible for the animals to move properly, if it gets too low the swarm disperses. Therefore it is useful to simulate these swarm behaviours by simulating the density profile inside these swarms.

Modelling swarm behaviour by partial integro-differential equations (PIDEs) has become really common in recent years and many authors have made different approaches. We have already discussed these approaches in Chapter 2. Now, we have a closer look at the formulation of Mogilner and Edelstein-Keshet, 1999. We discuss the properties of this model and afterwards we want to state some theoretical extensions for this special model formulation.

## 10.1 SIMULATING ANIMAL SWARMS

In Chapter 2 we have presented many different models for modelling animal swarms. Although the described models are very similar and describe swarm behaviour by similar techniques, they all have different assumptions concerning diffusion, velocity, velocity range and many other parameters. Therefore we want to focus in the following section on the PIDE formulation of Mogilner and Edelstein-Keshet, 1999 because its application is really near to a bat or bird swarm. Hence, it is most suitable for our problem.

Therefore we start by taking a closer look at the PIDE formulation

$$\frac{\partial f(x, t)}{\partial t} = \frac{\partial}{\partial x} \left( D \frac{\partial f(x, t)}{\partial x} - V(f)f(x, t) \right), \quad x \in \mathbb{R}, t \in (0, \infty) \quad (33)$$

where the velocity  $V(f)$  is given by

$$V(f) = K * f = \int_{\mathbb{R}} K(x - y)f(y, t)dy.$$

Furthermore we include the initial condition

$$f(x, 0) = f_0.$$

to the above equation. This initial condition gives us the density profile of the swarm at time  $t = 0$ .

Here the velocity is given as a convolution of a kernel function  $K$  and the population density function  $f$ . This means that the velocity is dependent on the population density at a certain surrounding of the actual space coordinate. The kernel function  $K$  can be interpreted as density function. Since the meaning of an individual  $y$  for individual  $x$  decreases the bigger the distance is between them, the kernel function  $K$  usually flatten near the boundaries. This means that the individuals usually orientate more on the individuals near them, in other words which they can sense (e.g. by seeing). Individuals which are outside their sense range are usually not relevant for their movement decisions, so we can ignore them in the model. Therefore we can restrict the integration domain to a bounded set  $S$  which describes exactly the sensation radius of the individual at position  $x$ . The solution of this problem  $f(x, t)$  can be interpreted as density function, as well.

A possible example for this kernel function is the normal distribution density function. It weights the distance between the actual space coordinate  $x$  and the surrounding space coordinates. For a normal density function this means, on the one hand, that the closer the two



coordinates  $y$  and  $x$  are, so the smaller  $|x - y|$  gets, the higher is the effect of the population density at  $y$ . On the other hand, if  $y$  is far away from  $x$ , the normal distribution function tends to 0 and the effect of  $p(y)$  on the velocity vanishes.

Hence, the velocity represents the non-local term in the above PIDE description and the kernel function controls the behaviour of the swarm. The structure of  $K$  has a big effect on whether the swarm will collide, drifts away or stays stable. For a closer look on these different scenarios see Mogilner and Edelstein-Keshet, 1999. There they discussed different types of kernel functions and their long-time effects on the swarm.

10.2 WEAK FORMULATION

Above we have presented the problem formulation and the meaning and the effects of the different variables. In this section we want to look closer to the problem formulation. Hence, we examine some existence and uniqueness results of Equation 33 and therefore, we start by introducing some definitions which we need later in this section.

We start with the definition of some function spaces.

**Definition 37.** *Function spaces*

We define the function spaces  $L^2(\mathbb{R})$  and  $H^1(\mathbb{R})$  and the corresponding norms:

1.  $L^2(\mathbb{R}) = \{v : \mathbb{R} \rightarrow \mathbb{R} : \int_{\mathbb{R}} |v(x)|^2 dx < \infty\}$  with inner product  $\langle v, w \rangle_{L^2(\mathbb{R})} = \int_{\mathbb{R}} v(x)w(x) dx$
2.  $H^1(\mathbb{R}) = \{v \in L^2(\mathbb{R}) : v' \in L^2(\mathbb{R})\}$  with inner product  $\langle v, w \rangle_{H^1(\mathbb{R})} = \langle v, w \rangle_{L^2(\mathbb{R})} + \langle v', w' \rangle_{L^2(\mathbb{R})}$

Endowed with the norm  $\|\cdot\|_V = \sqrt{\langle \cdot, \cdot \rangle_V}$ , where  $V = \{L^2(\mathbb{R}), H^1(\mathbb{R})\}$ ,  $L^2(\mathbb{R})$  and  $H^1(\mathbb{R})$  are Hilbert spaces.

Furthermore, we present a definition of Sobolev spaces.

**Definition 38.** *Sobolev spaces*

Let  $m$  be a positive integer and  $1 \leq p \leq \infty$ . Further, let  $\|\cdot\|_{m,p}$  denote a norm on the following spaces:

- $W^{m,p}(\mathbb{R}) = \{u \in L^p(\mathbb{R}) : D^\alpha u \in L^p(\mathbb{R}) \text{ for } 0 \leq |\alpha| \leq m\}$ , where  $D^\alpha u$  denotes the weak partial derivative.
- $W_0^{m,p}(\mathbb{R}) = \overline{C_0^\infty(\mathbb{R})}$

Endowed with the above described norms, these two spaces are Hilbert spaces.

**Remark 20.**

It holds  $W^{k,2}(\mathbb{R}) = H^k(\mathbb{R})$  and therefore  $W^{1,2}(\mathbb{R}) = H^1(\mathbb{R})$  and  $W_0^{1,2}(\mathbb{R}) = H_0^1(\mathbb{R})$ .

In this section, we want to have a closer look on the weak solutions of Equation 33. Therefore we introduce the weak formulation of this equation in the following definition.

**Definition 39.** *Weak formulation*

Let the problem equation be given as before, then we can derive the weak formulation

$$\begin{aligned} & \int_{\mathbb{R}} \frac{\partial f(x, t)}{\partial t} v(x) dx \\ &= \int_{\mathbb{R}} \frac{\partial}{\partial x} \left( D \frac{\partial f(x, t)}{\partial x} - \int_S K(x-y) f(y, t) dy f(x, t) \right) v(x) dx \end{aligned}$$

by using the arbitrary test function  $v(x) \in H_0^1(\mathbb{R})$ .

By integrating the right side by parts, we can reformulate the right side into

$$\begin{aligned} & \int_{\mathbb{R}} \frac{\partial}{\partial x} \left( D \frac{\partial f(x, t)}{\partial x} - \int_S K(x-y) f(y, t) dy f(x, t) \right) v(x) dx \\ &= \int_{\mathbb{R}} \left( D \frac{\partial f(x, t)}{\partial x} - \int_S K(x-y) f(y, t) dy f(x, t) \right) v'(x) dx. \end{aligned}$$

Since  $v(x) \in H_0^1(\mathbb{R})$ , the boundary terms of the partial integration are equal to zero.

This formulation is non-linear in  $f$  and because of that it is rather complicate to handle it. We simplify the above equation in the next two sections in two different ways before we examine this original equation in Section 10.5.

### 10.3 LINEAR CASE I

First, we simplify the non-linear equation by setting one density function  $f$  constant. This makes it possible to show an existence and uniqueness result very quickly.

**Assumption 6.**

We assume the last term  $f(x, t)$  to be a constant  $\bar{f} \in \mathbb{R}$  and obtain a linear formulation of our equation:

$$\int_{\mathbb{R}} \frac{\partial f(x, t)}{\partial t} v(x) dx = \int_{\mathbb{R}} \left( D \frac{\partial f(x, t)}{\partial x} - \int_S K(x-y) f(y, t) dy \bar{f} \right) v'(x) dx \quad (34)$$

With this assumption it is possible to show that the right side of our equation is a bilinear form.

**Theorem 14.**

With Assumption 6 it follows, that

$$a(u, v) = \int_{\mathbb{R}} \left( D \frac{\partial u(x, t)}{\partial x} - \int_S K(x-y) u(y, t) dy \bar{f} \right) v'(x) dx$$

is a bilinear form.

*Proof.* Let  $\lambda$  and  $\mu \in \mathbb{R}$  be constants,  $g$  and  $u$  suitable functions, then it follows:

$$\begin{aligned}
& a(\lambda(f+g), \mu(v+u)) \\
&= \int_{\mathbb{R}} \left( D \frac{\partial \lambda(f+g)(x,t)}{\partial x} - \int_{\mathbb{R}} K(x-y)(\lambda(f+g))(y,t) dy \bar{f} \right) \\
& (\mu(v+u))'(x) dx \\
&= \lambda \mu \int_{\mathbb{R}} \left( D \frac{\partial f(x,t)}{\partial x} - \int_{\mathbb{R}} K(x-y)f(y,t) dy \bar{f} \right) (v'(x) + u'(x)) dx \\
&+ \lambda \mu \int_{\mathbb{R}} \left( D \frac{\partial g(x,t)}{\partial x} - \int_{\mathbb{R}} K(x-y)g(y,t) dy \bar{f} \right) (v'(x) + u'(x)) dx \\
&= \lambda \mu \int_{\mathbb{R}} \left( D \frac{\partial f(x,t)}{\partial x} - \int_{\mathbb{R}} K(x-y)f(y,t) dy \bar{f} \right) v'(x) dx \\
&+ \lambda \mu \int_{\mathbb{R}} \left( D \frac{\partial g(x,t)}{\partial x} - \int_{\mathbb{R}} K(x-y)g(y,t) dy \bar{f} \right) v'(x) dx \\
&+ \lambda \mu \int_{\mathbb{R}} \left( D \frac{\partial f(x,t)}{\partial x} - \int_{\mathbb{R}} K(x-y)f(y,t) dy \bar{f} \right) u'(x) dx \\
&+ \lambda \mu \int_{\mathbb{R}} \left( D \frac{\partial g(x,t)}{\partial x} - \int_{\mathbb{R}} K(x-y)g(y,t) dy \bar{f} \right) u'(x) dx \\
&= \lambda \mu (a(f, v) + a(g, v) + a(f, u) + a(g, u))
\end{aligned}$$

□

So we can describe our weak formulation by the variational formulation

$$\int_{\mathbb{R}} \frac{\partial u(x,t)}{\partial t} v(x) dx = a(u, v). \quad (35)$$

Now we examine the existence and uniqueness properties of a weak solution of our simplified model Equation 34. Therefore we introduce the following assumptions:

**Assumption 7.**

1. The diffusion coefficient is bounded ( $D \in [D_{\min}, D_{\max}]$ ) and positive ( $D_{\min} > 0$ ).
2. The constant  $\bar{f}$  is nonnegative ( $\bar{f} \geq 0$ ).
3. The kernel function is positive and bounded above through a constant  $\bar{K} > 0$ . ( $0 \leq K(x-y)^2 \leq \bar{K} \forall x, y \in \mathbb{R}$ ).

Applying these assumptions to our problem formulation, we can derive the next theorem, which gives us further properties of our bilinear form  $a$ .

**Theorem 15.**

If assumptions 7 holds, the bilinear form  $\mathfrak{a}$  satisfies the following properties:

1. *Continuity:*  $|\mathfrak{a}(\mathbf{u}, \mathbf{v})| \leq c \|\mathbf{u}\|_{H^1(\mathbb{R})} \|\mathbf{v}\|_{H^1(\mathbb{R})}$
2. *Gårding inequality:*  $\mathfrak{a}(\mathbf{u}, \mathbf{u}) + c_1 \|\mathbf{u}\|_{L^2(\mathbb{R})}^2 \geq c_2 \|\mathbf{u}\|_{H^1(\mathbb{R})}^2$

where  $c, c_1 \geq 0$  and  $c_2 > 0$  are constants.

*Proof.*

For notation, we set in the following  $L^2(\mathbb{R}) = L^2$  and  $H^1(\mathbb{R}) = H^1$ .

**First inequality:**

With the Cauchy-Schwarz inequality it follows:

$$\begin{aligned}
|\mathfrak{a}(\mathbf{u}, \mathbf{v})| &= \left| \int_{\mathbb{R}} D\mathbf{u}'\mathbf{v}' - \int_{\mathbb{R}} K(x-y)\mathbf{u}\mathbf{d}\mathbf{y}\bar{\mathbf{f}}\mathbf{v}'\mathbf{d}\mathbf{x} \right| \\
&\leq D_{\max} \|\mathbf{u}'\|_{L^2} \|\mathbf{v}'\|_{L^2} + \bar{\mathbf{f}} \left| \int_{\mathbb{R}} \left( \int_{\mathbb{R}} K(x-y)^2 \mathbf{u}^2 \right)^{1/2} \|\mathbf{v}'\|_{L^2} \mathbf{d}\mathbf{y}\mathbf{d}\mathbf{x} \right| \\
&\leq D_{\max} \|\mathbf{u}'\|_{L^2} \|\mathbf{v}'\|_{L^2} + \bar{\mathbf{f}} \|\mathbf{v}'\|_{L^2} \left| \int_{\mathbb{R}} \left( \int_{\mathbb{R}} K(x-y)^2 \mathbf{u}^2 \mathbf{d}\mathbf{y} \right)^{1/2} \mathbf{d}\mathbf{x} \right| \\
&\leq D_{\max} \|\mathbf{u}'\|_{L^2} \|\mathbf{v}'\|_{L^2} + \bar{\mathbf{f}}\bar{\mathbf{K}} \|\mathbf{v}'\|_{L^2} \left| \int_{\mathbb{R}} \left( \int_{\mathbb{R}} \mathbf{u}^2 \mathbf{d}\mathbf{y} \right)^{1/2} \mathbf{d}\mathbf{x} \right| \\
&\leq D_{\max} \|\mathbf{u}\|_{H^1} \|\mathbf{v}\|_{H^1} + \bar{\mathbf{f}}\bar{\mathbf{K}} \|\mathbf{v}\|_{H^1} \|\mathbf{u}\|_{H^1} \\
&\leq c \|\mathbf{u}\|_{H^1} \|\mathbf{v}\|_{H^1}
\end{aligned}$$

with  $c = D_{\max} + \bar{\mathbf{f}}\bar{\mathbf{K}}$ .

**Second inequality:**

$$\begin{aligned}
\mathfrak{a}(\mathbf{u}, \mathbf{u}) &= \int_{\mathbb{R}} D\mathbf{u}'\mathbf{u}'\mathbf{d}\mathbf{x} - \int_{\mathbb{R}} K(x-y)\mathbf{u}\mathbf{d}\mathbf{y}\bar{\mathbf{f}}\mathbf{u}'\mathbf{d}\mathbf{x} \\
&\geq D_{\min} \int_{\mathbb{R}} \mathbf{u}'^2 \mathbf{d}\mathbf{x} - \int_{\mathbb{R}} \int_{\mathbb{R}} K(x-y)\mathbf{u}\mathbf{d}\mathbf{y}\bar{\mathbf{f}}\mathbf{u}'\mathbf{d}\mathbf{x} \\
&= D_{\min} \|\mathbf{u}'\|_{L^2}^2 - \int_{\mathbb{R}} \int_{\mathbb{R}} K(x-y)\mathbf{u}\mathbf{d}\mathbf{y}\bar{\mathbf{f}}\mathbf{u}'\mathbf{d}\mathbf{x} \\
&= D_{\min} (\|\mathbf{u}\|_{H^1}^2 - \|\mathbf{u}\|_{L^2}^2) - \int_{\mathbb{R}} \int_{\mathbb{R}} K(x-y)\mathbf{u}\mathbf{d}\mathbf{y}\bar{\mathbf{f}}\mathbf{u}'\mathbf{d}\mathbf{x} \\
&\geq D_{\min} (\|\mathbf{u}\|_{H^1}^2 - \|\mathbf{u}\|_{L^2}^2) - \bar{\mathbf{K}}\bar{\mathbf{f}} \|\mathbf{u}\|_{L^2} \|\mathbf{u}'\|_{L^2} \\
&\geq D_{\min} (\|\mathbf{u}\|_{H^1}^2 - \|\mathbf{u}\|_{L^2}^2) - \frac{k^2}{4} \|\mathbf{u}'\|_{L^2}^2 - \frac{\bar{\mathbf{K}}\bar{\mathbf{f}}^2}{k^2} \|\mathbf{u}\|_{L^2}^2 \\
&\geq D_{\min} (\|\mathbf{u}\|_{H^1}^2 - \|\mathbf{u}\|_{L^2}^2) - \frac{k^2}{4} \|\mathbf{u}'\|_{H^1}^2 - \frac{\bar{\mathbf{K}}\bar{\mathbf{f}}^2}{k^2} \|\mathbf{u}\|_{L^2}^2 \\
&= \left( D_{\min} - \frac{k^2}{4} \right) \|\mathbf{u}\|_{H^1}^2 - \left( D_{\min} + \frac{\bar{\mathbf{K}}\bar{\mathbf{f}}^2}{k^2} \right) \|\mathbf{u}\|_{L^2}^2
\end{aligned}$$

with  $k > 0$  an arbitrary constant,  $c_1 = D_{\min} + \frac{\bar{\mathbf{K}}\bar{\mathbf{f}}^2}{k^2}$  and  $c_2 = D_{\min} - \frac{k^2}{4} > 0$  follows the inequality for  $k$  small enough.  $\square$

We can now present a theorem, which lead to a existence and uniqueness result of our equation.

**Theorem 16.** (Wloka, 1982)

Let the two conditions of Theorem 15 be fulfilled, then the solution of Equation 35 exists and is unique.

**Remark 21.**

We define a new bilinear form  $b(\mathbf{u}, \mathbf{v}) = a(\mathbf{u}, \mathbf{v}) + c_1 \langle \mathbf{u}, \mathbf{v} \rangle$ . Then it holds with Theorem 15:

$$\begin{aligned} |b(\mathbf{u}, \mathbf{v})| &\leq |a(\mathbf{u}, \mathbf{v})| + |c_1 \langle \mathbf{u}, \mathbf{v} \rangle| \\ &\leq c \|\mathbf{u}\|_{H^1} \|\mathbf{v}\|_{H^1} + |c_1 \langle \mathbf{u}, \mathbf{v} \rangle| \\ &\leq c \|\mathbf{u}\|_{H^1} \|\mathbf{v}\|_{H^1} + c_1 \|\mathbf{u}\|_{L^2} \|\mathbf{v}\|_{L^2} \\ &\leq (c + c_1) \|\mathbf{u}\|_{H^1} \|\mathbf{v}\|_{H^1} \\ &\leq \tilde{C} \|\mathbf{u}\|_{H^1} \|\mathbf{v}\|_{H^1} \end{aligned}$$

with  $\tilde{C} = c + c_1$  and

$$\begin{aligned} b(\mathbf{u}, \mathbf{u}) &= a(\mathbf{u}, \mathbf{u}) + c_1 \langle \mathbf{u}, \mathbf{u} \rangle = a(\mathbf{u}, \mathbf{u}) + c_1 \|\mathbf{u}\|_{L^2}^2 \\ &\geq c_2 \|\mathbf{u}\|_{H^1}^2. \end{aligned}$$

With the Lemma of Lax-Milgram it follows the existence of a unique solution  $\mathbf{u} \in V$  for the following equation:

$$b(\mathbf{u}, \mathbf{v}) = \int_{\mathbb{R}} \left( \frac{\partial \mathbf{u}(x, t)}{\partial t} + c_1 \mathbf{u}(x) \right) \mathbf{v}(x) dx, \quad \forall \mathbf{v} \in V$$

Then we can follow that there exists a unique solution  $\mathbf{u}$  for Equation 35, as well.

Hence, we showed existence and uniqueness for the weak solution of our simplified linear model equation. But unfortunately this linear formulation does not simulate the biological phenomenon we want to analyse.

#### 10.4 LINEAR CASE II

We assume now the term  $f(x, t)$  inside the integral operator to be constant  $\bar{f} \in \mathbb{R}$  (instead of the outer term). Then we convert our partial differential equation as follows

$$\frac{\partial \mathbf{u}(x, t)}{\partial t} = D \frac{\partial^2 \mathbf{u}(x, t)}{\partial x^2} - \frac{\partial}{\partial x} \left( \bar{f} \int_{\mathbb{R}} K(x - y) dy \mathbf{u}(x, t) \right), \quad x \in \mathbb{R}, t \in (0, \infty)$$

Since the kernel  $K$  is a density function it holds  $\int_{\mathbb{R}} K(x - y) dy = 1$  and the above equation transforms to

$$\frac{\partial \mathbf{u}(x, t)}{\partial t} = D \frac{\partial^2 \mathbf{u}(x, t)}{\partial x^2} - \bar{f} \frac{\partial \mathbf{u}}{\partial x}, \quad x \in \mathbb{R}, t \in (0, \infty).$$

The equation above is called the one-dimensional Fokker-Planck equation with constant diffusion coefficient and its stationary solution is well known (see e.g. Risken, 1984).

This equation is a better model equation for simulating swarm behaviour but still does not exactly describe the same as the non-linear equation. It is important to simulate a variable density function inside the integral operator, because only then the non local effects were seen in the model result. A constant density is a too simple assumption to simulate the complex swarm behaviour.

### 10.5 NON-LINEAR CASE

In the previous sections, we proved existence and uniqueness of the weak solution for two linearised cases. But we also explained why the linear cases do not describe the behaviour that we want to simulate for our application. Especially the non-local effects are not simulated correctly and so the formulations in both linear cases do not describe swarm behaviour properly. Hence, we now consider the original non-linear case and show a uniqueness result of this equation. Therefore, we again consider the weak formulation of our original problem. Furthermore be  $W(0, T) = \{u \in L^2(0, T; H^1(\mathbb{R})) : D_t u \in L^2(0, T; H^{-1}(\mathbb{R}))\}$ .

**Theorem 17.** *Uniqueness*

Let  $u \in W(0, T)$  be a bounded solution of Equation 33, such that  $\|u\|_{L^2(0, T; H^1(\mathbb{R}))} \leq d$ . Then this solution is unique.

*Proof.*

Let  $u, v \in W(0, T)$  be solutions of our problem with  $u(0) = v(0) = u_0$  and be  $w = u - v$ . For a better notation we define the linear function  $T : L^2(\mathbb{R}) \rightarrow \mathbb{R}$  with

$$T(u) = \int_{\mathbb{R}} K(x - y)u(y)dy$$

Then it follows  $w(t) \in L^2(\mathbb{R})$  and  $w_t = Dw_{xx} - (T(u)u)_x + (T(v)v)_x$ ,  $w(0) = 0$ .

Without loss of generality let  $D$  be equal to one. Then for all  $t$  holds:

$$\begin{aligned}
 \frac{1}{2} \frac{d}{dt} \|w\|_{L^2}^2 &= (w, w_t) \\
 &= (w, w_{xx} - (T(u)u)_x + (T(v)v)_x) \\
 &= -(w_x, w_x) + (T(u)u, w_x) - (T(v)v, w_x) \\
 &= -\|w_x\|_{L^2}^2 + (T(u)u - T(v)v, w_x) \\
 &= -\|w_x\|_{L^2}^2 + (T(u)(u - v) + (T(u) - T(v))v, w_x) \\
 &= -\|w_x\|_{L^2}^2 + (T(u)w + T(w)v, w_x) \\
 &\leq -\|w_x\|_{L^2}^2 + \|w_x\|_{L^2} (\|T(u)w\|_{L^2} + \|T(w)v\|_{L^2}) \\
 &\leq -\|w_x\|_{L^2}^2 + \|w_x\|_{L^2} (\underbrace{\|T(u)\|_{\infty} \|w\|_{L^2}}_{\leq \|u\|_{L^2} \|w\|_{L^2}} + \underbrace{\|T(w)\|_{\infty} \|v\|_{L^2}}_{\leq \|w\|_{L^2} \|v\|_{L^2}}) \\
 &\leq -\|w_x\|_{L^2}^2 + c \|w_x\|_{L^2} \|w\|_{L^2} \\
 &= -(\|w_x\|_{L^2} - \frac{c}{2} \|w\|_{L^2})^2 + \frac{c^2}{4} \|w\|_{L^2}^2 \\
 &\leq \frac{c^2}{4} \|w\|_{L^2}^2
 \end{aligned}$$

where  $c$  is a positive constant. We apply the Gronwall's inequality theorem:

**Theorem 18.** *Gronwall's Inequality*

Let  $I = [t_0, t_1]$  and let  $a, b : I \rightarrow \mathbb{R}$  be continuous functions and  $u : I \rightarrow \mathbb{R}$  satisfies

$$\begin{aligned}
 u'(t) &\leq a(t)u(t) + b(t), \quad t \in I \\
 u(t_0) &= u_0
 \end{aligned}$$

Then the solution of the above described inequality fulfils

$$u(t) \leq u_0 e^{\int_{t_0}^t a(s) ds} + \int_{t_0}^t e^{\int_s^t a(k) dk} b(s) ds.$$

In our case  $u_0 = b = 0$  and therefore, it follows  $\|w\| \leq 0$ . Consequently  $u(t) = v(t) \forall t$  and this proves the theorem.  $\square$

So we showed the uniqueness of the weak solution of our original model equation. Showing the existence of this non-linear equation is very challenging. Therefore this is a target for further research.

In this chapter, we examined the model formulation of Mogilner and Edelstein-Keshet, 1999 and we were able to show some theoretical results. For future research, it would be interesting to have a look on the practical implementation and the application to our model species and the collision risk with wind turbines. It is expectable that

swarm behaviour has a negative effect on the number of fatalities caused by wind turbines. The examination of this topic is of great importance for swarming animals and their survival probabilities near wind turbines or whole wind parks.



## CONCLUSION AND OUTLOOK

---

We finish this thesis by concluding our results and by pointing out the most important steps of our work. Therefore we give a short summary of each chapter of this thesis by presenting the major findings to point out the relevance of this work for estimating the danger for bats caused by wind turbines. Furthermore, we present additional application possibilities of the derived models.

Finally we give an outlook on possible extensions of this thesis and interesting open questions concerning the wildlife conflict of bats and wind turbines.

### 11.1 CONCLUSION

We start with an overview of each chapter and our main results and findings therein.

#### CHAPTER 2: LITERATURE REVIEW

In Chapter 2, we present an overview of different mathematical models simulating animal movement behaviour. We illustrate the different approaches, e.g. random walk models, Brownian bridges, PDE based approaches and PIDE formulations. Furthermore, we mention the corresponding areas of application for most of the models. Then we embed our model in this theory and point out the relevance of building a new model for bats foraging behaviour due to the specific and very complex movement characteristics of bats.

#### CHAPTER 3: MODEL ASSUMPTIONS

In Chapter 3, we introduce all assumptions which we use to build our IBM in Chapter 4 and for our PDE model in Chapter 6. We separate them in biologically induced assumptions and practically induced assumptions. We document the biologically induced assumptions with results described in recent research papers and point out their relevance for a realistic simulation of bats' movement behaviour. For each assumption motivated by practical reasons, we explain its necessity for the implementation process and additionally we clarify the negligible effect on the output of the models.

## CHAPTER 4: INDIVIDUAL BASED MODEL

We present in Chapter 4 our individual based model. In this approach, we derive a model which simulates the behaviour of every single bat and illustrate the resulting movement characteristics for different landscape structures. Therefore, we split the habitat in three major parts, the sample paths, the one-dimensional and the two-dimensional attraction zones. Then we simulate the bats' movement behaviour by a combination of different stochastic processes and a symmetrized Euler-Maruyama discretization scheme of a reflected Brownian motion. Additionally we include a Voronoi separation into our model for simulating territorial behaviour inside the colony. This separation divides large two-dimensional attraction zones into multiple smaller zones and allocate individuals to these different subzones.

Then we include a Monte-Carlo simulation into our model in order to get an average behaviour of the population and to obtain an occurrence profile for every subregion of the considered habitat. At the end of the chapter, we present the numerical results for a habitat example for different parameter settings of the IBM and the Monte-Carlo simulation.

## CHAPTER 5 APPLICATION

We present the IBM results for a real parametrized landscape structure which is known for a pipistrelle (*Pipistrellus pipistrellus*) colony and which is focus of the research work of C. Lindemann. We choose different parameter settings and illustrate the resulting flight trajectories. This chapter gives a first idea of how the model is applicable on future research questions.

## CHAPTER 6: PARTIAL DIFFERENTIAL EQUATION MODEL

In addition to the IBM, we present a PDE based approach for bats' foraging behaviour in this chapter. We derive the PDE approach for all three subparts: Sample paths, one-dimensional and two-dimensional attraction zones. For the most challenging part, the two-dimensional attraction zones, we achieve this by using a recent result of Bossy, Gobet, and Talay, 2004 which allows us to transform our reflected Brownian motion into a parabolic PDE with Neumann boundary conditions. At the end of the chapter, we present the numerical results for these three subparts. Additionally we compare the results of the IBM and the PDE based models and we point out the advantages and disadvantages of both approaches in order to connect them to suitable applications. Furthermore, we explain the characteristics of the IBM which make it more suitable for our model purposes.

## CHAPTER 7: CALIBRATION

Every model has to be validated. So, we give a short introduction into model calibration and the general method, the Gauß-Newton algorithm. The main issue in all calibration methods is the calculation of the derivative of the residual function. This derivative is either approximated, e.g. by finite differences, or it is calculated exactly. The latter can sometimes be done analytically, but unfortunately this is not possible in our case. Another method for calculating the exact derivative is the sensitivity equation. However, this method produces a high computational effort. Hence, we use the adjoint equation. This method reduces the computational effort of the calibration model by simultaneously calculating the exact derivative. After a general introduction, we fit this method to our special model characteristics and present the final calibration model for our IBM.

## CHAPTER 8: DEATH RISK OF WIND TURBINES

Since the approaches of Chapter 4 and Chapter 6 only give us the occurrence rates for specific regions in the habitat, we need to calculate the number of fatalities caused by existing or planned wind turbines. Therefore, we present in Chapter 8 a model which calculates the number of bats actually being hit after reaching the wind turbine. This rate depends on various factors, e.g. the rotor height and the rotor radius. The result of this chapter is a formula which makes it possible to estimate the bats' risk of being killed by the wind turbine depending on the type of wind turbine, the wind velocity and the bat species. Hence, this model is also applicable to various bat species and their particular movement characteristics.

## CHAPTER 9: POPULATION MODEL

In Chapter 8, we estimate the number of fatalities caused by wind turbines. This number represents an additional death risk which we use for population size modelling in Chapter 9. We start this chapter with an introduction into the general theory of population models. There are a lot of different types of models in literature. We start with a simple discrete one and derive the corresponding ordinary differential equation (ODE) model which makes it possible to consider a continuous time development. Additionally, we include a carrying capacity which is an indicator for the food supply and the habitat quality and therefore limits the population growth.

Since there are different age-dependent fertility and death rates inside a bat colony, we introduce age-structured population models. We consider the discrete matrix population model formulation, called Leslie

Matrix, and also the continuous case, which uses a hyperbolic PDE formulation. A very challenging part of these age-structured models is the incorporation of the carrying capacity. We manage to include this carrying capacity, such that the population growth is again limited by this constant. We adapt all models to the characteristics of a bat population, include the additional risk caused by the wind turbines and compare the resulting population size developments.

#### CHAPTER 10: MODELLING SWARM BEHAVIOUR WITH PARTIAL INTEGRO-DIFFERENTIAL EQUATIONS

In this chapter, we present an interesting type of movement behaviour: The swarm. This type of movement is not only interesting for ecologically induced research, but it is also very fascinating to look at the mathematical techniques to represent this type of behaviour. We introduce the theoretical framework of simulating swarm behaviour with a partial integro-differential equation (PIDE) model. These models have been a focal issue in recent years and have been studied intensively. By moving as a swarm, individuals do not only move from A to B in the shortest or simplest way, but they orientate on the behaviour of the individuals surrounding them. This can be simulated by a non-local advection-diffusion term. We focus on the work of Mogilner and Edelstein-Keshet, 1999 and we get some existence and uniqueness results for a simpler version of their model and a uniqueness result for their original equation.

#### 11.2 OUTLOOK AND POSSIBLE APPLICATIONS

Here we want to sum up open questions and we would like to point out further research topics which might be interesting for evaluate the wildlife conflict of wind turbines and a local bat population. Additionally, we want to identify possible applications for the models described in this thesis.

##### 11.2.1 *Numerical calibration*

The numerical implementation of the calibration framework and the parameter fitting stays crucial for the application of the IBM. Therefore an appropriate empirical data set is necessary. The result of the calibration method can be used for validating the model assumptions or to find new model assumptions in order to obtain a more realistic model outcome. After this fitting process, it will be possible to use the model result in order to generate artificial trajectories of bats or to find better places for wind turbines.

### 11.2.2 *Planning tool*

The main goal of this work is to estimate the danger of existing or planned wind turbines for the local bat population. The next step is to derive a sort of planning tool which finds optimal locations for wind turbines. Here, we want to give a short outlook on how that can be achieved.

We present three different optimization approaches, which use specific target functions.

#### MAXIMISE ENERGY OUTPUT

The wind turbine produces an amount  $E$  of energy per year.  $E$  is dependent on the wind speed  $s$  and the type of the wind turbine. The wind speed is dependent on the location  $(x, y)$  where the wind turbine is built. The bats' annual death rate  $D$  must not exceed the limit  $\bar{D}$ . This limit should guarantee that the population does not become extinct. Just like  $E$ , the death rate is dependent on the wind speed  $s$  and the type of wind turbine considered. This rate is calculated in Chapter 8.

So we can set the optimization problem:

$$\begin{aligned} \max_{(x,y)} E(s(x, y)) \\ \text{s.t. } D(s(x, y)) \leq \bar{D}. \end{aligned}$$

#### MINIMISE DEATH RATE

In the second approach we define the minimal annual energy output  $\bar{E}$ . This limit identifies the amount of energy that is necessary for a economic efficient operation of the wind turbine.

Then we obtain the following optimization problem:

$$\begin{aligned} \min_{(x,y)} D(s(x, y)) \\ \text{s.t. } E(s(x, y)) \leq \bar{E}. \end{aligned}$$

We have to say that the two different optimization problems do not necessarily yield the same position coordinates for the wind turbine. In most of the habitats it is almost sure, that the results are different.

This occurs because in the first problem, we try to maximize the energy output. So we optimise over the set of points where the population does not extinct and search the optimal coordinates for energy production. In the second approach, we optimise on the set of economic reasonable locations for wind production and search the point where the bats have the highest survival rate.

## MULTI-OBJECTIVE OPTIMIZATION

Instead of considering these two different optimization problems it is also possible to formulate the multi-objective optimization problem

$$\begin{aligned} & \min_{(x,y)} \{\omega_1 D(s(x,y)), -\omega_2 E(s(x,y))\} \\ & \text{s.t. } (x,y) \in \mathbb{R}^2, \end{aligned}$$

here  $\omega_1$  and  $\omega_2$  denote two weighting functions, where  $\omega_1 + \omega_2 = 1$ . In the extreme cases ( $\omega_1 = 1$  and  $\omega_2 = 0$  or  $\omega_1 = 0$  and  $\omega_2 = 1$ ) we obtain the unconstrained cases from above. For the more interesting in-between cases we obtain new solutions which correspond to the choice of this weighting functions.

11.2.3 *Comparison to existing models*

The most mentioned technique for estimating the number of fatalities caused by wind turbines is the work of Behr et al., 2011. They propose a sort of shutdown algorithms which guarantee that the wind turbines are shut down in times with high bat activity and/or low wind velocities. Although this method is used for many wind parks, it is not known until today if these algorithms achieve the predicted reduction of fatalities. Hence, a comparison of our result to the approach of Brinkmann would be a very interesting project and could be a possibility for either validating both approaches or for giving ideas of improving the shutdown algorithms.

## LIST OF FIGURES

---

Figure 1	Space-time-prism . . . . .	12
Figure 2	Example for movement along sample path . .	24
Figure 3	Example for a movement inside a two-dimensional attraction zone . . . . .	26
Figure 4	Euler-Maruyama and symmetrized Euler-Maruyama scheme . . . . .	30
Figure 5	Voronoi separation scheme . . . . .	37
Figure 6	Model area . . . . .	39
Figure 7	IBM for four individuals . . . . .	40
Figure 8	IBM for two individuals with different preferences . . . . .	41
Figure 9	Effect of a Voronoi separation on the IBM result	42
Figure 10	Monte-Carlo simulation for four individuals .	43
Figure 11	Monte-Carlo simulation for two individuals with different preferences . . . . .	44
Figure 12	Example for a pipistrelle habitat . . . . .	45
Figure 13	Habitat example with sample paths, attraction zones, a roost and several wind turbine locations	46
Figure 14	Lettweiler 1 . . . . .	47
Figure 15	Lettweiler 2 . . . . .	48
Figure 16	Lettweiler 3 . . . . .	49
Figure 17	Lettweiler 4 . . . . .	50
Figure 18	Lettweiler 5 . . . . .	51
Figure 19	Lettweiler 6 . . . . .	52
Figure 20	PDE model for the path . . . . .	58
Figure 21	PDE model for the one-dimensional attraction zone . . . . .	59
Figure 22	PDE model for the two-dimensional attraction zone . . . . .	60
Figure 23	Comparison for the path . . . . .	61
Figure 24	Comparison for the two-dimensional attraction zone (1) . . . . .	62
Figure 25	Comparison for the two-dimensional attraction zone (2) . . . . .	63
Figure 26	Technical description of a wind turbine . . . .	81
Figure 27	Integration scheme for circ area . . . . .	82
Figure 28	Effect of the carrying capacity for the discrete and ODE model . . . . .	90
Figure 29	Effect of different birth rates for the discrete and the ODE model . . . . .	94
Figure 30	Effect of the carrying capacity for the matrix model . . . . .	104

Figure 31	Effect of the carrying capacity for the hyperbolic PDE model . . . . .	108
Figure 32	Age classes at time $T$ . . . . .	108



## BIBLIOGRAPHY

---

- Amorim, F., H. Rebelo, and L. Rodrigues (2012). "Factors influencing bat activity and mortality at a wind farm in the Mediterranean region." In: *Acta Chiropterologica* 14, pp. 439–457.
- Arnett, E.B., R.M.R. Barclay, and C.D. Hein (2013). "Threshold for bats killed by wind turbines." In: *Frontiers in Ecology and the Environment* 11, p. 171.
- Banks, H. T., P. M. Kareiva, and L. Zia (1988). "Analyzing Field Studies of Insect Dispersal Using Two-Dimensional Transport Equations." In: *Environmental Entomology* 17.5, p. 815.
- Behr, O. et al. (2011). "Fledermausfreundliche Betriebsalgorithmen für Windenergieanlagen." In: *Entwicklung von Methoden zur Untersuchung und Reduktion des Kollisionsrisikos von Fledermäusen an Onshore-Windenergieanlagen - Umwelt und Raum*. Vol. 4. Cuvillier, pp. 323–353.
- Björck, Å. (1996). *Numerical Methods for Least Squares Problems*. Society for Industrial and Applied Mathematics.
- Blackwell, P.G. (1997). "Random diffusion models for animal movement." In: *Ecological Modelling* 100.1–3, pp. 87–102.
- Bossy, M., E. Gobet, and D. Talay (2004). "Symmetrized Euler scheme for an efficient approximation of reflected diffusions." In: *Journal of Applied Probability* 41.3, pp. 877–889.
- Bovet, P. and S. Benhamou (1988). "Spatial analysis of animals' movements using a correlated random walk model." In: *Journal of Theoretical Biology* 131.4, pp. 419–433.
- Brillinger, D. R. (2003). "Simulating Constrained Animal Motion Using Stochastic Differential Equations." In: *Lecture Notes-Monograph Series* 41, pp. 35–48.
- Brillinger, D. R. et al. (2002). "Employing stochastic differential equations to model wildlife motion." In: *Bulletin of the Brazilian Mathematical Society* 33.3, pp. 385–408.
- Brown, R. (1828). "XXVII. A brief account of microscopical observations made in the months of June, July and August 1827, on the particles contained in the pollen of plants; and on the general existence of active molecules in organic and inorganic bodies." In: *Philosophical Magazine Series 2* 4.21, pp. 161–173.
- Budenz, T. et al. (in press). "Up and down: Western barbastes actively explore lattice towers – implications for mortality at wind turbines?" In: *Hystrix*.
- Bullard, F. (1991). "Estimating the Home Range of an Animal: A Brownian Bridge Approach." MA thesis. University of North Carolina at Chapel Hill.

- Burger, M., V. Capasso, and D. Morale (2006). "On an aggregation model with long and short range interactions." In: *Nonlinear Analysis: Real World Applications* 8, pp. 939–958.
- Caswell, H. (2001). *Matrix Population Models: Construction, Analysis, and Interpretation*. Sinauer Associates.
- Codling, E. A., M. J. Plank, and S. Benhamou (2008). "Random Walk Models in Biology." In: *Journal of the Royal Society* 5, pp. 813–834.
- Cohen, J. E. (1979). "Ergodic theorems in demography." In: *Bulletin (New Series) of the American Mathematical Society* 1.2, pp. 275–295.
- Costantini, C., B. Pacchiarotti, and Sartoretto F. (1998). "Numerical Approximation for Functionals of Reflecting Diffusion Processes." In: *SIAM Journal on Applied Mathematics* 58.1, pp. 73–102.
- Cryan, P. M. et al. (2014). "Behavior of bats at wind turbines." In: *Proceedings of the National Academy of Sciences* 111.42, pp. 15126–15131.
- Deuffhard, P. and A. Hohmann (2008). *Numerische Mathematik 1: Eine algorithmisch orientierte Einführung*. De Gruyter Lehrbuch Series. De Gruyter.
- Durstewitz, M. et al. (2017). *Windenergie Report Deutschland 2016*. Tech. rep. Fraunhofer IWES.
- Einstein, A. (1905). "Über die von der molekularkinetischen Theorie der Wärme geforderte Bewegung von in ruhenden Flüssigkeiten suspendierten Teilchen." In: *Annalen der Physik* 322, pp. 549–560.
- Fetecau, R C, Y Huang, and T Kolokolnikov (2011). "Swarm dynamics and equilibria for a nonlocal aggregation model." In: *Nonlinearity* 24.10, p. 2681.
- Fitzpatrick, S. and R.R. Phelps (1982). "Differentiability of the Metric Projection in Hilbert Space." In: *Transactions of The American Mathematical Society* 270.2.
- Gardiner, C. (2009). *Stochastic methods. A handbook for the natural and social sciences*. 4th revised and augmented ed. Berlin: Springer.
- Giles, M. B. and P. Glasserman (2006). "Smoking adjoints: fast Monte Carlo Greeks." In: *RISK* 19.1, pp. 88–92.
- Goldstein, S. (1951). "On Diffusion By Discontinuous Movements, and on the Telegraph Equation." In: *The Quarterly Journal of Mechanics and Applied Mathematics* 4.2, p. 129.
- Grimm, V. et al. (2006). "A standard protocol for describing individual-based and agent-based models." In: *Ecological Modelling* 198.1–2, pp. 115–126.
- Grünbaum, D. (1994). "Translating stochastic density-dependent individual behavior with sensory constraints to an Eulerian model of animal swarming." In: *Journal of Mathematical Biology* 33.2, pp. 139–161.
- Haraux, A. (1977). "How to differentiate the projection on a convex set in Hilbert space. Some applications to variational inequality-

- ties." In: *Journal of the Mathematical Society of Japan* 29.4, pp. 615–631.
- Harris, K.J. and P.G. Blackwell (2013). "Flexible continuous-time modelling for heterogeneous animal movement." In: *Ecological Modelling* 255, pp. 29–37.
- Helland, I. S., J. M. Hoff, and O. Anderbrant (1984). "Attraction of bark beetles (Coleoptera: Scolytidae) to a pheromone trap." In: *Journal of Chemical Ecology* 10.5, pp. 723–752.
- Hillen, J. et al. (2011). "Sex-specific habitat selection in an edge specialist, the western barbastelle bat." In: *Annales Zoologici Fennici* 48, pp. 180–190.
- Holmes, E. E. (1993). "Are Diffusion Models too Simple? A Comparison with Telegraph Models of Invasion." In: *The American Naturalist* 142.5, pp. 779–795.
- Holmes, E. E. et al. (1994). "Partial Differential Equations in Ecology: Spatial Interactions and Population Dynamics." In: *Ecology* 75.1, pp. 17–29.
- Kaebe, C., J. H. Maruhn, and E. W. Sachs (2009). "Adjoint-based Monte Carlo calibration of financial market models." In: *Finance and Stochastics* 13.3, pp. 351–379.
- Karatzas, Io. and S. E. Shreve (1991). *Brownian motion and stochastic calculus*. Graduate texts in mathematics. New York, Berlin, Heidelberg: Springer-Verlag.
- Kelm, D. H. et al. (2014). "Seasonal bat activity in relation to distance to hedgerows in an agricultural landscape in central Europe and implications for wind energy development." In: *Acta Chiropterologica* 16.1, pp. 65–73.
- Keyfitz, N. and H. Caswell (2006). *Applied Mathematical Demography*. Statistics for Biology and Health.
- Kushner, H. J. and P. G. Dupuis (1992). *Numerical Methods for Stochastic Control Problems in Continuous Time*. London, UK: Springer-Verlag.
- Langevin, P. (1908). *Sur la théorie du mouvement brownien*. Vol. 146. Comptes Rendues, p. 530.
- Langrock, R. et al. (2014). "Modelling group dynamic animal movement." In: *Methods in Ecology and Evolution* 5.2, pp. 190–199.
- Leslie, P.H. (1945). "On the Use of Matrices in Certain Population Mathematics." In: *Biometrika* 33.3, pp. 183–212.
- Lotka, A. J. (1925). *Elements of Physical Biology*. Williams and Wilkins, Baltimore.
- Malthus, T.R., D. Winch, and P. James (1992). *An Essay on the Principle of Population*. Cambridge Texts in the History of Political Thought. Cambridge University Press.
- Mansuy, R. and M. Yor (2008). *Aspects of Brownian Motion*. Springer Berlin Heidelberg.

- Meyer, C. D., ed. (2000). *Matrix Analysis and Applied Linear Algebra*. Other Titles in Applied Mathematics. Society for Industrial and Applied Mathematics.
- Miller, H. J. (2005). "A Measurement Theory for Time Geography." In: *Geographical Analysis* 37.1, pp. 17–45.
- Mogilner, A. and L. Edelstein-Keshet (1999). "A non local Model for a swarm." In: *Journal of Mathematical Biology* 38, pp. 534–570.
- Murray, J.D. (2011). *Mathematical Biology: I. An Introduction*. Interdisciplinary Applied Mathematics. Springer New York.
- Øksendal, B. (2003). *Stochastic Differential Equations: An Introduction with Applications*. Hochschultext / Universitext. Springer.
- Okubo, A. (1980). *Diffusion and Ecological Problems: Mathematical Models*. Biomathematics texts. Springer-Verlag.
- Okubo, A. and S. A. Levin (2001). *Diffusion and ecological problems: modern perspectives*. Interdisciplinary applied mathematics. Springer.
- Othmer, H. G., S. R. Dunbar, and W. Alt (1988). "Models of dispersal in biological systems." In: *Journal of Mathematical Biology* 26.3, pp. 263–298.
- Patlak, C. S. (1953). "Random walk with persistence and external bias." In: *The bulletin of mathematical biophysics* 15.3, pp. 311–338.
- Paul, W. and J. Baschnagel (1999). *Stochastic Processes: From Physics to Finance*. Springer.
- Peste, F. et al. (2015). "How to mitigate impacts of wind farms on bats? A review of potential conservation measures in the European context." In: *Environmental Impact Assessment Review* 51, pp. 10–22.
- Pettersson, Roger (1995). "Approximations for stochastic differential equations with reflecting convex boundaries." In: *Stochastic Processes and their Applications* 59.2, pp. 295–308.
- Preisler, H. K. et al. (2001). "Stochastic Differential Equations: A Tool for Studying Animal Movement." In: *Proc. IUFRO 4.11 Conference, Greenwich*, pp. 26–29.
- Risken, H. H. (1984). *The Fokker-Planck equation : methods of solution and applications*. Springer series in synergetics. Springer-Verlag.
- Rydell, J. et al. (2012). "The effect of wind power on birds and bats – a synthesis." In: *Swedish Environmental Protection Agency, report 5611*.
- Saisho, Yasumasa (1987). "Stochastic differential equations for multi-dimensional domain with reflecting boundary." In: *Probability Theory and Related Fields* 74.3, pp. 455–477.
- Santos, H. et al. (2015). "Using species distribution modelling to predict bat fatality risk at wind farms." In: *Biological Conservation* 157, pp. 178–186.
- Shapiro, A. (1994). "Existence and Differentiability of Metric Projections in Hilbert Spaces." In: *SIAM Journal on Optimization* 4.1, pp. 130–141.

- Śłomiński, L. (1994). "On approximation of solutions of multidimensional SDE's with reflecting boundary conditions." In: *Stochastic Processes and their Applications* 50.2, pp. 197–219.
- Smoluchowski, M. (1906). "Zur kinetischen Theorie der Brownschen Molekularbewegung und der Suspensionen." In: *Annalen der Physik* 326.14, pp. 756–780.
- Song, Y. and H. J. Miller (2014). "Simulating visit probability distributions within planar space-time prisms." In: *International Journal of Geographical Information Science* 28.1, pp. 104–125.
- Technitis, G. et al. (2015). "From A to B, randomly: a point-to-point random trajectory generator for animal movement." In: *International Journal of Geographical Information Science* 29, pp. 912–934.
- Topaz, C. M. and A. L. Bertozzi (2004). "Swarming patterns in a two-dimensional kinematic model for biological groups." In: *SIAM Journal on Applied Mathematics* 65.1, pp. 152–174.
- Topaz, C. M., A. L. Bertozzi, and M. A. Lewis (2006). "A Nonlocal Continuum Model for Biological Aggregation." In: *Bulletin of Mathematical Biology* 68.7, pp. 1601–1623.
- Tveito, A. and R. Winther (2006). *Introduction to Partial Differential Equations: A Computational Approach*. Texts in Applied Mathematics. Springer Berlin Heidelberg.
- Uhlenbeck, G. E. and L. S. Ornstein (1930). "On the Theory of the Brownian Motion." In: *Physical Review* 36 (5), pp. 823–841.
- Verboom, B. and H. H. Huitema (2010). "The influence of treeline structure and wind protection on commuting and foraging common pipistrelles." In: *Lutra - Journal of the Dutch Mammal Society*, pp. 63–80.
- Verhulst, P.F. (1845). "Recherches mathématiques sur la loi d'accroissement de la population." In: *Nouveaux mémoires de l'Académie Royale des Sciences et Belles-Lettres de Bruxelles* 18, pp. 14–54.
- (1847). "Deuxième Mémoire sur la Loi d'Accroissement de la Population." In: *Mémoires de l'Académie Royale des Sciences, des Lettres et des Beaux-Arts de Belgique* 20, pp. 1–32.
- Vogels, M. et al. (1975). "P. F. Verhulst's "notice sur la loi que la populations suit dans son accroissement" from correspondence mathématique et physique. Ghent, vol. X, 1838." In: *Journal of Biological Physics* 3.4, pp. 183–192.
- Voigt, C.C. et al. (2015). "Wildlife and renewable energy: Germans politics cross migratory bats." In: *European Journal of Wildlife Research* 61, pp. 213–219.
- Volterra, V. (1927). *Variazioni e fluttuazioni del numero d'individui in specie animali conviventi*. Atti della R. Accademia Nazionale dei Lincei. C. Ferrari.
- Wloka, J. (1982). *Partielle Differentialgleichungen: Sobolevräume und Randwertaufgaben*. Mathematische Leitfäden. Teubner.